

University of New Orleans

ScholarWorks@UNO

University of New Orleans Theses and
Dissertations

Dissertations and Theses

Spring 5-18-2012

Enhancement in Degradation of Environmental Pollutants: Fenton Degradation of 2,4,6-Trinitrotoluene and Photodegradation of Deepwater Horizon Crude Oil

Sarah M. King

University of New Orleans, samille3@uno.edu

Follow this and additional works at: <https://scholarworks.uno.edu/td>



Part of the [Analytical Chemistry Commons](#), [Environmental Chemistry Commons](#), and the [Oil, Gas, and Energy Commons](#)

Recommended Citation

King, Sarah M., "Enhancement in Degradation of Environmental Pollutants: Fenton Degradation of 2,4,6-Trinitrotoluene and Photodegradation of Deepwater Horizon Crude Oil" (2012). *University of New Orleans Theses and Dissertations*. 1451.

<https://scholarworks.uno.edu/td/1451>

This Dissertation is protected by copyright and/or related rights. It has been brought to you by ScholarWorks@UNO with permission from the rights-holder(s). You are free to use this Dissertation in any way that is permitted by the copyright and related rights legislation that applies to your use. For other uses you need to obtain permission from the rights-holder(s) directly, unless additional rights are indicated by a Creative Commons license in the record and/or on the work itself.

This Dissertation has been accepted for inclusion in University of New Orleans Theses and Dissertations by an authorized administrator of ScholarWorks@UNO. For more information, please contact scholarworks@uno.edu.

Enhancement in Degradation of Environmental Pollutants: Fenton Degradation of 2,4,6-Trinitrotoluene
and Photodegradation of Deepwater Horizon Crude Oil

A Dissertation

Submitted to the Graduate Faculty of the
University of New Orleans
in partial fulfillment of the
requirements for the degree of

Doctor of Philosophy
in
Chemistry

by

Sarah Miller King

B.A. Southeastern Louisiana University, 2005

May 2012

© 2012, Sarah Miller King

Acknowledgements

I would like to extend my deepest gratitude to my advisor Dr. Matthew Tarr. Throughout the past 5 years he has guided me with patience, encouragement, and support. I would also like to express my gratitude to my committee members, Dr. John Wiley, Dr. Edwin Stevens, Dr. Yang Cai, and Dr. Richard Cole for their comments and suggestions throughout my graduate research.

I would like to thank Dr. Thomas Soniat, Dr. Curtis Jarand, Aisa Carter, Anastasia Whitney, Masie O'Quinn, Peter Leaf, Elizabeth Balga, and Scott Gordon for their contributions to my research. I would also like to thank SDIX and Dr. Bhaskar Kura for the Microtox instrument. I would also like to thank my past and present group members for their support and wisdom: Sourav Chakraborty, Ashley Quach, Arriel Wicks, Venkata Kethineedi, Gayatri Sahu, Richie Provost, Angela Ellender, Ujwal Patil, Kristen Schexnayder, Parisa Pirani, Phoebe Ray, Donna Peralta, and Isbella Schmitt.

I would also like to thank my husband, Billy, for his love and support that he has giving me throughout my graduate career. I would like to also thank my parents, James and Darby Heine, for pushing me to become the best I could be and supporting me through every decision that I have made. I will also like to think my mother-in-law, Lorie Bowes, for the support she has given to me and my husband.

Lastly, none of this research would have been possible without funding. I wish to give thanks for the financial support from National Science Foundation (Grant CHE-0611902 and CHE-1111525), BP/The Gulf of Mexico Research Initiative via the Northern Gulf Institute (Grant 10-BP_GRI-UNO-01), the University of New Orleans College of Science, and the Academy of Applied Science (Grant W911NF-04-1-0226).

Table of Contents

List of Figures	v
List of Tables	viii
Abstract	x
Chapter 1: 2,4,6-Trinitrotoluene	1
Chapter 2: Enhancement of Fenton Degradation of TNT by Organic Modifiers	27
Chapter 3: Petroleum	47
Chapter 4: Photolytic and photocatalytic degradation of oil from the Deepwater Horizon spill.....	71
Chapter 5: Photolytic and Photocatalytic Degradation of Chemically Dispersed Surface Oil from the Deepwater Horizon Oil Spill.....	89
Chapter 6: Photolytic and Photocatalytic degradation of oil from the Macondo wellhead with and without dispersants.....	106
Chapter 7: Chemical and physiological measures on oysters from oil-exposed sites in Louisiana.....	128
Chapter 8: Summary and Future Work	137
References	142
Vita.....	159

List of Figures

Figure 1.1. Synthesis of TNT.....	1
Figure 1.2. The biotransformation of TNT	5
Figure 1.3. Location and number of TNT contaminated NPL superfund sites in the US ...	7
Figure 1.4. The proposed mechanism of Fenton oxidation of TNT	18
Figure 1.5. Structure of cyclodextrins.....	22
Figure 1.6. Torus structure of cyclodextrins.....	22
Figure 2.1. Normalized TNT concentration vs. reaction time for reactions without organic modifiers at neutral pH	33
Figure 2.2 The normalized TNT concentration vs. reaction time at near neutral pH of the Fenton degradation with cyclodextrins at varying iron concentrations.	36
Figure 2.3. The normalized TNT concentration vs. reaction time at neutral pH of the Fenton degradation with varying cyclodextrin concentrations	38
Figure 2.4. The normalized TNT concentration vs. reaction time at neutral pH of the Fenton degradation with 1 mM ether.....	40
Figure 2.5. The normalized TNT concentration vs. reaction time at neutral pH of the Fenton degradation with alcohols, polyols, and dextrans.....	40
Figure 2.6. The normalized TNT concentration vs. reaction time at neutral pH of the Fenton degradation with PEG 400.....	41
Figure 2.7. Plots of $\ln (C/C_0)$ vs. reaction time for TNT Fenton degradation.....	42
Figure 3.1. Areas impacted by the Deepwater Horizon oil spill.....	48
Figure 3.2. Sub-surface dispersant application theory.....	56
Figure 3.3. Schematic of the clean-up methods and weathering of the oil released from the Macondo well head	60
Figure 3.4. NOAA's proposed budget for oil released from the Macondo well	62
Figure 4.1. Appearance of oil as a function of irradiation time.....	77

Figure 4.2. Synchronous scan of the surface oil over irradiation time	78
Figure 4.3. EEM of the DCM diluted non-irradiated oil extracted and total fluorescence percent remaining of the DCM oil extracts over irradiation time.....	81
Figure 4.4. The GC-FID analysis of surface oil exposed over irradiation time.....	83
Figure 4.5 Microtox data of the toxicity of the aqueous layer of the irradiated surface oil samples.....	86
Figure 5.1. Appearance of surface oil with Corexit EC9500A as a function of irradiation time	93
Figure 5.2. Appearance of surface oil with Corexit EC9527A as a function of irradiation time	94
Figure 5.3. Synchronous scan of the irradiated samples containing Corexit EC9500A....	97
Figure 5.4. Synchronous scan of the irradiated samples containing Corexit EC9527A....	97
Figure 5.5. The total fluorescence percent remaining of the DCM oil extracts after irradiation of dispersed oil samples	98
Figure 5.6. The GC-FID analysis of oil with Corexit EC9500A.....	100
Figure 5.7. The GC-FID analysis of oil with Corexit EC9527A.....	100
Figure 5.8. Microtox data of the toxicity of the aqueous layer of the dark and irradiated samples containing dispersants without surface oil	102
Figure 5.9. Microtox data of the toxicity of the aqueous layer of the surface oil irradiated samples containing dispersants	104
Figure 6.1. Gas chromatogram of source and surface oils.....	113
Figure 6.2. Synchronous scan of the source oil irradiated samples containing no dispersant	114
Figure 6.3. Synchronous scan of the source oil irradiated samples containing Corexit EC9500A.....	114
Figure 6.4 Synchronous scan of the source oil irradiated samples containing Corexit EC9527A.....	115

Figure 6.5. The total fluorescence percent remaining of the source oil DCM extracts after irradiation	118
Figure 6.6. The GC-FID analysis of irradiated source oil without dispersant	120
Figure 6.7. The GC-FID analysis of irradiated source oil with Corexit EC9500A	120
Figure 6.8. The GC-FID analysis of irradiated source oil with Corexit EC9527A	121
Figure 6.9. Microtox data of the toxicity of the aqueous layer of the irradiated source oil samples with and without dispersants	125
Figure 7.1. Map of the oyster collection site and SCAT ground oil contaminated observations from May 8, 2011	131
Figure 7.2. LC-FLD chromatogram of the PAH standard, un-oiled and oiled samples ..	134
Figure 7.3. Florescence scan of the 12 minute peak: benzo[a]pyrene, purchased oyster, un-oiled oyster, and oiled oyster	134

List of Tables

Table 1.1. Physical properties of cyclodextrins	22
Table 2.1. Pseudo first order rate constants for the Fenton degradation of TNT in the presence of cyclodextrins and polyethylene glycol.	43
Table 2.2. Pseudo first order rate constants for the Fenton degradation of nitrotoluenes with and without PEG 400 present	44
Table 2.3. Concentration of nitrate and ammonia produced from Fenton degradation of TNT.....	45
Table 3.1. Structures and maximum water concentration for PAHs	51
Table 3.2. The physical properties of light and heavy crude oils	52
Table 3.3. Hydrocarbon composition of LSC oil from the Macondo Well	53
Table 4.1. The ratio of n-C17 to pristane and n-C18 to phytane over irradiation time in surface oil samples without photocatalyst	84
Figure 4.2. The ratio of n-C17 to pristane and n-C18 to phytane over irradiation time in surface oil samples containing photocatalyst.....	84
Table 5.1. The ratio of n-C17 to pristane and n-C18 to phytane over irradiation time in surface oil samples containing Corexit EC9527A	101
Table 5.2. The ratio of n-C17 to pristane and n-C18 to phytane over irradiation time in samples containing Corexit EC9500A.....	101
Table 6.1. The ratio of n-C17 to pristane and n-C18 to phytane over irradiation time in source oil samples without dispersants	122
Table 6.2. The ratio of n-C17 to pristane and n-C18 to phytane over irradiation time in source oil samples containing Corexit EC9500A	122
Table 6.3. The ratio of n-C17 to pristane and n-C18 to phytane over irradiation time in source oil samples containing Corexit EC9527A	122
Table 7.1. Environmental conditions at oyster collection sites.	130
Table 7.2. Weight and shell length of the oysters used for PAH analysis	132

Table 7.3. Mobile phase parameters for PAH analysis.....	132
Table 7.4. Fluorescence parameters for PAH analysis	132
Table 7.5. Percent recoveries of the PAHs monitored.....	133
Table 7.6. Reproductive, condition and disease metrics based on composites of 10 oysters	136

Abstract

Pollution poses serious threats to both the environmental and the organisms that depend on their environment for survival. Due to the toxicity of most contaminants, there is a dire need for remediation of polluted sites. Remediation studies were conducted on two high priority pollutants: 2,4,6-trinitrotoluene (TNT) and crude oil.

TNT was the most common explosive used in the 20th century. Continuous contamination has resulted in an urgent need for remediation. Fenton reagent provides an advanced oxidation process that is capable of remediating recalcitrant explosives, such as TNT. One drawback of Fenton chemistry is that the reaction requires acidic pH to prevent precipitation of iron. Our studies have investigated Fenton degradation of TNT at near neutral pH with several modifiers present: β -cyclodextrin, carboxymethyl- β -cyclodextrin, alcohols, and polyethylene glycol (PEG, MW 200, 400, or 600 g/mol). Fenton degradation was also carried out on other nitroaromatics to better understand the reaction mechanism with PEG 400. Further mechanistic studies investigated the production of nitrate and ammonium with and without PEG 400.

The Deepwater Horizon oil spill devastated the Gulf of Mexico and the surrounding wetlands. There are several mechanisms for degradation of oil released into aquatic environments. Bioremediation is one of the most important remediation methods; however degradation becomes stagnant in low nutrient waters. Furthermore, larger molecular weight alkanes and polycyclic aromatic hydrocarbons (PAHs) are not readily available for biodegradation. Transformation of these molecules often requires initial photodegradation. We have investigated the photochemical transformation of oil films with and without photocatalysts

present. To better understand the photochemical transformations that occur to the Deepwater Horizon oil, we have conducted additional studies with dispersants present.

Keywords: TNT, Fenton, Deepwater Horizon Crude Oil, Photolysis, Remediation

CHAPTER 1

2, 4, 6-Trinitrotoluene

2,4,6-Trinitrotoluene Chemical and Physical Properties

2,4,6-Trinitrotoluene (TNT) is also known as trinitrotoluol, Trotyl, and tilite. It exists as a colorless orthorhombic crystal or light yellow monoclinic needles with a crystal density of 1.654 g/cm^3 at 20°C .¹ TNT's solubilities in water, ethanol, toluene, and acetone are 0.013, 1.23, 55, 109 g/100g at 20°C , respectively. The melting point of TNT varies from $80.2\text{-}80.8^\circ\text{C}$ depending on the purity. TNT is synthesized by reacting toluene with concentrated nitric acid and concentrated sulfuric acid, Figure 1.1. This method of synthesis usually yields 95.5% 2,4,6-trinitrotoluene and 4.5% other trinitrotoluene isomers.² Unwanted trinitrotoluene isomers and dinitrotoluene species are removed by treating the reaction mixture with aqueous sodium sulfite.

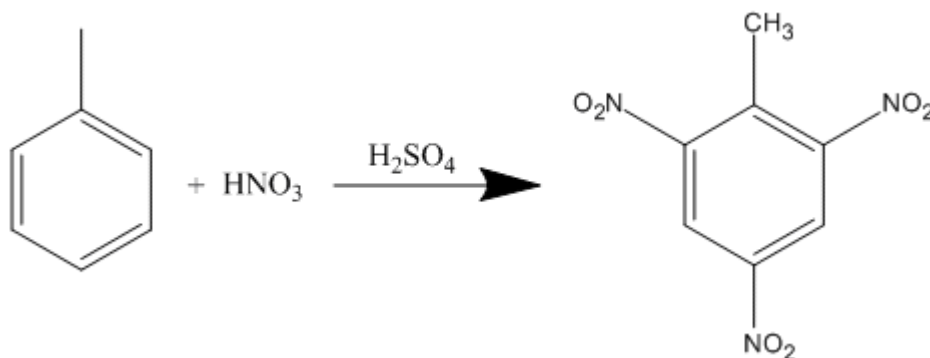
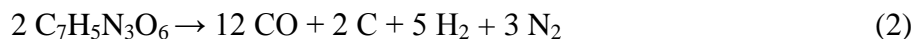


Figure 1.1. Synthesis of TNT

The energy and enthalpy of formation of TNT is -184.8 kJ/kg and -261.5 kJ/kg , respectively.³ The impact and friction sensitivity is 16 N m and 353 N , respectively. Reported

explosion temperatures for TNT range from 275-295°C, and the confined detonation velocity is 6,900 m/s. Decomposition of TNT via detonation can undergo two different transformations:



History of TNT

In 1835 Pelletier and Walter discovered toluene as a degradation product obtained by heating petroleum resin.⁴ In 1841, mononitration of toluene was accomplished. In 1863, Julius H. Wilbrand first prepared crude TNT.⁵ Further investigations on the detailed procedure of the preparation of TNT by Beilstrin and Kuhlberh led to the discovery of other isomers.⁶ TNT was prepared in its pure form in 1880 by Hepp and its structure was determined in 1883 by Claus and Becker.^{4, 7} Germany began manufacturing TNT as a yellow dye in 1891 and in 1899 aluminum was added to produce the explosive composition. In 1902 the Germans began to use TNT to fill their ammunition shells.⁸ Until this time picric acid was used as the explosive of choice, however after TNT explosive properties were identified it became the go to explosive due to many advantages over the former explosive including: less poisonous, completely unaffected by dampness, less dense, cheap to prepare, and less sensitive to impact than picric acid. In addition, TNT's low boiling point allowed for safer and easier shell filling. Britain tested TNT as a potential explosive in 1902 and 1905, but due to it being less powerful and harder to detonate than picric acid, Britain did not employ it as an explosive until 1913.⁹

TNT became a high demand explosive in World War I (WWI). It has been estimated that during WWI the Germans produced 2,500 tons of TNT a week, a massive amount in comparison to Britain's 20 tons a week production.⁹ Because of its advantages over previous explosives, TNT is known to be the most commonly used binary explosive in the 20th century. Binary

explosives are explosives that consist of two or more components. Commercial binary TNT compositions include: amatols (TNT and ammonium nitrate), tritonal (TNT and aluminum powder), octols (TNT and octahydro-1,3,5,7-tetranitro-1,3,5,7-tetrazocine (HMX)), cyclotols/Composition B (TNT and 1,3,5-trinitroperhydro-1,3,5-triazine (RDX)), pentolites (TNT and pentaerythritol tetranitrate), and tetryols (TNT and tetryl), Torpex (TNT, RDX, and aluminum powder), and HBX (TNT, RDX, and aluminum powder).¹⁰

Toxicity of TNT

Toxic effects have been observed for several explosives and components of explosive mixtures which lead to a potential for environmental risks. Toxicity of nitroaromatics have become of great importance due to the mass production of explosives during the 20th century. The first case of acute TNT toxicity in the United States was in 1917 when a factory worker died 24 hours after a jaundice diagnosis that was caused by atrophy of the liver.¹¹ During the first 7 months during WWI, 17,000 TNT poisonings were reported, and of these 475 poisonings resulted in death in the US.¹² From 1916 to 1917, 370 cases of TNT related jaundice was reported in England and 96 cases resulted in death. In Germany, during 1917 to 1918, 1000 cases were reported of TNT related jaundice with 113 of these cases resulting in deaths. Later during WWI the number of toxic TNT incidences decreased due to the increase in understanding of the toxicity, prevention, and treatment of TNT poisoning. During World War II, only 22 fatalities were reported in the US for all government owned explosive manufacturing plants.⁸

Several factors determine the severity of TNT's health effects including the dose, the duration, and the routes of exposure. Possible routes for TNT exposure include oral ingestion, dermal contact and inhalation. Orally ingested TNT travels throughout the blood stream and into all of the organs. Once TNT has reached the liver it is then broken down to several different

compounds. Most of these compounds have been identified and the mechanisms of TNT biotransformations are listed in Figure 1.2. Biotransformation of TNT occurs through a reductive pathway. The overall process is a 6 electron transfer that converts a nitro group to a nitroso group followed by further reduction to a hydroxylamine. Final reduction of the hydroxylamino group results in the formation of an amino group, which with further reduction can be released as ammonium. In addition to the amino substituted toluene and cresols, complexation of two 4-hydroxylamino-2,6-dinitrotoluenes can occur in reducing atmospheres to form azoxytetranitrotoluene.

Numerous studies have been conducted on the toxicity of TNT after oral exposure. Fatalities have been observed in rats, mice, and dogs after either single or multiple doses of TNT. From these studies it was observed that the lethal dose to kill 50 percent of the test species was dependent not only on the species of the animal, 1320 mg/kg/day for a rat versus 32 mg/kg/day for a beagle, but also on the sex of the animal, 1320 mg/kg/day for male rats versus 795 mg/kg/day for female rats.^{13, 14} In addition to fatalities, other less serious symptoms were observed for orally exposed test species. Dilley *et al.* reported that a low exposure (1.4-34.7 mg/kg/day) to TNT in rats resulted in no adverse effect; however when the TNT concentration was increased (160 mg/kg/day) anemia, high cholesterol, and a decrease in the body weight was observed.¹⁴ Levine *et al.* observed similar results in rats and found that the renal cortex discolored to a yellow-brown color.¹⁵ Dilley *et al.* and Levine *et al.* observed that with intermediate TNT exposure, the weight of the spleens of rats, mice, and dogs increased.^{14, 16} Additionally, they also found that that rats and dogs orally exposed became lethargic after exposure.^{13, 15, 17}

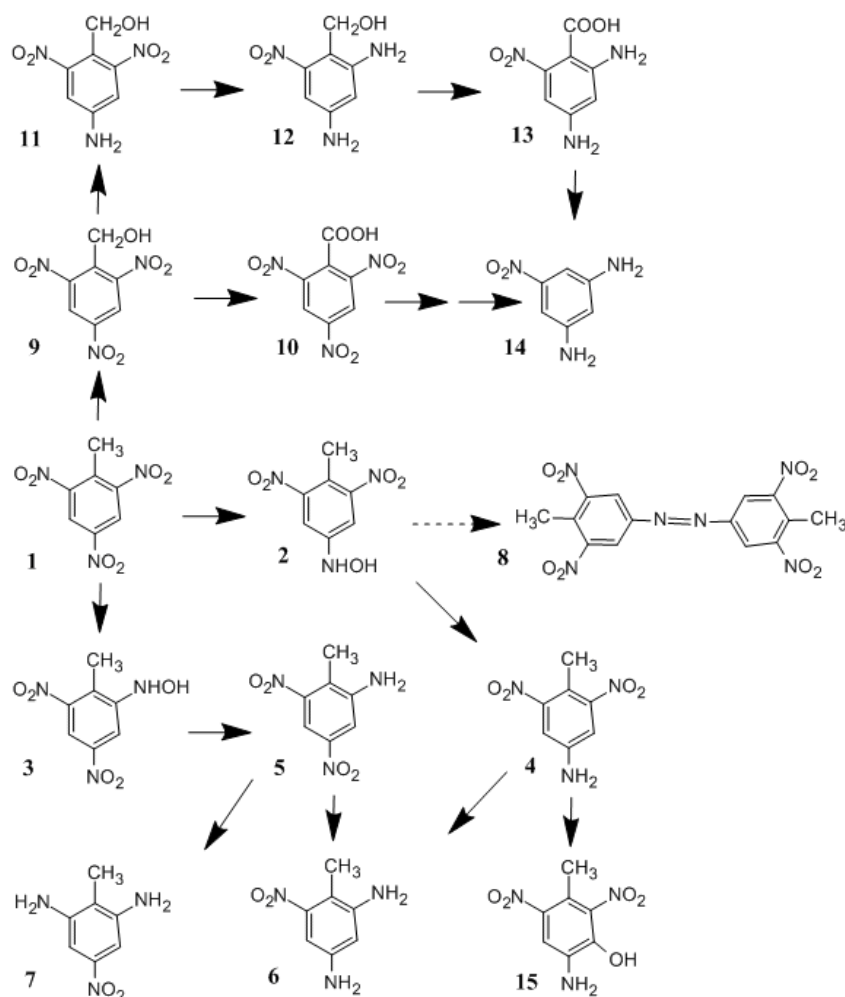


Figure 1.2. The biotransformation of TNT.¹⁸ Degradation products: TNT (1), 4-hydroxylamino-2,6-dinitrotoluene (2), 2-hydroxylamino-4,6-dinitrotoluene (3), 4-amino-2,6-dinitrotoluene (4), 2-amino-4,6-dinitrotoluene (5), 4,6-diamino-2-nitrotoluene (6), 2,6-diamino-4-nitrotoluene (7), 2,6,2',6'-tetranitro-4,4'-azoxytoluene (8), 2,4,6-trinitrobenzyl alcohol (9), trinitrobenzoic acid (10), 4-amino-2,6-dinitrobenzyl alcohol (11), 2,4-diamino-6-nitrobenzyl alcohol (12), 2,4-diamino-6-nitrobenzoic acid (13), 5-nitro-m-phenyleneamine (14), 4-amino-2,6-dinitro-m-cresol (15)

Currently, there are no reports of health effects of TNT after inhalation; however a 5 year study has reported levels of aminodinitrotoluenes in urine of workers of a TNT manufacturing plant.¹⁹ Hassman *et al.* surveyed 54 workers in a TNT manufacturing plant that averaged 13.9 years of exposure.²⁰ Of the workers surveyed 87% were diagnosed with cataracts and 9.3% have reported other toxic damage. Studies later by Hassmanova *et al.* reported liver steatosis in a 55 year old male TNT manufacture worker.²¹ Since there is no way to determine the amount of

TNT inhaled, these studies cannot differentiate whether these conditions were caused by inhalation or absorption through the skin.

Numerous studies have been conducted on the absorption of TNT via dermal contact. Moore claimed that the skin is the main means of entrance of TNT contamination for workers with oily and sweaty hands.²² Additionally, Barnes' studies found an increase in toxic TNT symptoms for workers with oily hands in comparison to workers with dry hands.²³ Studies by Voegtlin *et al.* examined the intensity of TNT skin contamination on workers during 1921 to 1922.²⁴ To measure the intensity of the contaminated area the skin was treated with alcoholic sodium hydroxide and the resulting color was noted. In these studies higher intensity of TNT on workers' hand palms and in the ankle region, areas not appropriately protected by clothing. Haythorn attempted to demonstrate the absorption of TNT through the skin by rubbing large amounts of TNT on his arms for several days; however, in these studies a positive Webster test was not observed.¹¹ Studies conducted by Neal *et al.* observed traces of TNT metabolites in urine after 500 mg of finely ground TNT was rubbed into the palms of human hands and covered with gloves for 8 hours.²⁵

The US Environmental Protection Agency (EPA) has classified TNT as a class C carcinogen and has regulated TNT contamination in soil to 17.2 ppm and in water to 2 µg/L.^{26, 27} In addition, sites that significantly exceed the EPA set concentrations of TNT contamination are listed on the National Priorities List (NPL), also known as superfund sites. Of the 1,338 NPL sites in the US, TNT contamination accounts for 20 superfund sites, Figure 1.3.²⁸ The US Army has estimated that in the US alone there is over 1.2 million tons of TNT contaminated soil.²⁹

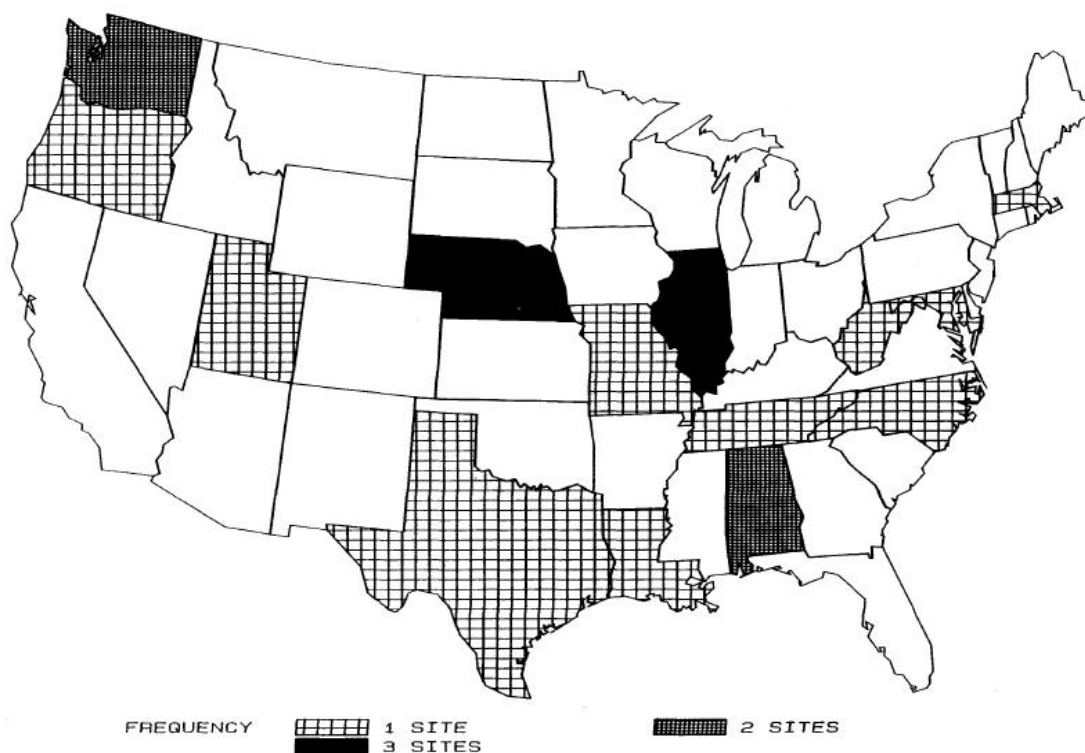


Figure 1.3. Location and number of TNT contaminated NPL superfund sites in the US.²⁸

Fate and Transport of TNT

There are many factors that affect the fate and transport of TNT including transformation, pH, absorption, and irreversible bonding to soil.³⁰⁻³⁴ Partition coefficients are used to express the probability of the TNT in the one phase over another. Partition coefficients are calculated by measuring the TNT in each phase and comparing the ratio. To determine the soil/water partition coefficient the concentrations are found in the equilibrium

$$[\text{TNT}]_{\text{soil}} \rightleftharpoons [\text{TNT}]_{\text{water}}$$

where $[\text{TNT}]_{\text{soil}}$ is the concentration of TNT in the soil and $[\text{TNT}]_{\text{water}}$ is the concentration of TNT in the water. These concentration are then used to calculate the soil/water partition coefficients

$$K_{\text{oc}} = [\text{TNT}]_{\text{soil}} / [\text{TNT}]_{\text{water}}$$

where K_{oc} is the soli/water partition coefficient of the TNT. TNT has a high affinity for soil (soil/water partition coefficient 6.38 L/kg) due to TNT's low water solubility (K_{ow} 1.6).³⁵ TNT migration is common and is found to be dependent on the soil conditions. Reduction of a nitro group on TNT to an amine group results in an increase in the soil/water partition coefficient to 7.91 L/kg thus increasing the adsorption of TNT to the soil. Further reduction of a second nitro group increases the soil/water partition coefficient to 11.96 L/kg. Studies have observed that the adsorption of TNT onto humic acids is pH dependent.³¹⁻³⁴ Brannon *et al.* studied the transformation of TNT at different pHs.³⁶ In these studies, TNT reduction to monoamino and diamino species was observed at all pHs; however, a drastic increase in reduction was observed for system at pH 8. Increased transformation would result in a higher content of amino substituted species, thus resulting in more of the original TNT binding to the soil.

Myers *et al.* studied the recovery of TNT though a column of 3 different soils.³⁷ These studies found that sandy soil (50 μ m-2mm particle size) columns resulted in 97.5% recovery of untransformed TNT, 0.6% of transformed TNT (0.2% 2,4-diaminonitrotoluene, 0.4% 2-aminodinitrotoluene) and 1.9% of TNT unrecoverable. Slit soil (2 μ m-50 μ m particle size) columns resulted in 0.1 % of TNT and 83.6% transformed TNT was recovered (59.4% 2,4-diaminonitrotoluene, 17.3% 2,6-diaminonitrotoluene, 3.7% 4-aminodinitrotoluene, 3.2% 2-aminodinitrotoluene). In the slit studies 15.9% of TNT was not recovered. In clay soil (<2 μ m particle size) columns, 0.1% TNT and 67.5% of transformed TNT was recovered (29.1% 2,4-diaminonitrotoluene, 14.3% 2,6-diaminonitrotoluene, 7.5% 4-aminodinitrotoluene, 16.6% 2-aminodinitrotoluene) and 32.3 of TNT was not recovered. These studies indicate that the adsorption of the TNT to the surface is depended on the grain size and the organic content of the soils. Clay soil samples in these studies had the highest organic content, thus more of the TNT

was adsorbed to the surface. Additionally, slit soils had an increase in the transformation products and the adsorption of TNT in comparison to sand which had similar organic content. The formation of higher percentage of diaminonitrotoluene in the slit soils than the clay soils suggested that the slit column has a higher tendency for TNT reduction. The unrecovered TNT was rationalized as loss due to irreversible binding to the soil, which has been previously observed.^{32, 38-40}

Haderlein *et al.* investigated nitroaromatic compound sorption on different clay minerals.⁴¹ In these studies researchers found that the different sorption of the nitroaromatics to the clays were high when exchangeable cations, K^+ and NH_4^+ , were present in the clays; however, low sorption was observed in the presence of homoionic (containing one cation species) Na^+ -, Ca^{2+} -, Mg^{2+} -, and Al^{3+} - clays. In addition, higher adsorption coefficients were reported for polynitrated aromatic compounds, such as TNT, but little absorption was observed for nonaromatic nitrated species, such as RDX. High adsorption coefficients were observed in the Haderlein *et al.*, however in these studies the adsorption to the clay was found to be reversible.

Remediation of TNT

Numerous contamination sites are present due to the detonation, manufacturing, and storage of TNT. Because of the toxic and mutagenic risk of TNT, there is a dire need for the remediation of contaminated sites. Methods for remediation of TNT from contaminated sites include physical removal (i.e. activated carbon), incineration, photodegradation, phytoremediation (plant based degradation), microbial degradation, and advanced oxidation processes. Various physical methods for the removal of TNT from contaminated soil have been studied.^{42, 43} While these studies did observe removal of TNT, they are very expensive and in many cases require ex-situ treatment. Phytodegradation has shown promise for TNT removal,

but it is limited by the depth of the roots in the soils.⁴⁴⁻⁴⁷ Furthermore, after excessive uptake of TNT, toxic effects are observed in plants. Microbial degradation has exhibited advantages over the aforementioned methods due to the ability to reach deep subsurface soil contamination sites. Microbial degradation transforms one or two nitro groups to amino groups.⁴⁸ The reduction of the nitro group increases the bonding to soil, thus increasing the probability of irreversible bonding. In addition, reductive products from TNT degradation can react with each other to form an azoxytetranitrotoluene, which has higher mutagenic effects than TNT.^{48, 49} In addition, some products of microbial transformation are recalcitrant to the microorganisms that formed them.⁵⁰ In order to fully mineralize TNT contaminated sites, other methods of degradation are need.

Advanced oxidation processes (AOP) have been shown to be very capable in degradation of a wide variety of inorganic and organic pollutants. In AOP generation of radical species, hydroxyl radical is mainly responsible for the oxidation of pollutants. Hydroxyl radical is a strong oxidant. Unlike most radicals, hydroxyl radical is a nonspecific radical, which allows for the transformation of a large variety of organic pollutants. In most cases the reaction of an organic pollutant with hydroxyl radical leads to complete mineralization of the pollutant to yield CO₂. Like previous remediation methods mentioned, AOP are ecofriendly and are inexpensive.

Various AOP for TNT removal include: photodegradation, electrochemical degradation, and Fenton reagent. Numerous studies have been conducted on photodegradation of TNT. In these studies photodegradation has been assisted with the addition of hydrogen peroxide, ozone, and photocatalysts. Hwang *et al.* studied hydrogen peroxide photo-assisted degradation of TNT contaminated water at different pHs and peroxide concentrations.⁵¹ Decolorization of the contaminated water was achieved within an hour of exposure, yet superior decolorization was observed with higher peroxide concentration and lower pHs. Further studies by Hwang *et al.*

examined the coupling of microbial and photodegradation.⁵² Minimal degradation was reported for samples not exposed to the light; however, photolysis samples exhibited 40 and 73% of TNT mineralized after 3 days of exposures for samples without and with riboflavin, respectively. Chen *et al.* examined photolytic TNT degradation with ozone present.⁵³ Degradation of TNT in spent acid was found to be independent of the irradiation intensity and the concentration of sulfuric acid in the solution; however, the removal was found to be dependent on the temperature of the system and the amount of ozone present.

An increasing number of studies have investigated photocatalytic degradation due to the ability to fully mineralize organic pollutants. Dillert *et al.* studied the photolytic and TiO₂ photocatalytic degradation of TNT with hydrogen peroxide.⁵⁴ These studies investigated a variety of parameters including pH and hydrogen peroxide concentration. Without hydrogen peroxide present, 78% and 57% of TNT was degraded from solutions at pH 7 and 11, respectively. When 0.1 mM hydrogen peroxide was added, 72% and 56% of the TNT was removed at pH 7 and 11, respectively. When TiO₂ was added to these same systems, an increase in the rate of degradation was observed at all pHs, and hydrogen peroxide addition only slightly increase degradation rate at pH 11. Son *et al.* examined the TiO₂ photocatalytic degradation of TNT at different pHs.⁵⁵ In agreement to the Dillert *et al.* studies, mineralization of TNT increased in the presence of photocatalyst and higher degradation rates were observed for neutral and basic pHs. Photodegradation is has been proven to be effective in the degradation of TNT, but it is not practical for subsurface contaminated sites.^{54, 56-61}

Electrochemical reactions utilize anodes in an aqueous solution to produce hydroxyl radical:



In addition to hydroxyl radical production at the anode, water can be oxidized at the anode and hydrogen peroxide can be produced by reduction of O₂ at the cathode:

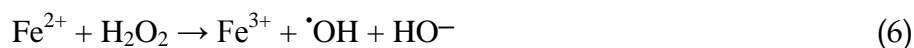


Chen and Liang have studied the electrochemical destruction of TNT in spent acids from the nitration of toluene.⁶² Complete mineralization of TNT as well as any other organic species was observed in these studies. Rabanal *et al.* studied the electrochemical degradation of TNT in concentrated sulfuric acid. To increase the oxidizing potential in this study, ozone was added to the system.⁶³ With addition of the ozone, 60% of the TNT was removed. Doppalapudi *et al.* reported successful reduction of TNT by electrochemical processes in waste water.⁶⁴ In these studies it was found that increasing current lead to an increase in the rate of TNT degradation; however, with the higher density currents mass transfer governed the degradation rates. Electrochemical degradation is a viable method for TNT removal from aqueous waste systems, but using this method for TNT removal from soil is not feasible.

Fenton's Reagent

In 1876, Henry J. Fenton observed the oxidation of tartaric acid in the presence of ferrous sulfate and hydrogen peroxide.^{65, 66} Fenton's studies noted minimal oxidation was observed with Fe³⁺ present, however when Fe²⁺ was present extensive oxidation was observed. Studies later by Haber and Weiss proposed the active oxidant species was the hydroxyl radical ([•]OH).⁶⁷ Additionally, Haber and Weiss proposed that the redox cycle of Fe²⁺/Fe³⁺ was responsible for the formation of the hydroxyl radical. Barb and various coworkers further investigated the various mechanisms of the formation of the active species.⁶⁸⁻⁷⁰

The Fenton reagent is an aqueous solution that contains Fe^{2+} and hydrogen peroxide. In the simplest terms, Fenton reaction is iron catalyzed hydroxyl radical formation:



While the formation of hydrogen peroxide is the key reaction, Barb *et al.* reported other important reactions that also occur:



Hydroxyl radical is produced in the first reaction (6), which happens with a larger rate constant in comparison to reaction 7, $k_f = 70 \text{ M}^{-1} \text{ s}^{-1}$ verses $k_f = 0.001\text{-}0.1 \text{ M}^{-1} \text{ s}^{-1}$. Reactions 7 and 10 recycle the Fe^{3+} to Fe^{2+} , which allows for the hydroxyl radical generation to be catalytic in iron. While the redox cycle in reaction 10 has a large rate constant ($k_f = 1.2 \times 10^6 \text{ M}^{-1} \text{ s}^{-1}$), it is dependent on the formation of hydroperoxyl radical in reaction 7 and 8. The drastically slower reaction rate of redox cycling of reaction 7 is the rate determining step of Fenton reactions. Hydroxyl radical can be scavenged by Fe^{2+} or by H_2O_2 , reactions 8 and 9 ($k_f = 3.2 \times 10^8 \text{ M}^{-1} \text{ s}^{-1}$ and $3.3 \times 10^7 \text{ M}^{-1} \text{ s}^{-1}$, respectively). In addition to hydroxyl radical, active reductive species formed include hydroperoxyl radical. The rate of hydroperoxyl radical formation is much lower than that of the hydroperoxyl radical formation for reaction 7. Formation of hydroperoxyl radical in reaction 8 is relatively fast, however for this reaction to occur high levels of hydrogen

peroxide (>0.3 M) are required. Although in the high peroxide solutions, the hydroperoxyl radical can disassociate to form the highly reductive species superoxide radical anion:

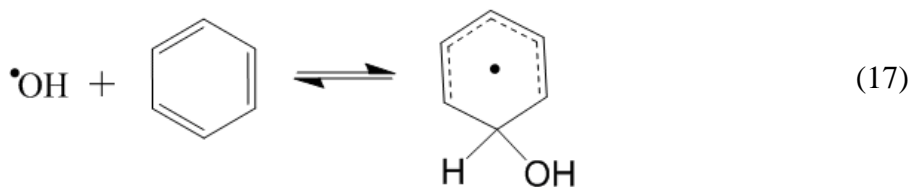
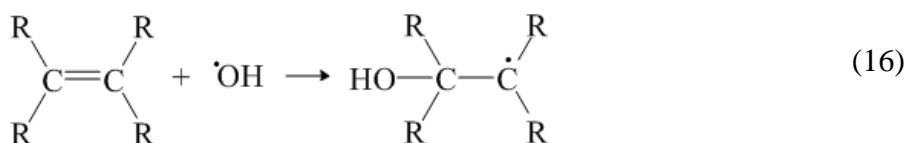
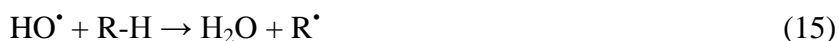


The biggest limitation to the Fenton's reagent is that Fe^{3+} precipitates out to amorphous ferric oxyhydroxides. Precipitation of Fe^{3+} reduces the amount of available Fe^{3+} which in turn reduces the amount to recycled Fe^{2+} . Without the recycled Fe^{2+} the production of hydroxyl radical ceases. To prevent iron precipitation Fenton reactions are normally carried out at pHs around 3, which is not ideal for environmental applications.^{71, 72} Additionally, iron chelating ligands can be added to reaction mixtures to reduce the precipitation of iron oxyhydroxides.⁷³ Wells and Salam observed an increase in rates of reaction 6 with increasing concentration of halide, sulfate, selenate, trimetaphosphate, and tripoylphosphate.^{72, 74, 75} While the rate of reaction 6 can increase, the likelihood of generating a high-valent oxoiron, such as ferryl, can also increase. Francis *et al.* studied the reaction of hydrogen peroxide with iron chelated by diethylenetriamine pentaacetic acid.⁷⁶ An increase in rate was observed, however in these studies the hydroxyl radical was not scavenged by typical hydroxyl radical scavengers, which suggest the formation of the high-valent oxoiron.

In addition to the pH limitations, the hydroxyl radical is a strong nonspecific oxidant; therefore degradation of the target pollutant is not always definite. Scavenging effects of a complex matrix, such as contaminated soil and water samples, is a concern for environmental Fenton applications. Preliminary studies by Lindsey and Tarr observed inhibition of Fenton degradation of polycyclic aromatic hydrocarbons (PAHs) with fulvic acid present.⁷⁷ Decrease in the degradation was attributed to the fulvic acid acting as a scavenger of the hydroxyl radical,

thus limiting the availability of the hydroxyl radical to react with the PAHs. Later studies by Lindsey and Tarr observed similar inhibition of degradation of PAHs with natural organic matter present.⁷⁸ Like the previous studies, the inhibition of degradation of the PAHs in these studies was credited to the natural organic matter scavenging the hydroxyl radical.

Oxidation of pollutants by hydroxyl radical occurs through hydrogen abstraction from C-H, N-H, or O-H bonds or through radical addition to C=C or aromatic rings:



Hydrogen abstraction and addition of the radical to double bonds are irreversible, but radical addition to the aromatic ring is reversible. In the presence of O_2 , organic radicals can react with oxygen to produce peroxy radicals or oxyl radicals:



The formation of peroxy and oxyl radicals from O_2 and R^\bullet is a fast reaction ($k_f = 10^9 \text{ M}^{-1} \text{ s}^{-1}$). Sequential addition of a second radical or hydrogen abstraction stabilizes the radical and produces the oxidized pollutant.

Reported second order rate constants of reactions with hydrogen peroxide have ranged from 10^7 to $10^8 \text{ M}^{-1} \text{ s}^{-1}$.⁷⁹ Several factors determine the reactivity of the hydroxyl radical with the target pollutant including: electrophilic character, strength of the C-H bond, stability of the prospective organic radical, number of equivalent H atom/position of attack, and steric effects.

Anbar *et al.* observed that strongly electropositive species have greater rate constants in comparison the strongly electronegative species.⁸⁰ It was concluded from that study that hydroxyl radical is weakly electrophilic, thus electrophilic character is important when consideration degradation rates. As previously discussed, hydroxyl radicals react with pollutants by abstracting hydrogen from the pollutant, thus the strength of the C-H bond determines the ease of hydrogen abstraction. The stability of the prospective organic radical is directly related to the strength of the C-H bond. The number of positions of attack and steric hindrance of the target pollutant are directly proportional to the probability of attack.

Due to the strong oxidizing potential of the hydroxyl radical, Fenton reagent may be applied to a wide variety of pollutants including polycyclic aromatic hydrocarbons, chlorinated aromatic and aliphatic compounds, and explosives. Przado *et al.* studied the Fenton degradation of a series of polychlorinated biphenyls (PCB 28, PCB 52, PCB 101, and PCB 138).⁸¹ A rapid increase the degradation of PCB 28 and 52 were reported for the first 24 hours; however PCB 101 and PCB 138 were poorly degraded. Decreases in the degradation for the PCB101 and PCB 138 were expected since they have higher chlorine substitutions, thus lower susceptibility to oxidation. Teel *et al.* studied modified Fenton degradation of carbon tetrachloride.^{82, 83} For their modified Fenton reactions high hydrogen peroxide concentrations were employed (> 0.3M) to produce reductive radical species (HO_2^\bullet and $^\bullet\text{-O}_2$). Carbon tetrachloride degradation in these studies was observed and was found to be dependent on the hydrogen peroxide concentration, with an increase in degradation observed for an increase in hydrogen peroxide concentration.

Li *et al.* has examined several parameters of TNT degradation in solution and soil slurries.⁸⁴⁻⁸⁶ In these studies similar extents of degradation were observed for hydrogen peroxide concentration over 0.1% and iron concentrations over 40 mg/L. Degradation of TNT did not

occur at the pH of 7, but when the pH was decreased to 2-4.5 ~95% of the TNT was removed. Higher degradation of TNT was observed for higher temperature (45 °C verses 23 °C) in soil slurry samples. When fulvic acid was added to the system an increase in degradation was observed, but when humic acid was added to the system inhibition of degradation was observed. Further investigation determined that the fulvic acid can reduce the Fe^{3+} to Fe^{2+} , thus increasing the availability of Fe^{2+} to react with hydrogen peroxide and the production of hydroxyl radicals. Increase in degradation was also observed in the presence of the clay component Ca^{2+} -montmorillonite. This increase was attributed to the sorption of the TNT and iron to the surface of the clay resulting in hydroxyl radical formation in close proximity of the TNT.

Matta *et al.* studied Fenton degradation of TNT with natural soils containing iron bearing minerals at acidic and neutral pH.^{87, 88} Higher percentages of TNT were removed for pyrite and magnetite in comparison to hematite, goethite, lepidocrocite, and ferrihydrite in both neutral and acidic pHs. From these results it is evident that oxidation state of the iron mineral was found to be a key parameter in the degradation of TNT. Solubility of the iron minerals and the sorption of TNT to the mineral surfaces were also determined to limit the rate of degradation at neutral pHs. Chelator addition in the magnetite systems increased the degradation of TNT by 3 fold. It was theorized that the increase in the degradation was credited to the increase in the iron dissolution rate, thus increasing the Fenton reaction efficiency.

Hess *et al.* examined degradation products from Fenton degradation of TNT via tandem mass spectroscopy.⁸⁹ From the Degradation products that were observed, a mechanism of oxidation was proposed, Figure 1.4. In some cases demethylation of TNT was the initial step of oxidation to 1,3,5-trinitrobenzene (TNB). Next, denitration occurred at the 2 position of the TNT or TNB to form either 2,4-dinitro-o-cresol or 3,5-dinitrophenol, respectively. At this time

the 2,4-dinitro-o-cresol can undergo demethylation to become 3,5-dinitrophenol. Further oxidation of the 3,5-dinitrophenol produced sequential denitration and alcohol formation and further decomposition to mineralization.

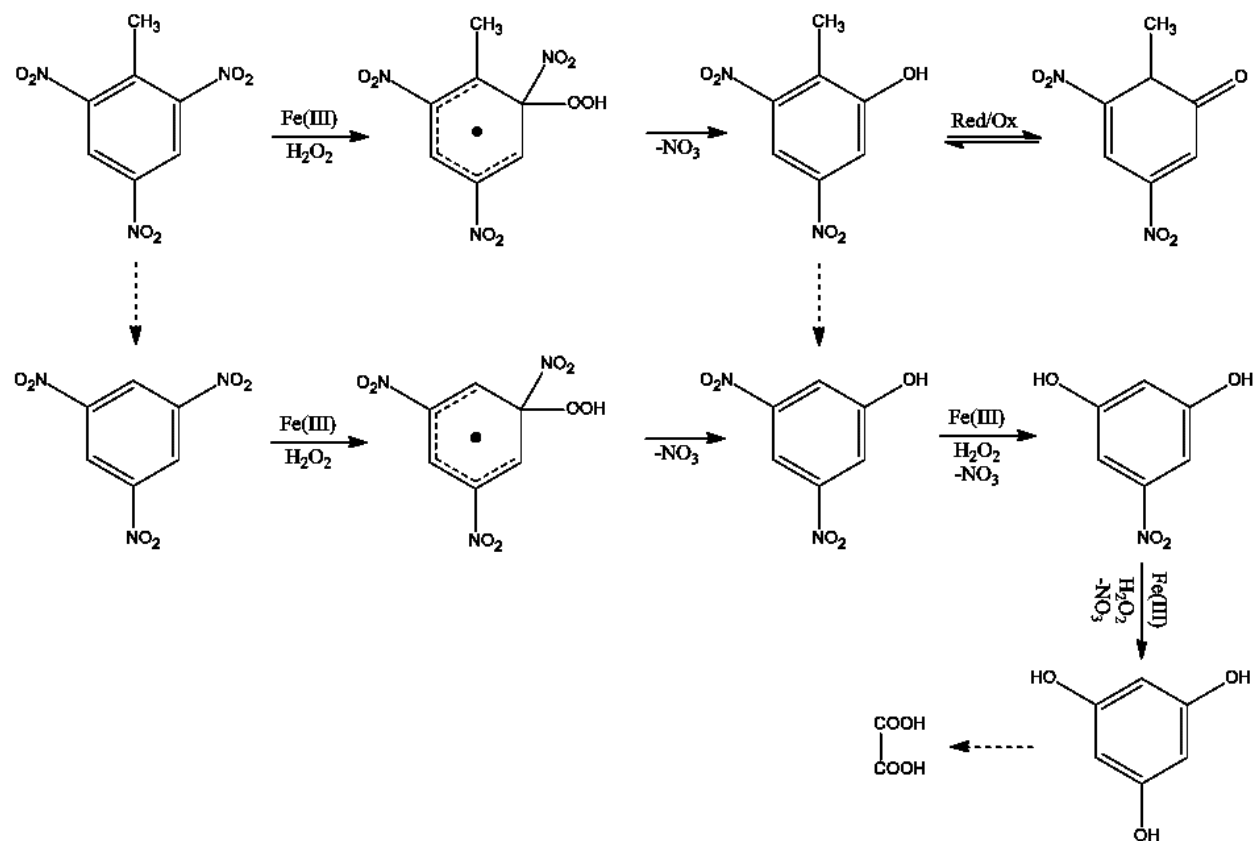


Figure 1.4. The proposed mechanism of Fenton oxidation of TNT.⁸⁹

Several studies have been conducted on the degradation of TNT with modified Fenton reagent. In these systems the Fenton reagent was assisted by either zero valent iron, UV irradiation, or by electrochemical reactions. Oh *et al.* monitored nitrogen production and total organic carbon (TOC) removed for TNT in Fenton systems pretreated with zero valent iron.^{90, 91} In these studies TNT was pretreated with the zero valent iron to reduce the nitro group to the amine. During the reduction the zero valent iron was oxidized to Fe²⁺ which was then used as the catalyst for Fenton reagent. An increase in TOC removal was observed in systems pretreated with zero valent iron. In TNT solutions not pretreated, only nitrate was observed as a

degradation product, however both nitrate and ammonium were observed in pretreated solutions which suggested that pretreatment reduces the TNT before Fenton oxidation. Barreto-Rodrigues *et al.* studied the Fenton degradation of TNT with zero valent iron.^{92, 93} With the pretreatment process, complete degradation of TNT was observed in 30 minutes. Additional studies with this system found that degradation was pH dependent and degradation drastically decreased at higher pHs.

In photo-Fenton degradation the UV produced photon is absorbed by FeOH_2^+ to produce hydroxyl radicals:



This reaction produces a hydroxyl radical which increases the hydroxyl radical formation by two-fold, thus increasing the oxidation potential of the reaction. Kitayama *et al.* studied the Fenton, photo-Fenton, and photocatalytic Fenton degradation of waste water from TNT manufacturing process.⁹⁴ With Fenton oxidation ~60% of the TNT was converted after 2.5 hours of degradation. In comparison to Fenton only samples, irradiated samples coupled to Fenton reaction increase the degradation by 25%. Degradation patterns for photocatalyst samples coupled to Fenton reagent were identical to those of irradiated samples without photocatalyst.

Chen *et al.* studied the photo-Fenton degradation of spent acid TNT solutions. In these studies the temperature, hydrogen peroxide concentration, and iron concentration were compared. Minute degradation difference were observed for photo-Fenton at varying temperatures and iron concentrations, however more organic carbon was removed at higher hydrogen peroxide concentration than at lower concentrations. No degradation was observed for photolytic processes only, however essentially identical degradation was observed for photo-Fenton and Fenton system.

Numerous studies have been conducted by Liou *et al.* on the photo-Fenton degradation of TNT.^{95, 96} Initial studies monitored the TNT concentration with the variety of degradation methods. Fenton degradation with high iron concentrations (1.44 mM) resulted in complete removal of TNT while lower iron concentrations (0.36 mM) resulted in only ~70% of the TNT degraded after 2 hours. With solely photolytic processes, minute losses of TNT were observed. Photo-Fenton treatments resulted in complete removal of TNT both at high and low iron concentrations. Further studies by Liou *et al.* investigated photolytic systems with hydrogen peroxide and at different intensity of irradiations. In these studies the hydrogen peroxide and UV systems had higher degradation rates than the UV only systems, but lower degradation rates than the UV/Fenton coupled reactions. Additionally, increases in the irradiation intensity resulted in increase in the degradation of TNT for photo-Fenton reactions. Similar to their previous studies, increases in iron concentration resulted in increases in TNT degradation for Fenton only systems, and photo-Fenton reactions were found to be independent of the iron concentrations.

Mechanism for electro-Fenton reactions are similar to that of electrochemical reaction in that anodes produce hydroxyl radical and the cathode produces hydrogen peroxide. In electro-Fenton reaction the hydrogen peroxide that is produced at the cathode reacts with iron to produce hydroxyl radical, thus increasing the production of hydroxyl radical. In addition, reduction of the ferric ions to ferrous ions occurs simultaneously at the cathode:



Chen *et al.* have investigated the electrochemical oxidation of TNT.^{62, 97, 98} In their studies, electrochemical Fenton reactions were carried out at different temperatures, iron concentrations, pH, electric potentials, and oxygen gas rates. Degradation of TNT was found to be independent of temperature at low iron concentration (15 mg/L); however in higher iron concentrations

(50mg/L), degradation rates were higher for lower temperatures (303 K) than higher temperature (343 K). When systems were held at the same temperature, minuscule variances in degradations were observed at different iron concentrations. Degradation was determine to be dependent on the pH of the system, and lower pHs (0.2 verses 2) resulted in increases in the TNT degradation. Electric potential applied effected the degradation of TNT. An increase in the potential resulted in an increase in the TNT degradation. Oxygen gas bubbled into the reaction system was found to have no effect on the TNT degradation.

Cyclodextrins

In 1891, Villiers reported the unidentified crystals were formed during the fermentation of starch.⁹⁹ Years later, Schardinger discovered that *Bacullius macerans* was responsible for the deterioration of foods and two distinct crystals were produced during the decomposition, which he called α -dextrin and β -dextrin.¹⁰⁰⁻¹⁰² It wasn't until 1930s that the structures of these dextrins were know. Numerous studies by Freudenberg and coworkers describe the aforementioned crystals were actually maltose units that were connected only by α -1,4 linkages.¹⁰³⁻¹⁰⁵ In 1936 they further identified that the crystal dextrins were cyclic in structure.¹⁰⁶ Year later Freudenberg and Cramer discovered in addition to the alpha and beta dextrins, gamma dextrins were also present.¹⁰⁷

Cyclodextrins (CD) are cyclic oligosaccharides that contains 6 (α), 7 (β), or 8 (γ) D(+)-glucopyranose units that are connect by α -1,4 linkages, Figure 1.5. Reacting starch with the amylase of *Bacullius macerans* produces multiple cyclodextrins which are then separated out by precipitation with different organic solvents. Cyclodextrins have a torus-like shape with all of the glucose units in an undistorted C1 (D) (chair) conformation, Figure 1.6. The interior of the torus structure consist of a ring C-H, followed by a ring of glucosidic oxygens and another C-H

ring. This configuration of CD allows for a polar exterior with a nonpolar interior¹⁰⁸. Primary hydroxyls along the smaller orifice can partially move and can block the cavity; whereas the secondary hydroxyls on the larger orifice are rigid and do not allow movement thus they do not block the cavity. A list of cavity dimensions and physical properties are listed in Table 1.1.

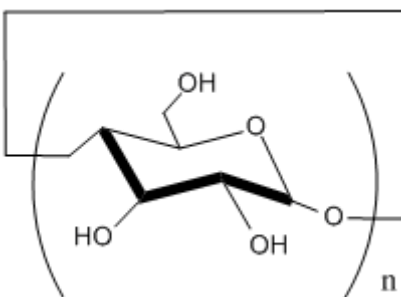


Figure 1.5. Structure of cyclodextrins. $n = 6, 7$, or 8 for α , β , and γ cyclodextrin, respectively

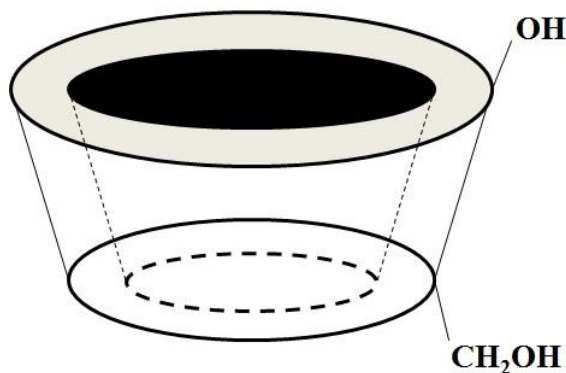


Figure 1.6. Torus structure of cyclodextrins

Table 1.1. Physical properties of cyclodextrins

Cyclodextrin	Number of Glucose Rings	Molecular Weight (g/mol)	Water Solubility (g/100 mL)	Cavity dimensions (Å)	
				Internal Diameter	Depth
α -cyclodextrin	6	972	150.5 ± 0.5	~ 5.2	8
β -cyclodextrin	7	1135	162.5 ± 0.5	~ 6.6	8
γ -cyclodextrin	8	1297	177.4 ± 0.5	~ 8.4	8

One of the most important characteristics of CD is the ability to form guest-host complexes. An abundance of theoretical and experimental studies has been conducted to better

understand CD inclusion complexes. Theoretical studies have studied the bonding of CD to guest molecules.¹⁰⁹⁻¹²¹ In many of these studies it was concluded that the complex form was mostly stabilized by Van der Waal's interactions, with a small contribution from electrostatic forces.^{110, 112, 115-117, 121} While these studies help to better understand the CD complexes, they are limited due to studies conducted in the gas phase which lack solvent interactions with the guest and CD. Experimental studies have been conducted in both aqueous and organic solvents.¹²²⁻¹²⁴ In these studies it was observed that the type of solvent can control the formation of the complexes. Additionally, it was found that organic solvents can inhibit complexation due to the stability of the nonpolar guest in the solvent.^{122, 125-127}

Zheng and Tarr studied cyclodextrin complexes.¹²⁸⁻¹³⁰ In initial studies formation of a 1:1 binary complex formed with iron and carboxymethyl- β -cyclodextrin (CM- β -CD). Further studies with two pollutants, 2-naphthol and anthracene, identified formation of a ternary complex between the CM- β -CD, pollutants, and iron. Further investigations by Zheng and Tarr examined the binary and ternary complexes with an array of CDs: hydroxylpropyl- β -cyclodextrin (HPCD), sulfated- β -cyclodextrin (SCD), α -cyclodextrin (α -CD), and β -cyclodextrin (β -CD).¹³⁰ Binary complexes were observed with the different CDs, however only the CM- β -CD formed a ternary complex. Binary 2-naphthol/HPCD complexes were formed, but due to the low binding to metals, ternary complexes were not observed. The sulfated groups of the SCD are strong metal ligands so binary complexes were formed with the Fe^{2+} ; however the large sulfate groups blocked the entry to the hydrophobic cavity, thus pollutant binding did not occur. Like HPCD, β -CD is a weak metal chelator, so only the binary complex was observed with the β -CD/2-naphthol. Complexation between α -CD/pollutant was observed, but unlike the 1:1 β -CDs: 2-naphthol complexes a 1:2 α -CD:2-naphthol complex was formed. Cai *et al.* examined the formation of

complexes in a gas phase by electrospray mass spectrometry.¹³¹ Toluene and β -CD have a high probability to form binary complexes in the aqueous phase, however in these studies complexes were not observed in the gas phase due to the lack of hydrophobic interactions in the presence of a proton or alkali metal ion acting as an attaching cation. To overcome this limitation, dication Fe (II) was added to the reaction system. Addition of iron (II) to the system stabilized the ternary complex by modifying the conformation of β -CD ring. Further studies of the ternary complexation of iron (II), β -CD, and 2,4,5-trichlorophenoxyacetic acid (2,4,5-T) suggest that polar portion of the 2,4,5-T is favored in the β -CD cavity and not the non-polar aromatic portion.

CDs are non-toxic, inexpensive, ecofriendly, and can be chemically altered with different functional groups. These properties with the ability for complexation has allowed for a vast amount of applications for CD including food, cosmetic, pharmaceutical, environmental cleanup, and the ability to catalyze chemical reactions.

Fenton degradation of pollutants has been studied in the presence of CDs. Veignie *et al.* studied the Fenton degradation of benzo[a]pyrene in the presence of β -CD, HPCD, and other randomly methylated β -cyclodextrins. Significant increase in the solubility was observed for the benzo[a]pyrene when cyclodextrins were present in the solution, and increased cyclodextrin concentration resulted in an increased solubility of the pollutant. Increase in the solubility of the benzo[a]pyrene with increase in cyclodextrin concentration was theorized to be due to pollutant/cyclodextrin complexation. While Fenton degradation with the cyclodextrins increased the rate of degradation of the benzo[a]pyrene, it was found to be dependent on the ability of the cyclodextrin to solubilize the pollutant. When hydroxyl mannitol, a radical scavenger, was added to solutions with HPCD, inhibition of degradation was observed.

Ko *et al.* studied the Fenton degradation of hydrophobic organic compounds with surfactants.¹³² When CM- β -CD was used as a surfactant 90% of phenanthrene was degraded; however when synthetic surfactants were added, a decrease in the degradation occurred. Synthetic surfactants added to the solution scavenged the hydroxyl radical, but the CM- β -CD did not. The observed increase in the phenanthrene degradation with the CM- β -CD present suggested a ternary complex where the hydroxyl radical was produced in close proximity to the pollutant, thus increasing the likelihood of reacting with the phenanthrene.

Previous studies have investigated Fenton degradation of TNT with cyclodextrins present. Yardin and Chiron studied photo-Fenton degradation of TNT obtained from soil flushing with CDs.¹³³ In these studies methylated- β -CD (M- β -CD) and CM- β -CD were employed to increase the aqueous solubility of the TNT and flushing it from the soil. After the TNT was extracted from the soil, the solution underwent photo-Fenton processes. In comparison to water only samples, a 2.1 and 1.8 fold increase in degradation was observed for solutions containing M- β -CD and CM- β -CD, respectively. This increase was attributed to complexation between the CD, TNT, and iron. Calculations from experiment results reported association complexation constant (K) of 338 M^{-1} and 163 M^{-1} for TNT and M- β -CD and CM- β -CD, respectively. These association constants were in agreement to previously reported constants by Sheremata and Hawari.¹³⁴

Jarand *et al.* studied the Fenton degradation of TNT with a variety of CDs: β -CD, CM- β -CD, 6A-[bis(carboxylatomethyl)amino]-6A-deoxy- β -cyclodextrin (β -CD-ida), and 6A-[tri(carboxylatomethyl)(2-aminoethyl)amino]-6A-deoxy- β -cyclodextrin (β -CD-EDTA).¹³⁵ An increase in TNT degradation was reported for CD solutions in comparison to water only solutions of TNT. At pH of 3.1 greater enhancements was observed for the β -CD (7X) than for

other substituted CDs, 2.4, 1.8 and 3.8 for β -CD-ida, β -CD-EDTA, and CM- β -CD, respectively. Further studies were conducted to better understand the mechanism for degradation. Mass spectroscopy data of the degradation processes suggested that CD assisted Fenton degradation of TNT underwent both reductive and oxidative mechanisms. To further confirm the presence of reductive pathway, the samples were analyzed via ion chromatograph (IC) to monitor the nitrate and ammonium production. Only nitrate was observed in IC analysis of the Fenton reaction without CD present, which suggests the degradation occurs only through an oxidative pathway. For Fenton degradation of TNT with CD present, both nitrate and ammonium were detected, which indicates both the oxidative and reductive pathway occurs.

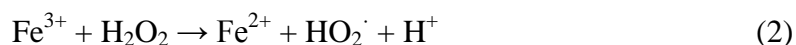
TNT is a toxic, high priority environmental pollutant due to the numerous sites contaminated during manufacturing, testing, and disposal processes. Physical methods for remediation can be costly and require ex-situ treatment. Phytoremediation has demonstrated to be effective for TNT degradation, but after continuous contamination plants exhibit detrimental effects. Biodegradation of contaminated site does occur, but the reduction products can irreversibly bind to soil and some degradation products are more toxic than TNT. Advance oxidative processes have displayed promise for TNT degradation. Photodegradation allows for in situ degradation of TNT; however it is limited by the penetration depth. Fenton degradation provides rapid removal of TNT in laboratory studies; however the high pH requirement is problematic for real world applications. While the previous studies have proven effective in the degradation of TNT, limitation still lies with in situ degradation.

CHAPTER 2

ENHANCEMENT OF FENTON DEGRADATION OF TNT BY ORGANIC MODIFIERS

Introduction

In World War I and World War II 2,4,6-trinitrotoulene (TNT) had become the explosive of preference due to the number of advantages over the previously used explosives, including low cost to manufacture, safety of handling, and low sensitivity of impact.⁴ Consequently, residues of TNT from battle fields and ammunition manufacturing sites contaminate soils and groundwater worldwide. Contaminated sites pose severe hazards due to the toxicity and mutanigency of TNT to living organisms.¹³⁶ For that reason, there is an important need for remediation of TNT in contaminated sites. The most common remediation methods that have been previously studied are bioremediation, incineration, photodegradation, and advance oxidation processes.^{45, 46, 137-144} Advance oxidation processes (AOPs) have shown enormous potential for large scale treatment of recalcitrant, hazardous organic pollutants in water and soils. The AOPs depend on generation of strong oxidants, such as hydroxyl radicals.¹⁴⁵ Fenton chemistry generates hydroxyl radicals by reacting iron with hydrogen peroxide, with two of the many important reactions being:



Cyclodextrins (CDs) are cyclic oligosaccharides made of 6 (α -CD), 7 (β -CD), or 8 (γ -CD) glucose rings connected by α -1,4 linkages. Cyclodextrins have a torus structure that includes a hydrophobic interior which allows for binding of hydrophobic molecules in the cavity. This property of CDs increases the aqueous solubility of hydrophobic organic molecules, thereby improving drug delivery of hydrophobic molecules and removal of pollutants from soil via soil flushing.^{133, 146} Previous studies have shown that in the presence of cyclodextrins, the Fenton degradation rate of TNT is vastly increased partially due to the binary and ternary complexes that are formed between TNT/CD/ Fe^{2+} .^{133, 134, 147} In addition, studies have further verified formation of Fe^{2+} , CD, and pollutant ternary complexes.¹²⁸⁻¹³⁰ Studies have further suggested that the binary complexes are formed by coordination of the nitro groups to the alcohol groups of the CD.^{148, 149} The increase in rate for the binary and ternary complexes is credited to the close proximity of the TNT to the site of formation of the hydroxyl radical. Furthermore, studies have shown that the increase in the degradation rate in the presence of CD is due to the formation of secondary radicals that are more efficient at attacking the TNT.¹⁵⁰

Lindsey *et al.* studied the effect of hydroxyl radical scavengers on the Fenton oxidation of naphthalene.¹⁴⁷ In the presence of the radical scavenger ethyl ether, the degradation of naphthalene was decreased by 70%; however, with carboxymethyl- β -cyclodextrin present in the solution the degradation was inhibited by only 10%. These results suggested that formation of the CD-naphthalene complex or the ternary iron-CD-naphthalene complex played a role in the naphthalene degradation efficiency, possible through formation of radicals in close proximity to naphthalene in binary or ternary complexes.

Previous studies have investigated the kinetics of Fenton degradation of different nitroaromatics under acidic conditions ($\text{pH} = 3$).¹⁵¹ For these studies a correlation was found

between the reaction rate and the number of nitro group on the ring, more nitro substitutions gave lower rates of degradation. The same correlation was also observed in previous Fenton degradation studies by Li *et al.* on nitroaromatics.¹⁵² Other studies investigated and compared the Fenton reagent to photodegradation methods.¹⁵³ In these studies it was found that the Fenton reagent was more effective at oxidizing the TNT than the photolytic methods. In addition, previous researchers have studied the Fenton degradation with natural iron bearing minerals: goethite, ferrihydrite, hematite, and lepidocrocite.^{87, 88} These studies were conducted in soil slurries at neutral pH to mimic contaminated soil environments. From these studies it was discovered that degradation of TNT can occur with the natural iron bearing minerals. In the previous study carboxymethyl- β -cyclodextrin was also added to the soil slurries and an increase in solubility of TNT was observed.⁸⁸

We have studied the Fenton degradation of TNT in aqueous samples at neutral pH values. For these studies, reactions were conducted with systems containing TNT alone and in systems containing organic modifiers: β -cyclodextrin, carboxymethyl- β -cyclodextrin, polyethylene glycol (MW = 200, 400, 600 g/mol), diethylene glycol, diethyl ether, dipropyl ether, ethanol, ethyl acetate, or methanol. Pseudo first order rate constants were calculated and compared for Fenton reaction with and without organic modifiers. In addition to TNT, Fenton degradation was examined for 2-nitrotoluene, 2,4-dinitrotoluene, and 2,6-dinitrotoluene. Pseudo first order rate constants were calculated for these reactions and comparison was made for samples with and without polyethylene glycol (MW 400). Furthermore, TNT degradation products in the presence of polyethylene glycol (MW 400) were studied to better understand the pathway of degradation.

Experimental Materials and Methods

TNT (98% purity, 30 % water) was obtained from Chem Service. 2-Aminotoluene (2-AT) and dipropyl ether were from EM Science and 2-nitrotoluene (2-NT) was from TCI America. 2,6-dinitrotoluene (2,6-DNT) and β -cyclodextrin were from Alfa Aesar. Ferrous sulfate heptahydrate (A.C.S. grade) was obtained from Fisher Scientific. Hydrogen peroxide (30 % wt, A.C.S. grade), 2,4-dinitrotoluene (2,4-DNT), diethylene glycol, and ethyl acetate were obtained from Sigma Aldrich. Acetonitrile (HPLC grade), sulfuric acid, and methanol were from EMD. Carboxymethyl- β -cyclodextrin was obtained from Cerestar. Diethyl ether was from Mallinckrodt Chemicals. Ethanol was from Parmco-AAPER. Polyethylene glycol (MW 400) and polyethylene glycol (MW 600) were from Aldrich. Polyethylene glycol (MW 200) was from Sigma. All aqueous solutions were prepared with purified water from a Barnstead Nanopure UV water purification system with a distilled water feed.

To prepare TNT solutions in water, solid TNT (98% purity, 30% water) was dried in a vacuum desiccator for 1 hour. The appropriate amount of TNT was then dissolved in acetonitrile and the acetonitrile was then evaporated under a stream a nitrogen gas. The TNT crystals were then reconstituted in nanopure water and allowed to mix overnight.

The Fenton reactions for high performance liquid chromatography (HPLC) analysis were carried out by adding 300 mM H_2O_2 at 1 mL/min to an 7 mL aqueous solution containing ferrous sulfate heptahydrate and an organic modifier (if any) under constant stirring. After 2 minutes of peroxide addition, 3 mL of a solution containing the pollutant, ferrous sulfate heptahydrate and the organic modifier (if any) was added and stirring was maintained. This approach was used to allow the Fe/peroxide system to come to steady state before adding the pollutant. Addition of iron and the modifier in the pollutant solution prevented changes in the iron or modifier

concentrations upon pollutant addition. 300 μ L samples were periodically withdrawn and quenched by addition 90 μ L of acetonitrile. The quenched samples were then centrifuged and filtered to remove the precipitated iron before being analyzed via HPLC. Procedure for ion chromatography (IC) was similar to that for HPLC analysis with a few exceptions. For the initial reaction 5mL of ferrous sulfate heptahydrate and organic modifier (if any) solution was allowed to react with the H_2O_2 , and after 2 minutes of addition of 5 mL of pollutant, ferrous sulfate heptahydrate, and organic modifier (if any) was added. Similar to the HPLC analysis samples 300 μ L samples were periodically withdrawn; however, the samples were quenched with either 30 μ L methanol and 20 μ L of 1N H_2SO_4 for cation analysis or 10 μ L of 0.05M NaOH for anion analysis.

TNT was analyzed on an Agilent 1100 HPLC equipped with a reverse phase Alltech Econosphere C18 column (150 X 4.6 mm i.d., particle size 5 μ m) and a diode array absorbance detector that collected the full spectrum from 200-400 nm. The injection volume of the sample was 50 μ L and the wavelength used for quantitation was 254 nm. The solvent programming for the HPLC analysis was 30% acetonitrile: 70% water for 0-3 minutes, and then a linear ramp to 100% acetonitrile from 3-18 minutes.

Ionic products of Fenton treatment were analyzed by IC using a Dionex GP40 gradient pump coupled to an ED40 electrochemical detector. The samples were analyzed in both anion and cation modes. For anion mode, the IC was equipped with an Ion Pac AG14 guard column (4 mm X 50 mm) with an Ion Pac AS14 column (4 mm X 250 mm) and an ASRS300 (4-mm) anion suppressor. For cation mode, the IC was equipped with an Ion Pac CG12A guard column (4 mm X 50 mm) with an Ion Pac CS14A column (4 mm X 250 mm) and a CSRS300 (4-mm) cation

suppressor. Mobile phases for anion and cation modes were 2.1 mM Na₂CO₃/0.6 mM NaHCO₃ and 15 mN sulfuric acid, respectively.

Results and Discussion

Before Fenton degradation of TNT could be carried out with organic modifiers, a further understanding was needed for the Fenton degradation of TNT without modifiers. Extensive studies have been performed on the degradation of TNT via Fenton reagent; however most of these studies were conducted under acidic conditions (pH~3, which is not cost efficient or feasible for in situ applications). The goal for this portion of the research was to examine the reaction at near neutral pH. Fenton degradation of TNT was first carried out with different iron concentrations to better understand the role of the iron. Results are presented in Figure 2.1. As can be seen in this figure, the largest amount of TNT degraded in this system was 44%. In general, TNT degradation was minimal at times beyond one minute of reaction, and most of the degradation occurred in the first minute. This hindrance in the degradation is mainly attributed to precipitation of iron as iron (III) hydroxide. At lower iron concentrations (0.25-0.75 mM), the maximum TNT loss was 30%. The low percent of TNT removed is likely due to the lower rate of radical formation at lower iron concentrations. However in the mid-concentration region (0.75 – 1 mM) the degradation was increased to 44% of TNT removed after 2 minutes followed by a plateau region that is likely due to precipitation of iron at the neutral pH. When the iron concentration was increased to 5 or 10 mM, the degradation decreased in comparison to the mid-concentration ranges. This decrease is suspected to be due to the iron acting as a radical scavenger. Overall, Fenton degradation of TNT was observed to cease after about one minute of reaction, the extent of degradation increased with increasing [Fe²⁺], but then decreased at 5 mM Fe²⁺ or higher. Precipitation of iron is the most likely cause for the cessation of degradation after

one minute, and the higher iron concentrations likely had lower degradation due to scavenging by the excess iron in solution.

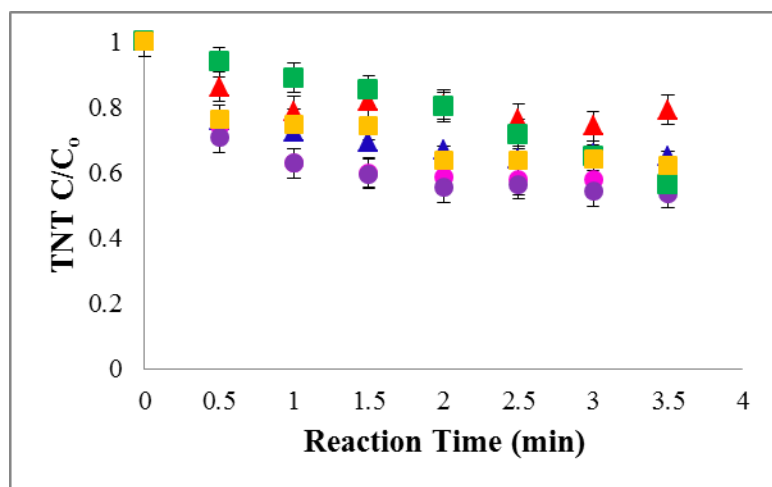


Figure 2.1. Normalized TNT concentration vs. reaction time for reactions without organic modifiers at neutral pH. 300 μ L of the initial 60 μ M TNT solution; 300 mM H_2O_2 added at 1 mL/hr; initial iron (II) sulfate concentrations: 0.25 (\blacktriangle), 0.5 (\blacktriangle), 0.75 (\bullet), 1 (\bullet), 5 (\blacksquare), and 10 mM (\blacksquare). Error bars represent one standard deviation for triplicate experiments. Representative error bars are present.

Fenton degradation of TNT was studied in the presence of β -cyclodextrin (β -CD) and carboxymethyl- β -cyclodextrin (CM- β -CD). These studies were carried out at different concentrations of the CD and Fe^{2+} . In comparison with reactions without CD, the reactions with CD exhibited more extensive degradation of TNT under many conditions but also showed inhibited degradation under certain conditions. Results are presented in Figure 2.2. In the presence of β -CD at low initial concentrations of Fe^{2+} (0.25 and 0.5 mM), degradation of TNT was totally inhibited. At 0.75 mM initial Fe^{2+} , the TNT degradation was slightly decreased compared to experiments with no CD. As the iron concentration was increased further, TNT degradation was enhanced substantially compared to experiments with no CD. For initial $[\text{Fe}^{2+}]$ of 5 mM, TNT was completely degraded within 3 minutes. Furthermore, the degradation under these conditions did not stop after 1 minute of reaction as it did in the absence of CD. Further increasing the initial Fe^{2+} concentration to 10 mM resulted in slower degradation compared to 5

mM Fe^{2+} , but the degradation was still substantially greater than for experiments with no CD. The observed enhancements in TNT degradation in the presence of β -CD can be caused by two different mechanisms. The first mechanism involves binary (Fe-CD or CD-TNT) and ternary complexes (Fe-CD-TNT) that are formed in solution. Formation of Fe-CD complexes would enhance iron solubility and increase the likelihood of formation of CD radicals since the iron catalyst would be in close proximity to the CD. Although CD-TNT complexes can enhance TNT solubility, these studies were conducted below the aqueous solubility of TNT, so enhanced TNT solubility should not have been a factor in these experiments. However, formation of CD-TNT complexes would enhance the likelihood for interaction between TNT and CD radicals formed via interaction with Fenton generated species simply due to the enhanced proximity of TNT to CD molecules. If ternary Fe-CD-TNT complexes form, the complex would allow the TNT be in proximity to the site where Fenton generated radicals are formed, thus enhancing the rate of TNT reaction with these radicals. CD inhibition of TNT degradation at low iron concentrations indicates that the cyclodextrin is acting as a scavenger which is not likely to interact with the TNT. Effective isolation of the CD radicals from the TNT results in prevention of TNT degradation. At higher iron concentrations, sufficient CD radicals are formed so that these radicals are likely to react with TNT, switching the CD from a scavenger to a propagator of the radical chain. This process represents the second possible mechanism in which the CD reacts with hydroxyl radical to form secondary radicals through hydrogen abstraction from the cyclodextrin. Subsequent reaction of the cyclodextrin radical with TNT can result in degradation of the TNT, most likely via a reductive pathway. Previous research discovered that in the presence of CDs, 4-amino-2,4-dinitrotoulene was formed, which indicated a reductive pathway.¹⁵⁴ In addition, research has revealed hydrogen abstraction from CD by the hydroxyl

radical occurs specifically at the C4, C5, and C6 locations on the CD ring.¹⁵⁵ These abstraction sites are located inside the CD cavity, which suggests that binary CD/TNT complexes should be important in this reductive pathway. Since the hydrogen abstraction is favorable for the inner cavity of the CD, the CD-TNT complex would bring the TNT in closer proximity to the radical site, thus yielding a higher efficiency for the reaction with TNT. At higher concentrations of iron (10 mM), the degradation of TNT was inhibited compared to degradation at 5 mM iron. This phenomenon is likely due to iron acting as a radical scavenger ($\text{Fe}^{2+} + \text{HO}^\cdot \rightarrow \text{Fe}^{3+} + \text{OH}^-$ or $\text{Fe}^{2+} + \text{CD}^\cdot \rightarrow \text{Fe}^{3+} + \text{CD}^-$).

Results for Fenton degradation of TNT with CM- β -CD present are shown in Figure 2.2b. These results are similar to those for β -CD, although the extent of TNT degradation is slightly smaller when CM- β -CD was used. Initial iron loadings of 5 and 10 mM showed enhanced TNT degradation compared to experiments with no CD. Experiments with 5 mM iron showed the most TNT degradation and showed continued degradation for the entire 3.5 minute treatment. The slightly decreased enhancement of TNT degradation caused by CM- β -CD compared to β -CD could be due to lower reactivity with Fenton reagents caused by the carboxymethyl substitution or could be due to different binding with Fe^{2+} or TNT. At lower iron concentrations (0.25-0.75 mM) the degradation of TNT was completely inhibited. This observation is thought to be due to: 1) at the lower concentration of iron, added cyclodextrin acts as an effective radical scavenger but secondary radical concentrations are too low to be important and 2) binary CD-TNT and/or Fe-CD complexes isolate the TNT away from the initial Fenton radical formation site.

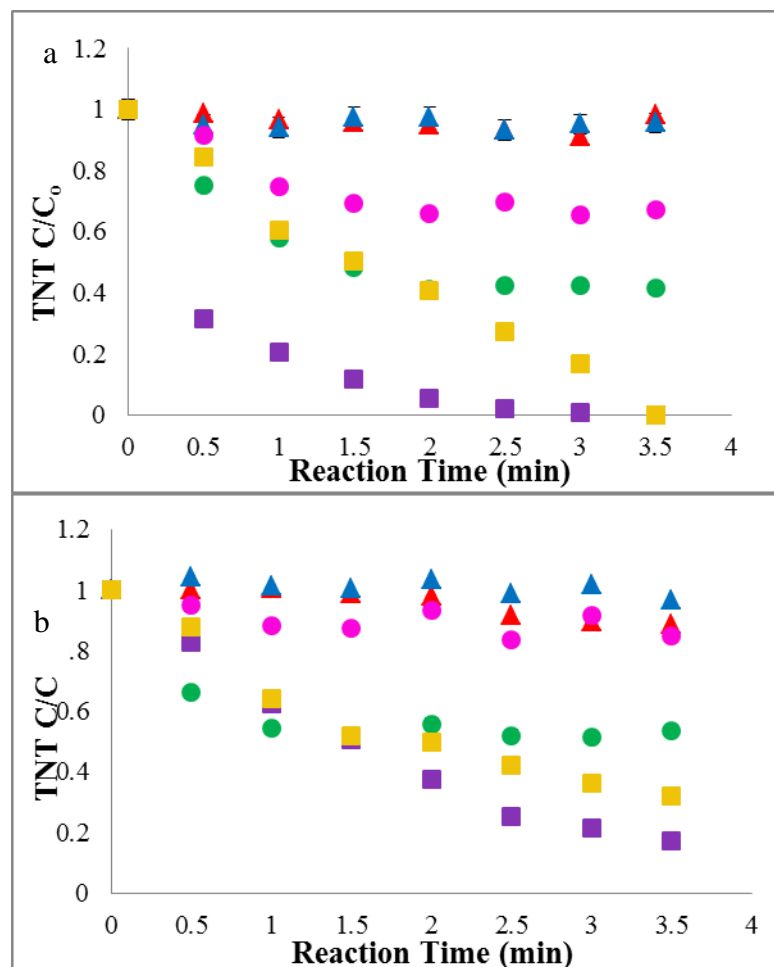


Figure 2.2. The normalized TNT concentration vs. reaction time at near neutral pH of the Fenton degradation with (a) 1 mM β -cyclodextrin and (b) 1 mM carboxymethyl- β -cyclodextrin. 300 μ L of the initial 60 μ M TNT solution; 300 mM H_2O_2 added at a rate of 1 mL/hr; initial iron (II) sulfate concentrations: 0.25 (\blacktriangle), 0.5 (\blacktriangle), 0.75 (\bullet), 1 (\bullet), 5 (\blacksquare), and 10 mM (\blacksquare). Representative error bars are present.

In order to investigate the effect of CD concentration, we repeated TNT degradation experiments at 5 mM initial Fe^{2+} with varying concentrations of β -CD or CM- β -CD. These results are presented in Figure 2.3. For β -CD the fastest TNT degradation occurred at 1 mM β -CD. Further increases in of β -CD concentration actually resulted in less degradation as the β -CD concentration increased. This result can be explained by a competition between two reaction pathways: 1) direct Fenton degradation TNT and 2) indirect reaction of TNT with a CD radical intermediate. As CD concentration increased, the first pathway was increasingly inhibited by

more prevalent CD scavenging. At the same time, the second pathway was enhanced by increased concentration of the CD radicals. However, further increases in β -CD may have caused substantial inhibition of the direct Fenton pathway without an equivalent replacement by the CD radical pathway. For CM- β -CD, the extent of TNT degradation increased with increasing CD concentration, although the degradation rate was similar at 2 and 5 mM CM- β -CD. The different results for CM- β -CD compared to β -CD are consistent with CM- β -CD being a poorer scavenger and less likely to produce secondary radicals. When the CD was in high excess in relation to the TNT concentration, then few CD molecules had a TNT molecule bound inside the cavity. Statistically, the likelihood of a CD radical reacting with TNT becomes unfavorable under these conditions. Previous studies by Yardin and Chiron investigated association complexes constants for β -cyclodextrins.¹³³ It was reported in their studies that with 5 mM cyclodextrin and 0.88 mM TNT 63% of the TNT formed a complex with methylated- β -cyclodextrin and 45% bound to hydroxypropyl- β -cyclodextrin. The decrease in the association constant for the hydroxypropyl- β -cyclodextrin was attributed to the steric hindrance of the hydroxypropyl group with the methyl group of the TNT. Similar steric hindrance could attribute for the decrease in the Fenton degradation of TNT in the presence of CM- β -CD in comparison to β -CD.

Lindsey *et al.* examined Fenton degradation of polychlorinated biphenyls (PCB) with and without cyclodextrins present.¹⁴⁷ For these studies it was observed that the rate constants for reactions with cyclodextrins present were double in comparison to reactions without cyclodextrin present. These observations contradict theoretical values that predict the cyclodextrin would decrease the degradation rate of the PCB degradation by 1600 fold due to the higher pseudo first order rate constant of the cyclodextrin's with the hydroxyl radical then that of the PCB and the

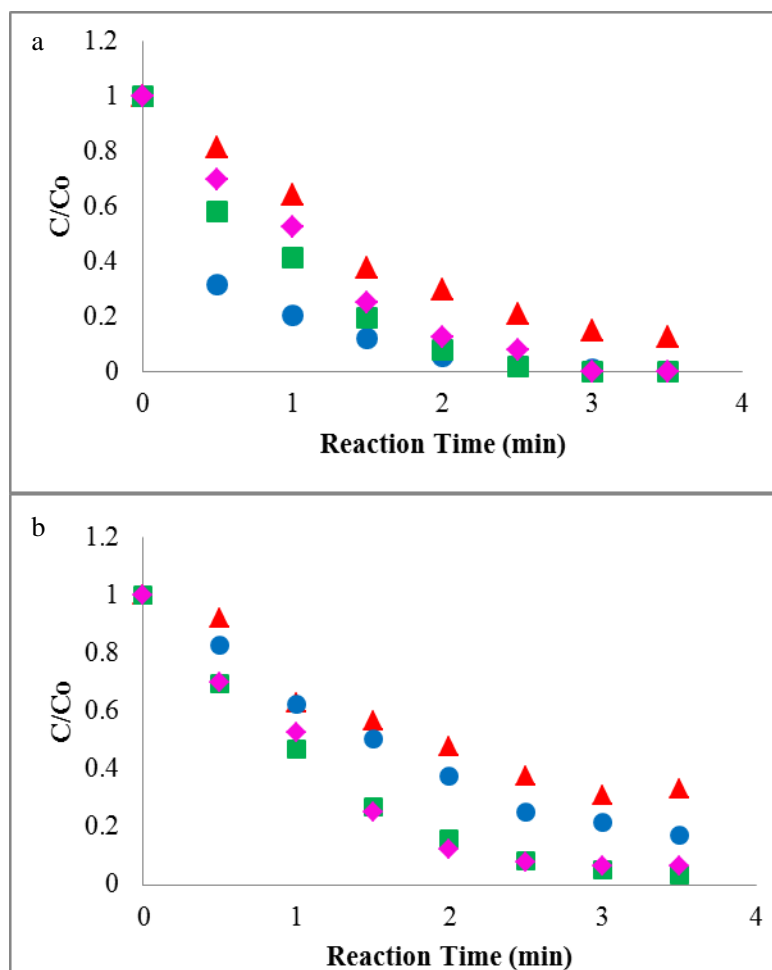


Figure 2.3. The normalized TNT concentration vs. reaction time at neutral pH of the Fenton degradation with (a) cyclodextrin and (b) carboxymethyl- β -cyclodextrin. 300 μ L of the initial 60 μ M TNT solution; 300 mM H_2O_2 added at a rate of 1 mL/hr; initial iron (II) sulfate concentration 5 mM; CD concentrations: 0.5 (\blacktriangle), 1 (\bullet), 2 (\blacksquare), and 5 mM (\blacklozenge). Representative error bars are present.

hydroxyl radical. The higher hydroxyl radical scavenging ability of the cyclodextrin with the increase in the rate constant further suggests that the increase in the degradation of the PCB with cyclodextrin present is due to the formation of a ternary complex. Absorbance studies by Lindsey *et al.* indicated that a binary complex was formed between the iron and cyclodextrin. Additionally they calculated the binary binding constant to be 120 ± 10 . Zheng and Tarr conducted studies on the ternary complexes formed between iron, cyclodextrin, and 2-naphthol.^{129, 130} Their studies found that binding between 2-naphthanol and carboxymethyl- β -

cyclodextrin was in a 1:1 ratio. Furthermore, fluorescence quenching experiment suggested that a binary complex was formed between the iron and the carboxymethyl- β -cyclodextrin. NMR studies of solutions containing pollutant, iron, and carboxymethyl- β -cyclodextrin further suggested a ternary complex was formed between the 3 species present in the solution.

To better understand the mechanism for the Fenton degradation of TNT, studies were carried out in the presence of hydroxyl radical scavengers. In contrast to the results from Lindsey *et al.* for naphthalene, the degradation of TNT with diethyl ether present was significantly enhanced, as shown in Figure 2.4. Low concentrations of iron (0.25, 0.5, 0.75 mM) resulted in complete inhibition of TNT degradation, but 5 mM of iron with diethyl ether showed an enhancement similar to that observed for CM- β -CD. Since diethyl ether cannot form a complex with TNT and is unlikely to bind strongly to iron in aqueous solution, these effects are likely due to scavenging effects as discussed above. Scavenging by the ether at low iron concentrations prevents direct reaction of hydroxyl radical (or other Fenton derived radicals) with dissolved TNT. Secondary radicals formed from the ether are present at too low of a concentration to have appreciable reaction rates with TNT. However, at higher iron concentrations, sufficient secondary radicals are formed to overcome the loss of hydroxyl or other Fenton generated radicals.

To find a low cost, environmental friendly organic modifier, the Fenton degradation of TNT was studied in the presence of additional organic modifiers: polyethylene glycol (MW = 200, 400, 600), diethylene glycol, dipropyl ether, ethanol, ethyl acetate, and methanol. Results from degradation studies with these modifiers are presented in Figure 2.5. Methanol exhibited no effect or a slight inhibition. Ethanol resulted in a modest increase in extent of TNT degradation but was not as effective as other modifiers. The polyethylene glycols showed the

fastest TNT degradation rates, which were comparable to those observed for the β -CD. This correlation can be related to two possibilities: 1) complexation of the TNT and/or the Fe^{2+} with the ether groups on the organic modifiers, and 2) the increase in the number of sites that are available for hydrogen abstraction.

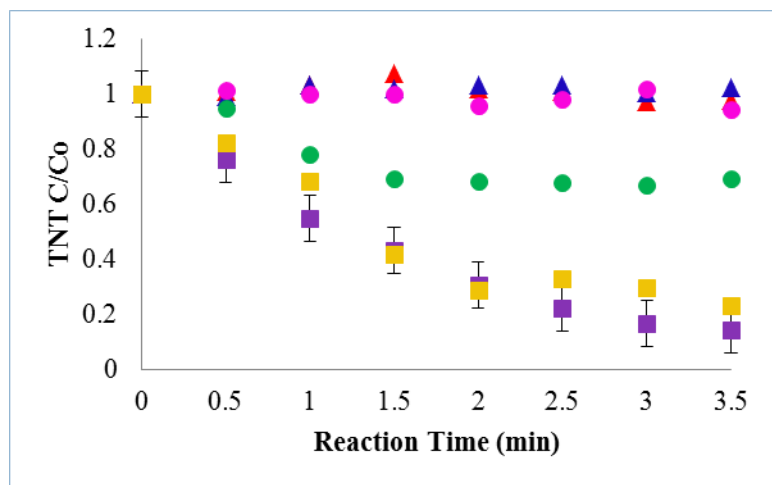


Figure 2.4. The normalized TNT concentration vs. reaction time at neutral pH of the Fenton degradation with 1 mM ether. 300 μ L of the initial 60 μ M TNT solution, 300 mM H_2O_2 added at a rate of 1 mL/hr, initial iron (II) sulfate concentrations: : 0.25 (\blacktriangle), 0.5 (\blacktriangle), 0.75 (\bullet), 1 (\bullet), and 5 mM (\blacksquare). Without ether: 5 mM iron (\bullet). Representative error bars are present.

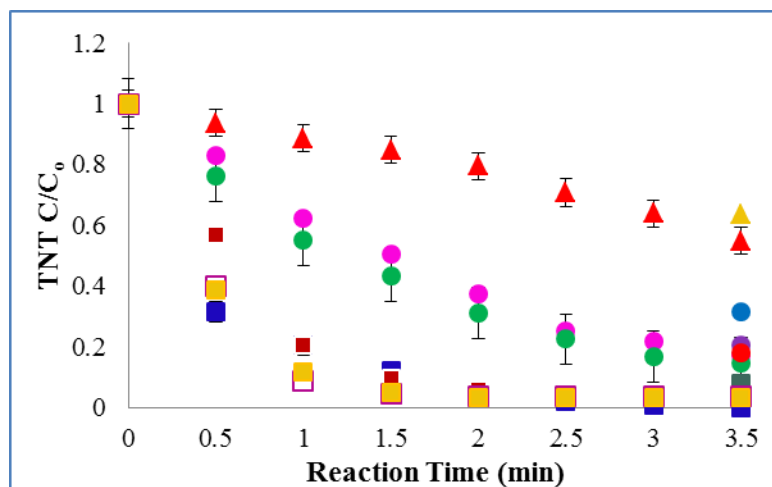


Figure 2.5. The normalized TNT concentration vs. reaction time at neutral pH of the Fenton degradation with 1 mM organic modifiers. 300 μ L of the initial 60 μ M TNT solution ; 300 mM H_2O_2 added at a rate of 1 mL/hr; initial iron (II) sulfate concentration 5 mM; organic modifiers: No modifier (\blacktriangle), β -CD (\blacksquare), carboxymethyl- β -CD (\bullet), diethyl ether (\bullet), propyl alcohol (\bullet), methanol (\blacktriangle), diethylene glycol (\bullet), ethyl acetate (\blacksquare), ethanol (\bullet), polyethylene glycol (MW 200) (\blacksquare), polyethylene glycol (MW 400) (\blacksquare), polyethylene glycol (MW 600) (\blacksquare). Representative error bars are present.

The degradation of TNT in the presence of polyethylene glycol (PEG 400, MW 400) was further examined at different concentrations of iron as shown in Figure 2.6. Similar degradation patterns were exhibited for the PEG 400 as for the CDs. At lower iron concentrations (0.25-0.5 mM) the degradation of TNT was inhibited, and at 1-5 mM initial Fe^{2+} the TNT degradation was enhanced. This enhancement in the degradation is likely due to the formation of PEG radicals similar to the mechanism suggested for the CDs. At low iron concentrations, initial Fenton radicals are scavenged by the organic modifier, but too few secondary radicals are formed to effectively degrade the TNT. At higher iron concentrations, enough secondary radicals are formed to cause efficient TNT degradation.

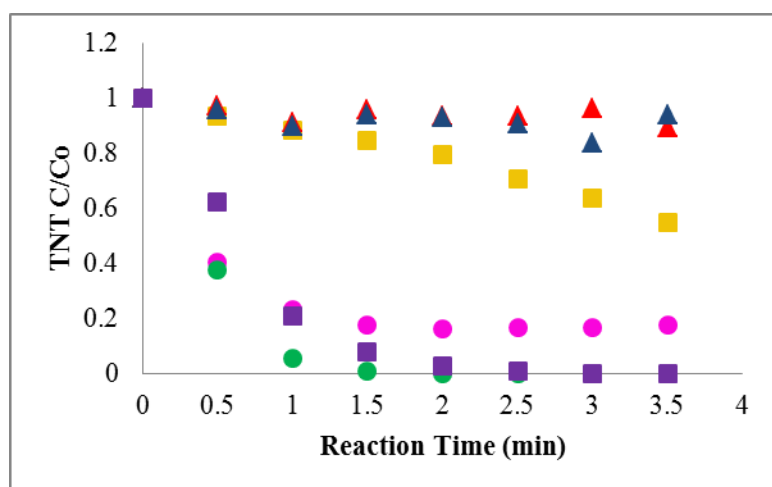


Figure 2.6. The normalized TNT concentration vs. reaction time at neutral pH of the Fenton degradation with 1 mM PEG 400. 300 μL of the initial 60 μM TNT solution; 300 mM H_2O_2 added at a rate of 1 mL/hr; initial iron (II) sulfate concentrations: .25 (▲), 0.5 (▲), 0.75 (●); 1 (●), and 5 mM (■). Without PEG 400: 5 mM iron (■). Representative error bars are present.

Fenton degradation of TNT exhibited pseudo first order kinetics, Figure 2.7. Good linearity (>0.98) was observed in the pseudo first order graphs for most samples; however a few samples slightly deviated from acceptable linearity. For these kinetic reactions a semi-wave like pattern is observed. This wave like pattern is thought to be due to the cycling of the Fe^{3+} to Fe^{2+} and vice versa. Pseudo first order rate constants for TNT degradation were calculated with and without organic modifiers. These results are presented in Table 2.1. The enhancement of TNT

degradation in the presence of organic modifiers followed the trend: PEG 600 ~ PEG 400 > β -CD ~ PEG 200 > CM- β -CD. The greatest enhancement over the aqueous only Fenton reaction (14 and 13 fold increase) was observed for the PEG 400 and PEG 600, respectively; with β -CD and PEG 200 enhancements closely following (9 and 8 fold, respectively). Of the modifiers studied, the smallest enhancement (~4 fold increase) was observed for CM- β -CD.

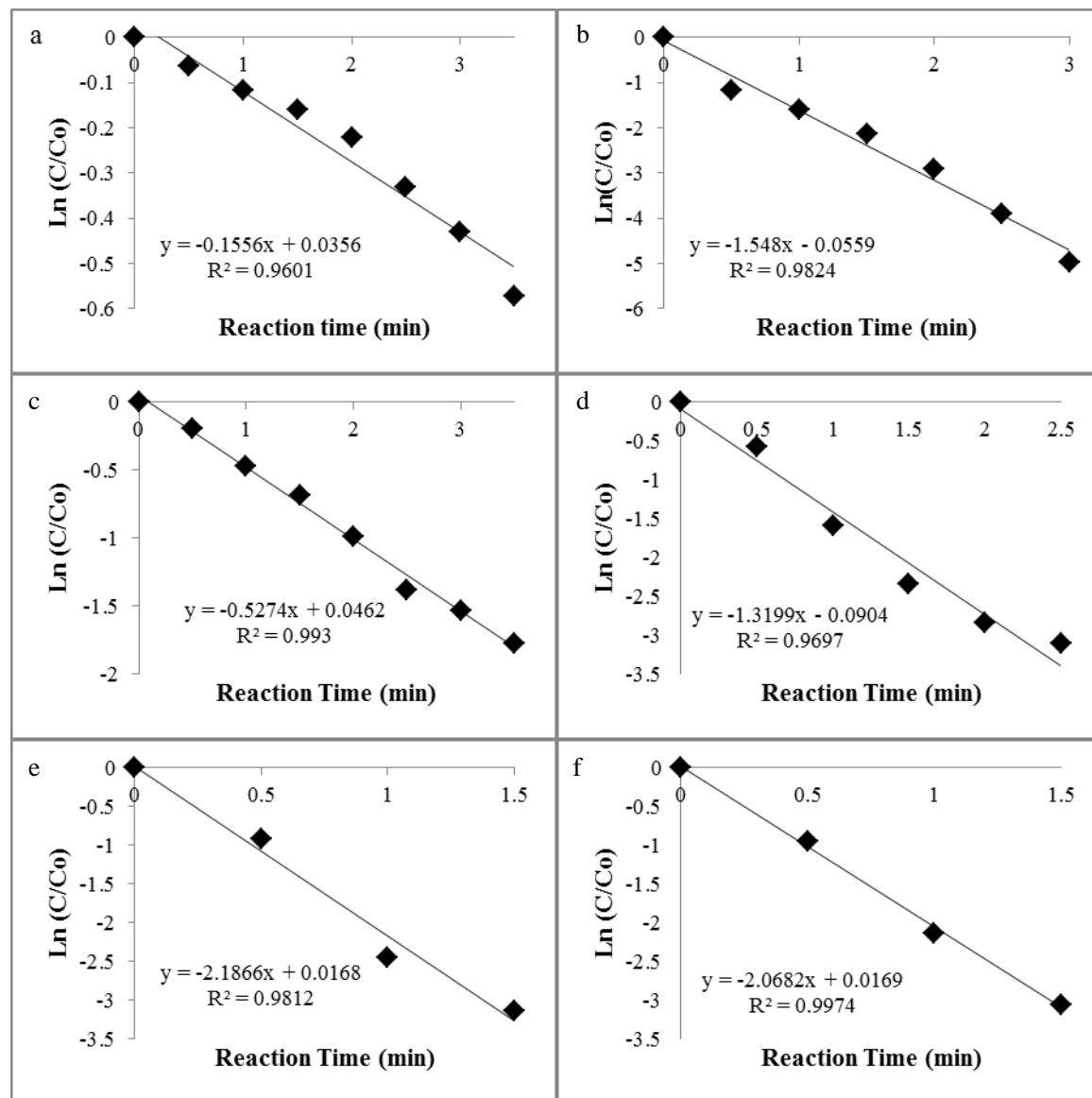


Figure 2.7. Plots of $\ln(C/C_0)$ vs. reaction time for TNT Fenton degradation for (a) water only and with 1 mM: (b) β -CD, (c) cm- β -CD, (d) PEG 200, (e) PEG 400, and (f) PEG 600.

Table 2.1. Pseudo first order rate constants for the Fenton degradation of TNT in the presence of cyclodextrins and polyethylene glycol. k_o' is the pseudo first order rate constant in the absence of any modifiers. 300 μ L of the initial 60 μ M TNT solution; 300 mM H_2O_2 added at a rate of 1 mL/hr; initial 5 mM iron (II) sulfate, 1 mM organic modifier

	Measured k' (min^{-1})	Enhancement over pure water (k'/k_o')
Pure Water	0.16 ± 0.03^a	--
β CD	1.5 ± 0.2^a	9 ± 2
CM β CD	0.52 ± 0.02^a	3.3 ± 0.6
PEG (MW 200)	1.3 ± 0.1^a	8 ± 2
PEG (MW 400)	2.2 ± 0.2^a	14 ± 3
PEG (MW 600)	2.1 ± 0.2^a	13 ± 3

^astandard error

To better understand the mechanism for the enhancement of TNT degradation, the Fenton degradation of nitrotoluene, 2,4-dinitrotoluene, and 2,6-dinitrotoluene were studied. Pseudo first order degradation rate constants are presented in Table 2.2. Based on these rate constants it is evident that when PEG 400 is present in the system the rate constants for 2-nitrotoluene degradation decrease in comparison to the reactions without PEG 400 present. In fact, an approximate 5-fold decrease was observed in the rate constant for 2-NT when PEG 400 was present. 2-Nitrotoluene is known to be more prone to undergo oxidative reactions than reductive reaction. The decrease in 2-NT degradation when the PEG is added indicates that the oxidative reaction is impeded while the reductive pathway is not prevalent enough to overcome the loss of the oxidative pathway. Since 2-NT is not likely to undergo reduction, it is clear that the PEG is acting as a scavenger that removes radicals that are otherwise capable of oxidizing 2-NT. For 2,4-DNT, the rates of degradation were essentially the same with and without PEG. Since 2,4-DNT is more likely to undergo a reductive process, the secondary radicals produced by PEG scavenging were sufficient to offset the decrease in the oxidative pathway. For 2,6-DNT, a similar effect was observed, although a slight decrease in degradation rate occurred. As previously discussed, 2,4,6-TNT showed a dramatic enhancement in degradation in the presence

of PEG. Since TNT is the most easily reduced species in this series of nitrotoluenes, it is sensible that PEG radicals produced from scavenging hydroxyl radical (or other Fenton produced radicals) would enhance the observed TNT degradation rate more than the decrease in degradation rate due to the loss of the oxidative pathway.

Table 2.2. Pseudo first order rate constants for the Fenton degradation of nitrotoluenes with and without PEG 400 present. 300 μ L of the initial 60 μ M TNT solution; 300 mM H₂O₂ added at a rate of 1 mL/hr; initial 5 mM iron (II) sulfate, 1 mM PEG 400

	Measured k' (min ⁻¹)	
	Without PEG 400	With PEG 400
2-Nitrotoluene	1.28 \pm 0.07 ^a	0.24 \pm 0.01
2,4-Dinitrotoluene	0.26 \pm 0.01 ^a	0.22 \pm 0.03
2,6-Dinitrotoluene	0.47 \pm 0.03 ^a	0.24 \pm 0.06
2,4,6-Trinitrotoluene	0.13 \pm 0.02 ^a	2.2 \pm 0.2 ^a

^astandard error

In order to confirm the switch from oxidative to reductive pathways, we investigated ionic degradation products. Previous studies have found that nitrate and nitrite are produced in the oxidative degradation of TNT.⁸⁹ In addition, studies found that ammonium is produced during reductive degradation.¹⁵⁴ To further investigate the prevalence of the oxidative and reductive pathways, nitrate and ammonium production were monitored via IC. Table 2.3 reports the observed nitrate and ammonium formation during degradation of TNT with and without added PEG. Nitrate production was observed in both reactions with and without PEG 400 present. However, reactions without PEG present produced 77% less nitrate than reactions with PEG present. These values were found to be statistically different using a paired t-test. Since nitrate is a product of oxidative degradation of TNT, these results confirm that the oxidative pathway is inhibited by addition of PEG. Nitrite production could not be quantified in these systems due to interference from formate produced during the reaction. In contrast to the nitrate results, ammonium production was undetectable in TNT degradation reactions without PEG present; however, ammonium production was observed in all TNT degradation reactions

containing PEG. The formation of ammonium is indicative of a reductive pathway. The production of ammonium and the simultaneous decrease in nitrate production in the presence of PEG provides strong evidence of a shift away from an oxidative pathway in favor of a reductive pathway. The data presented in Tables 2.2 and 2.3 are all consistent with this conclusion. It is important, however, to emphasize that TNT is an easily reduced species, so the behavior observed in this study cannot be extrapolated to all pollutants. For example, 2-NT showed only a decrease in degradation rate in the presence of PEG since 2-NT is not readily susceptible to degradation via the reductive pathway observed for TNT. Furthermore, previous studies with naphthalene did not show the reactive pathway when diethyl ether was added, suggesting that naphthalene did not readily undergo reductive degradation in those studies.¹⁴⁷ Pollutants that are not readily reduced will not show the behavior observed here for TNT. Consequently, it is important to understand both the oxidative and reductive mechanisms of individual pollutants in order to determine the expected impact of organic modifiers. The role of cyclodextrins is slightly more complicated since they can act as scavengers, can produce secondary radicals that can act as reducing agents, and can change the solubility of both iron and pollutants through formation of binary or ternary complexes.

Table 2.3. Concentration of nitrate and ammonia produced from 300 μ L of 100 μ M TNT solution after 3.5 minutes of Fenton degradation. 300 mM H_2O_2 added at a rate of 1 mL/hr; initial iron (II) sulfate concentration 5 mM; 1 mM PEG 400

	Concentration (ppm)	
	Without PEG 400	With PEG 400
NO_3^-	1.76 ± 0.62	0.40 ± 0.33
NH_4^+	n.d.	0.91 ± 0.49

n.d. – not detected

Conclusion

Fenton degradation of TNT was examined at near neutral with and without organic modifiers. Without modifiers a maximum of 44% of the TNT was removed. After 1.5 minutes, degradation ceased in the water only systems due to the precipitation of iron at the near neutral pHs. Addition of CDs to the system increased the rate of degradation and 100% of the TNT was removed after 3 minutes with β -CD. The increase in the degradation with CD present is attributed to 2 different mechanisms: (1) formation of binary and ternary complexes between the CD, iron, and TNT and (2) formation of secondary radicals that are more efficient at attacking the TNT than hydroxyl radical. Increase in degradation was also observed with the addition of PEG, with 100% of the TNT removed after 1.5 minutes. Mechanistic studies of the Fenton degradation concluded that TNT undergoes both oxidative and reductive pathways with PEG 400 preset; however without PEG 400 only oxidative pathway is observed.

CHAPTER 3

PETROLEUM

On the night of April 20th, 2010 an explosion occurred on the Deepwater Horizon (DWH) oil rig. That night 11 men lost their lives and another 17 men were injured. The Coast Guard fought to contain the fire and save the 700,000 gallons of diesel from contaminating the Gulf of Mexico. They were defeated in their fight when the Deepwater Horizon sank on April 22, 2010. On April 25, 2010 British Petroleum (BP) made the first reports of oil leakage from the Macondo well. Crude oil continued to surge into the Gulf of Mexico until July 15, 2010 when BP capped off the well head. Over the 86 days of the oil spill it has been estimated that 4.9 million barrels of oil was released into the gulf, making the Deepwater Horizon oil spill the largest in United States history and the second largest oil spill in the world.¹⁵⁶

History of Oil

The first record of offshore drilling was in 1896 by Henry Williams in Summerland, California.¹⁵⁷ In his previous drilling he noted that the quality of the wells increased the closer that he was to the shore line. To get the best well, Williams decided to drill an oil well off a 300 foot pier. It wasn't until 15 years later that the first stand-alone well was drilled in Caddo Lake in Louisiana. Years after the first stand-alone platforms, Brown and Root drilled the first free standing platform 1 mile off Louisiana's coast in the Gulf of Mexico. Subsequent discoveries of floating platforms led to drilling the Kermac 16 well 10 miles offshore in 20 feet of water in 1947. As demand for oil increased, so did the platform technologies. Invention of a jack up rig pioneered well drilling in deeper waters. At the time jack up rigs were the only oil platforms that could drill wells in up to 500 feet of water. In 1961, Blue Water Drilling Company and Shell Oil

teamed up to build a semi-submersible oil rig which allowed for deep and ultra-deepwater drilling in up to 10,000 feet of water. The semi-submersible rigs are currently the most commonly used oil rig to date, including the Deepwater Horizon rig.

The DWH oil spill was a catastrophic event that devastated the Gulf of Mexico and the surrounding coastlines. Figure 3.1 represents the path and areas affected by the DWH oil spill. The United States government has estimated the flow rate on April 22, 2010 to be 62,200 barrels of oil per day and on July 14, 2010 to be 52,700 barrels of oil per day. Based on these averages it has been estimated that 4,928,100 barrels of oil were released. Only one oil spill to date has been more disastrous, the Gulf War in 1991. During the Gulf war, Iraqi forces opened the valves of oil wells and pipelines in order to slow the American troops. It was estimated that this intentional oil release distributed 5.7-8 million barrels of oil into the Persian Gulf.¹⁵⁸ Unlike the DWH oil spill, serious recovery efforts were not employed until after the Gulf War ended over a month later. The Intergovernmental Oceanographic Commission at UNESCO has reported that half of the oil from the Gulf War was evaporated, an eighth of the oil recovered, and a fourth of the oil was washed up inland mainly on the shores of Saudi Arabia.

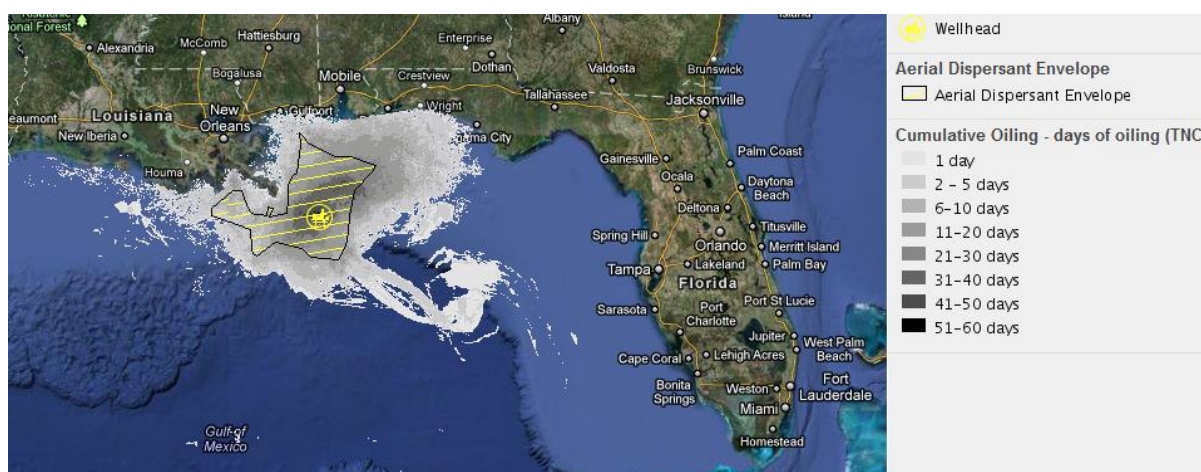


Figure 3.1. Areas impacted by the Deepwater Horizon oil spill.¹⁵⁹

While there have been numerous oil spills to date, the Deepwater Horizon oil spill was like no other. In 1989, the Exxon Valdez oil spill devastated the Prince William Sound in Alaska. Until the DWH oil spill, the Exxon Valdez was considered to be the worst oil spill in U.S. history. Unlike the DWH oil spill, the Exxon Valdez was a small oil spill (257,000 barrels).¹⁶⁰ In addition, the Exxon Valdez spill was from a tanker, therefore the oil did not spend an extensive amount of time traveling through the water column to reach the surface. The diminutive of time in the water column decreases the extent of dissolution of the oil into the aqueous phase. The limited dissolution of the oil along with the cold temperatures of Alaska allow for easier clean-up of the oil. Furthermore, biodegradation was the key for clean-up during the Exxon Valdez spill; however biodegradation of the DWH oil was limited due to the lack of nutrients in the Gulf of Mexico.

In 1979 the Ixtoc I well released an estimated 3.33 million barrels of oil into the Gulf of Mexico over the course of 10 months. The Ixtoc spill happened in the same tropical environment as the DWH oil spill, which would entail that the same chemical transformation would occur for both oils. However, unlike the DWH oil spill the Ixtoc spill was a shallow well (50 m versus 1500 m) which allowed for divers at the well head. In addition, the oil from the DWH oil spill passed through several stratifications of the gulf which allowed for more oil to be lost through dissolutions and emulsification and for the formation of deep-water plumes.

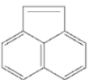
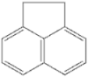
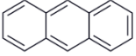
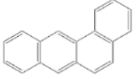
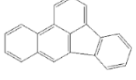
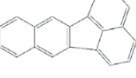
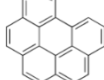
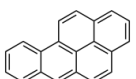
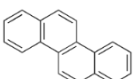
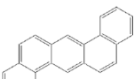
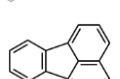
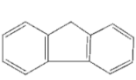
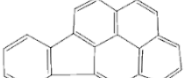
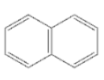
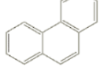

Crude Oil Components

Crude oil is a complex mixture of compounds that contain hydrocarbons, metals and polar compounds. Hydrocarbon fractions of crude oil contain n-paraffins, isoparaffins, olefins, cycloparaffins, and aromatics. N-paraffins are straight chain saturated alkanes. Isoparaffins consist of branched alkanes. Olefins are unsaturated hydrocarbons also known as alkenes.

Cycloparaffins are cycloalkanes and are commonly called naphthenes. The n-paraffins, isoparaffins and the cycloparaffins account for the largest portion of the oil. Aromatics consist of monocyclic (benzene), dicyclic (naphthalene), or polycyclic aromatic hydrocarbons (PAHs), which are multi-ring aromatic molecules. PAHs are known to be toxic and mutagenic, and due to these concerns the EPA has listed 16 PAHs on its National Priority List, Table 3.1.

In addition to hydrocarbons, metals and polar compounds are commonly found in crude oil. Common metals found in crude oil include iron, arsenic, cadmium, copper, chromium, nickel, lead, and vanadium.¹⁶¹ In comparison to other crude oil components, metals only make up a minute fraction (<0.1%). Polar compounds that are present in crude oils include an array of nitrogen, oxygen, and sulfur species. Common polar species that are found in crude oil are resins and asphaltenes. Both of the species are normally present at low concentrations, and the chemical composition varies between different oils. Resins are smaller polar compound such as thiols. Asphaltenes are larger polar compounds and have been previously defined as a component in crude oil that is insoluble in pentane or heptane; however, they can readily dissolve in toluene.

Table 3.1. Structures and maximum water concentration for PAHs established by the EPA

Pollutant	Structure	Maximum Water Concentration (ppm)
Acenaphthylene		0.059
Acenaphthene		0.059
Anthracene		0.059
Benz[a]anthracene		0.059
Benzo[b]fluoranthene		0.11
Benzo[k]fluoranthene		0.11
Benzo[g,h,i]perylene		0.0055
Benzo[a]pyrene		0.061
Chrysene		0.059
Dibenz[a,h]anthracene		0.055
Fluoranthene		0.068
Fluorene		0.059
Indeno[1,2,3-c,d]pyrene		0.0055
Naphthalene		0.059
Phenathrene		0.059
Pyrene		0.067

The combinations of the compounds in crude oil are dependent on the geological formation of the area where oil is found.¹⁶² Based on the composition, oil is classified as either light or heavy crude oil. Properties of these two types of oil are dependent on the oil's composition and are listed in Table 3.2. Light crude oils are produced in great abundance in Louisiana and Western Canada. This oil consists mainly of paraffins, isoparaffins, cycloparaffins, and olefins with low concentrations of polar compounds, metals, and sulfur. Like light crude oil, heavy crude oil consist of mainly paraffins, isoparaffins, and cycloparaffins; however concentrations of olefins are much lower and the concentrations of polar compounds and sulfur are higher than that of light crude oil. Heavy oil is commonly found in Arabic countries and off the coast of Newfoundland and California. In addition to the light and heavy classification of oils, oil has also been classified by their sulfur content. Oils with low sulfur content are categorized as sweet oils, whereas high sulfur containing oils are called bitter oil.

Table 3.2. The physical properties of light and heavy crude oils¹⁶²

Property	Units	Light Crude	Heavy Crude
Viscosity	mPa•s at 15°C	5-50	50-50,000
Density	g/mL at 15°C	0.78-0.88	0.88-1.00
Water Solubility	ppm	10-50	5-30
API Gravity		30-50	10-30

The oil that was from the Macondo well was classified as Louisiana sweet crude (LSC) oil. Chemical analysis of the LSC oil determined that paraffins, isoparaffins, and naphthenes were the most abundant hydrocarbon components in the oil and the percent composition determined from PIANO (paraffin, isoparaffins, aromatic, naphthene, and olefin) analysis is listed in Table 3.3.¹⁶³ The American Petroleum Institute (API) gravity of the LSC oil at 15°C is 36.2, which classifies it as a light crude oil. The low sulfur content (0.26%) classifies the oil as sweet crude oil. Nitrogen content of the oil was measured to be 690 ppm. Quantification of the metal content has determined undetectable amounts of cobalt, barium, and vanadium. Iron and

nickel were present in the oil samples at 0.9 and 1.8 ppm, respectively. In addition to the other components of the oil, water was measured in the LSC oil at 1680 ppm.

Table 3.3. PIANO analysis of hydrocarbon composition of LSC oil from the Macondo Well¹⁶³

Compound Type	Weight % in oil
Paraffin	22.0
Isoparaffin	31.3
Aromatic	25.3
Naphthene	21.0
Olefin	0.4

Clean-Up

Advancement in oil spill clean-up technology has been almost stagnant since the Exxon Valdez and Ixtoc I oil spills. The DWH oil spill employed various physical and chemical methods to contain the oil.¹⁵⁶ One physical method that BP utilized was boom. It has been estimated that during the DWH oil spill, 13.5 million feet of boom was used, and of the boom used, 3.8 million feet was hard boom and 9.7 million feet of soft boom. Hard boom, also known as containment boom, is used to corral the oil or block the oil from shore lines. This type of boom is normally made of a vinyl coated polyester or nylon which is ultraviolet resistant. Soft boom, also known as sorbent boom, is used to absorb the oil. Soft boom has been called sausage boom due to its fishnet style casing that is stuffed with polypropylene, an absorbent material. In addition to boom, BP also employed boats to skim the oil from the surface of the Gulf of Mexico. Skimming of the oil from the surface used hard boom to collect the oil. The oil can then be recovered, or in some cases the collected oil was burned.

In addition to the physical methods for clean-up, chemical methods were employed. To reduce the presence of oil slicks on the surface of the Gulf, chemical dispersants were utilized. There are three basic different types of dispersants: water based, solvent based, and concentrates.¹⁶² Water based dispersants require longer time lengths for dispersion to occur and some sort of an external source of mixing for dispersion to occur. Solvent based dispersants are

commonly used for waxy and heavy oils. Solvent based dispersants can easily disperse the oils, however more dispersant is needed in comparison to the water based dispersants. Concentrates are dispersants with minimum diluents. Concentrates are commonly known as third generation or self-mixing dispersants because they require minimum energy to disperse oil films. With self-mixing dispersants the chemical surfactants is compatible with the bulk of the oil. When the oil phase comes into contact with the aqueous phase the surfactant has a strong driving force to diffuse out of the oil phase and into the aqueous phase. Upon diffusion into the aqueous phase the surfactant pulls some of the oil with it, thus producing small oil droplets.

Dispersants contain solvents and surfactants.¹⁶⁴ The surfactant is the main component in the dispersant that is responsible for the increasing the aqueous solubility of the oil. A surfactant is a compound that has both oil-compatible and water compatible groups. Surfactants form oil droplets by reducing the interfacial tension between the water and oil layers. There are three main types of surfactants: anionic, cationic, and nonionic. Anionic surfactants are the oldest type of surfactants. They are the most commonly used surfactants and account for roughly 50% of surfactant production. They consist of a long chain of fatty acids such as sodium oleate (soap), sodium lauryl sulfate (foaming agent), alkylbenzene sulfonates (detergents), and di-alkyl sulfosuccinate (wetting agents). A large portion of cationic surfactants corresponds to nitrogen compound (amines or quaternary ammonium salts) and a halogen type, such as cetyl trimethyl ammonium bromide. Nonionic surfactants are the second largest type of surfactant produced. Instead of containing an ionized compound, nonionic surfactants contain a hydrophilic group of a non-dissociating type, such as alcohol, phenol, ether, or ester.

There have been numerous reports of benefits for using dispersants. By increasing the aqueous solubility of the oil, dispersants lower the amount of oil on the surface of a body of

water which has a number of advantages. A major advantage of the absence of oil slicks is the decrease in the number of birds contaminated. Many birds feed on different marine species and in order to catch their feed they dive under the surface of the water. When surface oil is present on the water layer these birds become covered in oil and as a result cannot fly. In extreme contaminated cases oiling of birds has resulted in death. In addition to advantages with marine feeding birds, the absence of oil slicks reduces the fire hazard. By dispersing the oil into the water column the combustible components on the water surface are eliminated. In select studies the rate of biodegradation of chemically dispersed studies has increase.¹⁶⁵⁻¹⁶⁷ The increase in the biodegradation of the oil has been attributed to the increased solubility of the oil and smaller droplet size of oil present, thus increasing the oils surface area that comes into contact with the degrading microbes. In contrast, abundant studies have found chemically dispersed oil to inhibit the biodegradation of the oil.^{168, 169}

Previously there are two main ways to apply dispersants to the oil, via boats or aerially. Both application methods utilize spray nozzles to apply droplets of dispersant to the oil slick. Boats allow for a large load of dispersant on the boat itself; however application area is limited to the extension of the boom arms on the vessel. Additionally, boat applications can be very time consuming in comparison to aerial application. Aerial distribution of dispersants allows for fast application of dispersants to the oil slicks; however it is limited by the capacity of dispersant that can be transported on the plane. While planes do not have the high cargo capacities of the boats, they are much faster, thus allowing for multiple reloading in the time frame of one boat voyage. In addition to the aforementioned dispersant applications, during the DWH oil spill dispersants were applied at the well head. This is the first sub-surface application in the history of dispersants use. Wellhead application was approved by the Environmental Protection Agency

(EPA) to reduce and possibly eliminate oil slick on the surface of the Gulf of Mexico. In addition to the previous advantages listed, it was proposed that sub-surface dispersant application will reduce the number of volatile components, thus reducing many inhalation health related concerns. For this application to be successful, a jet was placed at the well head and the dispersant was to be applied directly in the flow of the oil, Figure 3.2.¹⁷⁰ However due to multiple variables in the operation of the well head, the jet was not always applying dispersant, nor was it always in the oil and gas flow stream, thus the oil was not fully dispersed before reaching the water's surface.

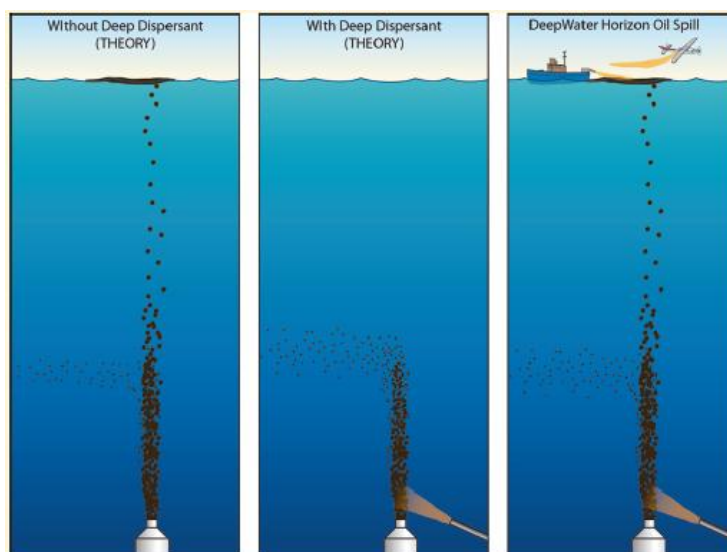


Figure 3.2. Sub-surface dispersant application theory. Reprinted with permission from Kujawinski, E. B.; Kido, S. M. C.; Valentine, D. L.; Boysen, A. K.; Longnecker, K.; Redmond, M. C., Fate of dispersants associated with the deepwater horizon oil spill. *Environ. Sci. Technol.* **2011**, *45*, 1298-1306. Copyright 2012 American Chemical Society.

The Environmental Protection Agency has approved 20 dispersants in the National Contingency Plan. Of the 20 previously approved dispersants, BP chose Corexit EC9500A and Corexit EC9527A due to their large availability. These dispersants are self-mixing, anionic dispersant containing dioctyl disodium sulfosuccinate (DOSS).¹⁷¹ In addition to the DOSS, arrays of sorbitan surfactants are present in the dispersants including Tween 85, Tween 80, and Span 80.¹⁷¹ Both dispersants contain propylene glycol as a solvent. Additionally, Corexit

EC9500A contains hydrotreated light petroleum distillates and Corexit EC9527A contains 2-butoxyethanol as added solvents. Suggested application rates for oil spills treated with Corexit EC9500A and Corexit EC9527A ranges from 50:1 to 10:1 oil to dispersant.^{172, 173}

Since oil's composition can vary with the source of the oil, the effectiveness of dispersants has found to be dependent on the oil source. Belore *et al.* studied the effectiveness of Corexit EC9500A and Corexit EC9527A with various oils.¹⁷⁴ In these studies it was observed that the oils with higher densities had a lower percentage of oil dispersed with the dispersants. Additionally, they observed in some oils that samples with Corexit EC9500A had a slightly lower overall percentage dispersed in the aqueous layer. Moles *et al.* studied the effectiveness of Corexit EC9500A and Corexit EC9527A on Alaska North Slope Crude oil at low temperatures and variable salinities.¹⁷⁵ In these studies dispersion of oil into the aqueous phase with both dispersants did not occur at temperatures below 10°C with low salinities (22 ppt); however when the salinity was increased to 32 ppt dispersion did occur. No dispersion was observed with either of the dispersants at 3°C. Trudel *et al.* studied the dispersant effectiveness with oils of different viscosities.¹⁷⁶ Oils with viscosities over 30,000 cP were not chemically dispersed and oils with viscosities of 2,500 to 18,690 cP were only partially dispersed with Corexit EC9500A. Additionally droplet size was found to be dependent on the viscosity of the oil. The EPA has reported dispersant effectiveness for Corexit EC9500A and Corexit EC9527A to be 54.7% and 63.4% effective on south Louisiana crude, respectively.¹⁷¹

The EPA has estimated that 1.85 million gallons of dispersants were used during the duration of the DWH oil spill.¹⁵⁶ In these estimation it was approximated that 0.77 million gallons of Corexit EC9500A were applied at the wellhead and a combined 1.07 million gallons of Corexit EC9500A and Corexit EC9527A were applied on the Gulf's surface. In the history of

oil spills never have dispersants been used to this extent. Before the DWH oil spill, the largest application of dispersant in United States history was the Exxon Valdez oil spill of 1989. In this spill it was estimated that 5,500 gallons of Corexit 9580 was used.¹⁷⁷

One aspect of concern with such large dispersant application is the potential toxicity of the dispersants to marine organisms. Hemmer *et al.* has studied the toxicity of dispersants since the DWH oil spill.¹⁷⁸ These studies examined the toxicity of eight dispersants, including Corexit EC9500A, with and without Louisiana sweet crude oil on two different marine species, mysid shrimp and inland silverside. Mysid shrimp lethal concentrations to kill 50 percent of the test species (LC₅₀) were in agreement with previously reported values from NCP for the Corexit EC9500A (42 verses 32.2); however LC₅₀ values for the inland silverside were over 5 times the NCP previously report value (130 verses 25.2). Toxicity tests conducted on Louisiana sweet crude indicated that the crude oil only samples were more toxic for both marine species than oil-dispersant samples. Additionally, Corexit EC9500A only samples were found to be practically or slightly toxic per NPC standards, but when mixed with Louisiana sweet crude the samples become moderately toxic.

Scarlett *et al.* studied the toxicity of 2 dispersants, including Corexit EC9527A, on different marine species: a sediment-dwelling amphipod, a mussel, an anemone and seagrass.¹⁷⁹ In these studies the anemone was found to be more susceptible to the dispersant with the lowest-observable-effect concentration (LOEC) of 20 ppm after 48 hours of exposure. The mussel on the other hand had the highest LOEC of 250 ppm for the 48 hour exposure. Irreversible damage of the respiratory system was observed, however, depending on the exposure time neurological damage was reversible. Judson *et al.* studied the toxicity of dispersant via endocrine activity.¹⁸⁰ As postulated, Corexit EC9500A did not show endocrine activity. Nonexistent endocrine

activity for Corexit EC9500A was due to the absence of nonylphenol ethoxylates, which can degraded to the highly toxic nonylphenol.

In addition to toxicity issues, the effect of underwater dispersant application is uncertain and of great concern. Fluorescence studies conducted after the DWH oil have identified chemically dispersed underwater plumes 900-1300 m from the surface.^{181, 182} Plume formation was also identified in DeSoto Canyon by researchers at the University of South Florida, which was later confirmed by the National Oceanic and Atmospheric Administration.¹⁸³ DeSoto Canyon is a nutrient rich area that is a vital area for commercial fish spawning; therefore, oiling in this region has a large commercial impact. Ramachandran *et al.* studied the effects of chemical dispersed oil on fish.¹⁸⁴ In this study, an increase in the uptake of PAH was observed for Corexit EC9500A dispersed samples. The EPA has reported that application of dispersant will not increase toxicity.¹⁸⁵ These finding are challenged by the scientific community due to limitations in the research.¹⁸⁶ In the EPA studies only Corexit EC9500A was tested and not Corexit EC9527A, which is known to be more toxic and bioaccumulates. Additionally, studies were only conducted on two marine species, which do not mimic the species diversity in the Gulf of Mexico especially in deep waters. Furthermore these studies were short term, thus long term effects (i.e. reproduction, mutation) on marine organisms are not known.

Fate and Degradation of Oil

Oil spilled in marine environments can undergo various processes, Figure 3.3. Several environmental factors determine the fate of the oil. After release of sub-surface oil the oil begins to travel through the water column. During its duration in the water column, the water soluble polar fractions of oil dissolve in the aqueous layer. In addition to dissolution, oil biodegradation can occur in the water column. Once oil has reached the water surface, the lighter more volatile

portions of the oil evaporate into the atmosphere. Oil slicks on the surface undergo atmospheric oxidation which is intensified by solar irradiation. As the oil sits on the surface of the water, water in oil emulsion (mousse) can form. Previous studies observed increases in the frequency of water in oil emulsions in the presence of oxidative degradation products.^{187, 188}

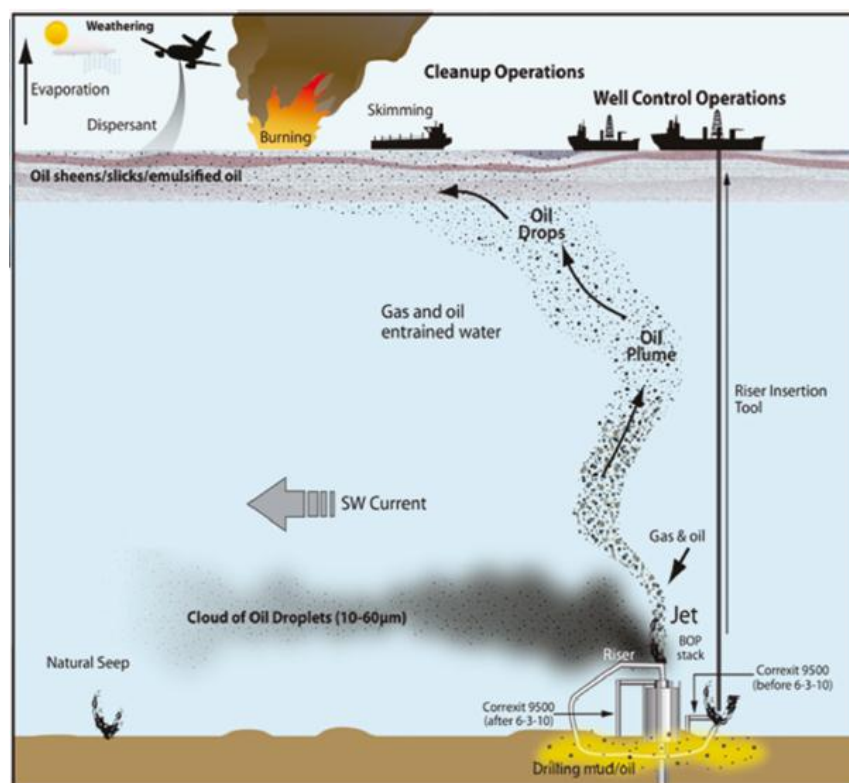


Figure 3.3. Schematic of the clean-up methods and weathering of the oil released from the Macondo well head. Reprinted adapted with permission from Atlas, R. M.; Hazen, T. C., *Oil Biodegradation and Bioremediation: A Tale of the Two Worst Spills in U.S. History*. *Environ. Sci. Technol.* **2011**, 45, 6709-6715. Copyright 2012 American Chemical Society.

Boehm *et al.* studied the weathering of n-alkanes and aromatics in crude oil released from the Ixtoc I oil spill.¹⁸⁹ In these experiments, evaporation and dissolution of lower molecular weight alkanes and aromatics was observed. Rates of evaporation were almost identical for alkanes and aromatics; however dissolution favors the lower molecular weight aromatics due to the increase in solubility of the aromatics. Additionally, biodegradation was virtually stagnant in the studies due to the low nutrient waters of the Gulf of Mexico. Payne *et al.* employed

modeling methods to study the weathering on Prudhoe Bay crude oil.¹⁹⁰ Simulations concluded that the uptake of water by the oil increased over weathering time. Additionally, the density and the viscosity of the oil increased with weathering time. Increases in the density and viscosity were expected due to the loss of the lighter fractions by evaporation and dissolution. Interfacial tension between the oil and air increased over time; however, the interfacial tension between the water and oil layer decreased over time. Various degradation processes produce polar oxidation products that are more soluble in water thus the interfacial tension between the water in the oil layers decreases. Field experiments were conducted and experimental results were found to be in agreement with the predicted results from modeling.

Douglas *et al.* examined the weathering of crude oil from the OSSA II spill over a series of 12 months.¹⁹¹ In these studies both lab and field experiments were conducted. To determine the maximum amount of oil that could be lost due to evaporation, a gentle stream of nitrogen gas was directed on the oil surface while a hot plate heated the oil to 75°C. A maximum of 45% of oil was lost in the laboratory evaporation studies and almost complete removal of C3-C18 n-alkanes was observed. In addition to the removal of the lower molecular weight alkanes, loss of C20 to C35 was also reported. The loss of some of the mid-range n-alkanes were theorized due to the enhanced evaporation or aerosol partitioning. In addition the lab studies suggest that the aqueous vapor extraction was responsible for the loss of the mid-range alkanes, which has been discussed in previous studies.¹⁹² In the field samples nearly complete loss of the lighter alkane fractions, C8 to C15, and partial loss of the mid-range alkanes, C15 to C40, were reported.

The National Oceanic and Atmospheric Administration (NOAA) proposed a budget to account for the oil from the DWH oil spill, Figure 3.4.¹⁸³ In this budget they reported that 17% of the oil was recovered directly from the wellhead and an additional 8% was removed through

BP's physical clean-up methods. They estimated that 25% of the oil was evaporated from the surface of the gulf or was dissolved in the gulf due to the travel from the wellhead. Naturally dispersed oil accounted for 16% of the oil removed while chemical dispersion accounted for only 8% of the oil removal. An estimated 26% of the oil is considered to be residual oil. They defined the residual oil as tar balls that have washed up on the shore, oil that is just below the surface or on the surface as sheen, and oil that is located in the lower portions of the shore's surface. The residual oil and the dispersed oil has not been collected, thus these portions are still present in the ecosystem and are being degraded.

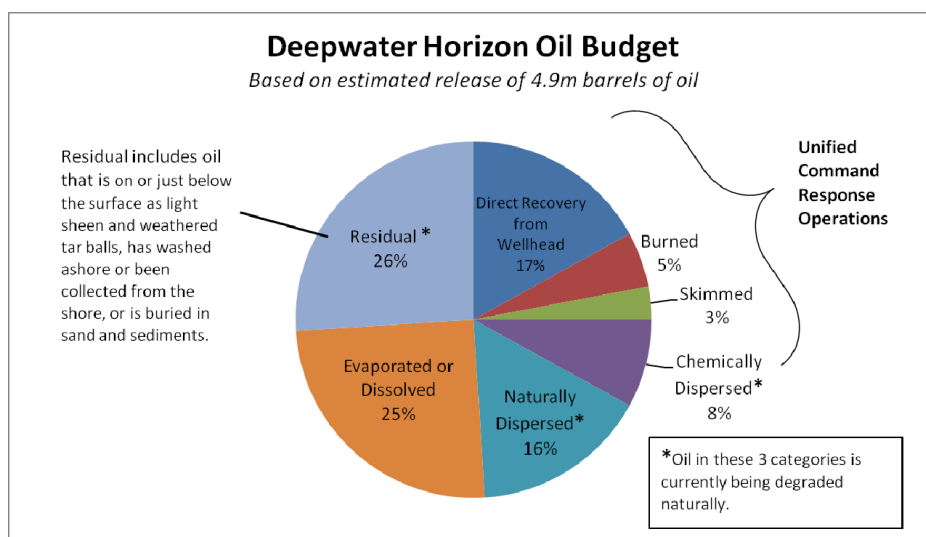


Figure 3.4. NOAA's proposed budget for oil released from the Macondo well¹⁸³

The two major pathways for oil degradation are biodegradation and photodegradation. Many studies have examined the biodegradation of crude oils. Wong *et al.* carried out laboratory studies on the biodegradation of oil.¹⁹³ Fluorescence intensities of oil samples drastically decreased between 3 and 5 days of microbial degradation, and after 15 days of exposure fluorescence was nonexistent. Alkane degradation in these studies was rapid, and almost complete degradation of linear alkanes was observed after 9 days. Mille *et al.* investigated the biodegradation of oil in differ salinities.¹⁹⁴ Increase in degradation was observed for salinities up

to 0.4 mol/L. Salinities above 0.4 mol/L exhibited a decrease in biodegradation with increasing saline concentrations.

After the DWH oil spill studies found fluorescent underwater plumes miles away from the Macondo wellhead.¹⁸² These plumes were suspected to be chemically dispersed oil from the wellhead that was picked up by an underwater current 900 to 1300 meters below the surface. Initial reports of the plume indicated that the plume was monoaromatic compounds that persisted in the gulf's water column for months without substantial biodegradation. Further investigation of the deep-sea plume found low concentrations of phosphate, nitrate, and dissolved oxygen with higher concentrations of ammonium.¹⁹⁵ Differences in the nutrient concentrations suggested that these plumes contain high concentration oil degrading microorganisms that were not present in the non-plume areas. The presence of biodegrading microorganisms were attributed to light nature of the oil containing a large portion of readily biodegradable volatile compounds. While these recent studies have observed increases in the microbial activity in deep underwater plumes, larger molecules, such as PAHs, are normally recalcitrant biodegradation.¹⁹⁶ Additionally, biodegradation of insoluble oil fractions are limited by oil-water interface area, thus biotransformation is slow. Dispersant addition increases the oil to water surface contact area. Studies with dispersant addition have observed an increase in the biodegradation of oil, however in contradicting studies inhibition of biodegradation of oil with dispersant was observed.

Zahed *et al.* studied the biodegradation of oil with and without nutrients present in the system while varying the initial oil concentration.^{197, 198} In these studies increase in total petroleum hydrocarbon degradation was observed when nutrients were added for all oil concentrations; however, the greatest enhancement was observed for lower oil concentrations. Further investigations were conducted to determine the effect of Corexit EC9500A on the

biodegradation of the oil.¹⁹⁹ Increase in the degradation was reported for all samples with dispersant present with varying initial oil concentrations; however, higher overall percent oil remaining was observed for higher initial oil concentrations. Macnaughton *et al.* studied the microbial colonization and biodegradation of crude oil with and without nutrients.²⁰⁰ Colonization of microorganisms in oil droplets was delayed for systems without Corexit EC9500A in contrast to systems with dispersant present, thus increase in biodegradation was observed for dispersed samples. In comparison to samples without nutrients, an increase in microbial degradation of n-alkanes was observed in samples with nutrients present (55% versus 90% respectively). Wrenn *et al.* studied the biodegradation of oil with ammonium and nitrate present as nutrients.²⁰¹ In these studies nutrients were added both continuously and intermittently to determine if continuous nutrient source increased biodegradation. With these studies, biodegradation was found to be independent of the nitrogen source and the abundance of the nutrient. Additionally, after 2 weeks of exposure, biodegradation ceased in systems with and without nutrient addition.

Fought *et al.* studied the biodegradation of n-alkanes and aromatics with and without Corexit EC9527A.²⁰² In contrast to studies by Zahed *et al.*, samples with dispersant had a decrease in the alkane degradation in comparison to samples without dispersant. Minute differences were observed for aromatic hydrocarbon biodegradation with or without dispersant. Sequential studies by Fought *et al.* examined the degradation of sulfur containing heterocyclics with different concentrations of Corexit EC9527A.²⁰³ For these studies inhibition of the degradation was observed with high concentrations of dispersant present.

Previous studies have observed that biodegradation is sluggish in low nutrient environments, such as the Gulf of Mexico. In addition large molecules are resistant to

biodegradation; therefore, alternative methods are needed for degradation to occur. Photooxidation is an important mechanism for the degradation of crude oil. Photooxidation reactions have been defined as either type 1 or type 2 reactions.²⁰⁴ In type 1 reactions the light absorbed photodissociates the absorbing compound to produce radicals. The radical products then react with oxygen to yield oxidation products. In type 2 reactions, excited state singlet oxygen is formed, which can then react with compounds in the system to form oxygenated products. In addition to formation of singlet oxygen, studies have suggested superoxide radical anion is a reaction intermediate in some photooxidation reactions.

Numerous studies have been conducted on the photooxidation of crude oil and different fractions of crude oil. Berthou *et al.* examined the photodegradation of the water soluble acid compounds in Arabian light oil.²⁰⁵ Increase in the fluorescence intensity was observed over irradiation time in these studies due to the increase in products that were more water soluble than the parent compound. Additionally drastic increases were observed in the unresolved complex mixture portion of the gas chromatogram after 70 days of irradiation due to the increase in degradation products, some which act as photosensitizers. Thominet and Verdu studied the photooxidation of light crude oil.²⁰⁶ They observed a decrease in the lower molecular weight compounds and the formation of a high molecular weight species due to polymerization or coupling reactions. D'Auria *et al.* studied the effect of UV irradiation of crude oil by high pressure mercury lamps.²⁰⁷ In these studies linear hydrocarbon intensity increased and alkenes were eliminated after irradiation. It was hypothesized that the surge in the linear hydrocarbon concentration was due to the degradation products formed from branched and cyclic alkanes.

Aromatics are highly photoactive due to their ability to absorb light in the UV regions, thus many studies have been conducted on the photodegradation of aromatics. Plata and Reddy

examined the photochemical decomposition of selected PAHs, benzo[e]pyrene (BEP), benzo[a]pyrene (BAP), benzo[a]anthracene (BAA), and chrysene (CHR), in oil contaminated coastal zones.²⁰⁸ These studies found that the bent isomers, BEP and CHR, are resistant to photodegradation in comparison to their linear counterparts, BAP and BAA. The preference for degradation of linear PAHs suggests that the direct photodegradation is the mechanism for degradation. Lower degradation rates were observed for studies of PAHs conducted in hexane than in water, which implies that direct photolysis contributes a smaller role in PAH degradation in oil films than in aqueous systems. Further investigations by Plata *et al.* studied the role of singlet oxygen in the degradation of the above mentioned PAHs.²⁰⁹ In these studies, degradation was almost stagnant in hydrophobic solvents. The inhibition in the degradation was attributed to the unstable environment for the single oxygen in the hydrophobic solvents.

Studies have been conducted on the photodegradation of PAHs under different gas streams: O_3/N_2 , O_2/N_2 , $O_2/O_3/N_2$.²¹⁰ In these studies, increases in rate constants for anthracene and phenanthrene were observed in the presence of O_2/N_2 . Higher rate constants for perylene and pyrene were reported for O_3/N_2 , which suggests that direct photolysis is not the mechanism for degradation. Fasnacht and Blough studied the mechanism of PAH photodegradation through cation radicals and the role of O_2 in the degradation in aqueous systems.²¹¹ In these studies PAH degradation was found to be independent of the wavelength of irradiation, which suggests that indirect photoionization was occurring. Additionally, photodegradation quantum yields of PAHs increased with increasing concentrations of oxygen, which confirms the importance of oxygen in the photodegradation mechanism. A small effect was observed on PAH degradation reactions in the presence of an electron donor at low oxygen concentrations; however, with high oxygen concentrations the rate of PAH degradation drastically decreased. From these studies it was

concluded that the photodegradation of PAHs occurs through the excited singlet state, primarily through an electron transfer to oxygen, while triplet oxygen degradation happens through a direct reaction of oxygen with the PAH.

Alkanes are readily biodegraded, however due to the lack of the ability to absorb ultraviolet irradiation, they are resistant to photodegradation. In order for photodegradation of alkanes to occur, a photosensitizer must be present. Rontani *et al.* studied the photosensitized degradation of pristane with over 15 days with anthraquinone present.²¹² Anthraquinone is commonly chosen as a photosensitizer due to its abundance in marine environments. With the photosensitizer present, pristane was oxidized to produce secondary or tertiary photodecomposition products, including alcohols and ketones. The ratios of pristane to eicosane were compared to study the patterns of photodegradation. In these comparisons the ratios did decrease over the reaction time, which suggested that branched alkanes are more readily photodegraded than linear alkanes. Further studies by Rontani *et al.* investigated the photosensitized degradation of linear alkanes with natural sunlight over 28 days.²¹³ Alkane loss was observed over the course of the irradiation period. The ratios of heptadecane to pristane and octadecane to phytane were compared. Decreasing ratios confirmed the higher photochemical reactivity of the branched alkanes.

Photocatalysts have been added to increase the rate of photodegradation and to assist in the degradation of alkanes. Most of the studies of oil degradation employ titanium dioxide (TiO₂) as the photocatalyst. Titanium dioxide is a common photocatalyst due to its relatively low toxicity, resistance to corrosion, and ability to be excited in the UV region. Titanium dioxide has three different crystal structures: brookite, anatase, and rutile.²¹⁴ While rutile is the most thermodynamically stable form of TiO₂, anatase TiO₂ is more photochemically active.

However, studies have shown that 70:30 anatase to rutile is optimal for maximum photoactivity. Anatase TiO_2 is excited by wavelengths lower than 387 nm and has a band gap of 3.2 eV.²¹⁵ When TiO_2 is irradiated with light, the absorbed photon excites an electron from the valence band into the conduction band. When the electron is excited into the conduction band a hole is also produced. Coupling of the produced excited electron and the hole is commonly called an electron-hole pair. The excited electron can undergo direct degradation by being absorbed by a pollutant, thus reducing the pollutant. Additionally, the excited electron can react with molecular oxygen to produce a superoxide radical ($\text{O}_2^{\cdot-}$), which can then react with the pollutant or with water to form other radicals. The hole can diffuse to the particle surface where it can react to degrade the organic compound either directly or indirectly.²¹⁶⁻²¹⁸ Direct degradation is when the hole directly oxidizes the organic compound. In the indirect degradation pathway, the hole at the particle's surface reacts with a water molecule to produce hydroxyl radical ($\cdot\text{OH}$). The hydroxyl radical produced is a nonspecific oxidant that can degrade the pollutant, sometimes yielding complete mineralization if sufficient oxidant is present. In addition to TiO_2 , iron oxide can be excited by photons to produce an electron-hole pair. In comparison to the band gap of TiO_2 , the Fe_2O_3 band gap is 2.2 eV, allowing Fe_2O_3 to absorb in the visible region. However, Fe_2O_3 has a higher probability of electron and hole recombination, which limits its effectiveness as a photocatalyst.^{215, 219}

Ziulli and Jardim studied the photocatalytic degradation of the water soluble fractions of oil with TiO_2 .²¹⁶ Increase in reduction of dissolved organic carbon was reported for systems with TiO_2 present. Additionally, FT-IR analysis indicated that mineralization of the water soluble fraction was observed with catalyst present, but not without photocatalyst. Over the course of 5 days, samples without photocatalyst remained toxic; however, samples with photocatalyst were

no longer toxic after 3 days of irradiation. Further investigations by Ziolli and Jardim on the photodegradation of the water soluble fractions observed no significant difference in the gas chromatogram without photocatalyst; conversely with TiO_2 of the complete removal of the compounds present in the water soluble fraction was observed.²²⁰

Pernyeszi and Dekany studied the photocatalytic degradation of sodium dodecylsulfate (SDS) stabilized toluene and asphaltene dissolved in toluene with TiO_2 and hydrogen peroxide present.²¹⁸ Hydrogen peroxide was added in these systems to trap the hole of the electron-hole pair, thus decreasing the probability of recombination. After 10 hours of irradiation, 85% of the asphaltene and toluene mixture was removed with photocatalyst and hydrogen peroxide, whereas 65% of toluene was removed in toluene only systems. In addition to the asphaltene and toluene studies, photodegradation of crude oil was examined with and without hydrogen peroxide. In these studies enhancement was observed in high peroxide (1 M) systems; however at low peroxide concentrations (0.1 M) total organic carbon removed after 10 hours of irradiation was identical.

A number of studies have investigated the degradation products from photolysis. Ehrhardt and Weber examined the products of anthraquinone photosensitized reactions with tetradecane and two Brazilian oils.²²¹ Acetaldehyde, acetone, and formaldehyde were identified as products of the reactions. Attempts to quantify acetaldehyde and acetone were unsuccessful due to the irregular changes in the concentrations, which were postulated to be due to the volatility of the compounds. Formaldehyde was quantified and the rate of formation was determined to be dependent on the source of the oil. Hansen studied photodegradation products of petroleum surface films on seawater irradiated by mercury lamps.²²² When glass was inserted in the pathway of the irradiation, no photodegradation products were observed. Lack of

photodegradation products was suggested to be due to the filtering out of wavelengths below 350 nm, which is where photoactivity is the highest. When irradiation was performed with wavelengths below 350 nm, the intensity of the photodegradation products were increased by tenfold in comparison to full solar spectrum irradiation. The principle photodegradation products that were detected were carboxylic acids. Additionally, alcohols and aldehydes were detected, but it was implied that these products were further phototransformed to carboxylic acids.

Burwood and Speers investigated the photooxidation product of Middle Eastern crude oil.²²³ In these studies, photooxidation resulted in the increase in the unresolved complex mixture and the formation of sulfoxides. Larson *et al.* examined the products of photooxidation and their toxicities on baker's yeast.²²⁴ Increase toxicity was observed over irradiation time and was initiated by the formation of polar oxidative products including carbonyls and phenols. Supplementary investigations by Larson *et al.* identified that in addition to the formation carbonyls and phenols, hydroperoxides were formed.²²⁵ In addition to the above mentioned photooxidation products, studies have reported the formation of epoxides, sulfones, esters, fatty acids, anhydrides, and quinones.^{188, 226-228}

CHAPTER 4

PHOTOLYTIC AND PHOTOCATALYTIC DEGRADATION OF OIL FROM THE DEEPWATER HORIZON SPILL

Introduction

The Deepwater Horizon oil spill in the Gulf of Mexico was an enormous disruption to the entire ecosystem. It was estimated that 4.9 million barrels of oil gushed into the gulf over 86 days until BP capped the well head.¹⁵⁶ The impacts are widespread and a full understanding of the long term impacts is still under investigation. To better understand the impacts that the oil spill has on the ecosystem, a full knowledge is need of the fate of the oil after it is released.

There are several mechanisms for the degradation and dispersion of aquatic released oil including dissolution, emulsification, absorption, mixing, evaporation, biodegradation, photodegradation, and chemical reactions.^{187, 229-233} Contributions from dissolution were higher for the Deepwater Horizon oil spill than other Gulf of Mexico oil spills due to the depth of the oil head (1500m) and the addition of chemical dispersants. In addition, biodegradation and photodegradation have been shown to be two of the most significant degradation mechanisms in previous oil spills.^{234, 235} Initial studies report of biodegrading bacteria in water plumes from the Deepwater Horizon oil spill.¹⁹⁵ Biodegradation has been shown to be useful for the degradation of small molecules; however, it is slower in the nutrient deficient waters of the open Gulf of Mexico.^{201, 236, 237} Furthermore, higher molecular weight alkanes and polycyclic aromatic hydrocarbons (PAH) are resistant to biodegradation, as well as dissolution and evaporation. For

these recalcitrant compounds, photochemical transformations become of extreme importance for the initial step in promoting bioavailability and further degradation.

Numerous studies have been conducted on the photodegradation of oil. In most of these studies a mercury lamp or fluorescent lamps were used as an irradiation source.^{216, 220, 238, 239} These sources do not accurately mimic the optical spectrum of the sun. In addition, in some of the previous studies the oil was separated into different fractions before irradiation.^{213, 216, 240} The chemical and physical interactions of the different fractions were therefore not included in these studies, thus the degradation rates and mechanisms do not necessarily mimic those of true crude oil samples in an environmental setting.

Few studies have been conducted on oil in the presence of photocatalysts.^{217, 218, 241, 242} In those studies, the samples with photocatalysts have shown an increase in the degradation rate of the different components of the oil. The most common photocatalyst that has been studied in the degradation of oil is titanium dioxide. In comparison to the rutile form, the anatase form of TiO_2 is more photochemically active. Anatase has a band gap of 3.2 eV and is excited by electromagnetic radiation with wavelengths that are shorter than 387 nm. The absorbed photon excites an electron from the valence shell into the conduction band, thus producing an electron-hole pair. The excited electron can undergo direct degradation by being absorbed by a pollutant, thus reducing the pollutant. Additionally, the excited electron can react with oxygen to produce a superoxide radical ($\text{O}_2^{\cdot-}$), which can then react with the pollutant or with water to form other radicals. The hole can diffuse to the particle surface where it can react to degrade the organic compound either directly or indirectly.²¹⁶⁻²¹⁸ Direct degradation is when the hole directly oxidizes the organic compound. In the indirect degradation pathway, the hole at the particle's surface reacts with a water molecule to produce hydroxyl radical ($\cdot\text{OH}$). The hydroxyl radical

produced is a nonspecific oxidant that can degrade the pollutant, sometimes yielding complete mineralization if sufficient oxidant is present. In addition to TiO_2 , hydroxyl radicals can be formed by iron oxides. Iron oxide is excited by photons which then produce an electron-hole pair similar to the TiO_2 . Comparable to TiO_2 the electron hole pair can then react with a water molecule to produce hydroxyl radicals that degrades the organic pollutant. In comparison to the band gap of TiO_2 , the Fe_2O_3 band gap is 2.2 eV, allowing Fe_2O_3 to absorb in the visible region. However, Fe_2O_3 has a higher probability of electron and hole recombination, which limits its effectiveness as a photocatalyst.^{24,25}

In this chapter, photodegradation of surface oil from the Deepwater Horizon spill was studied. Photodegradation studies were conducted with and without the photocatalysts TiO_2 and Fe_2O_3 . Analysis of the phototransformation of crude oil was achieved using GC-FID for alkanes and fluorescence for PAH. In addition, Microtox was utilized to study the toxicity of the water exposed to oil with and without photochemical treatment.

Experimental Materials and Methods

Crude oil and water samples were collected on May 26, 2010 at N 28° 48.316, W 89° 07.949, which is approximately 47 miles northwest of the Deepwater Horizon spill site. Oil samples collected were thick and dark brown. The water samples were collected from a nearby area in the Gulf of Mexico that was not visibly contaminated with oil. After collection the water samples were filtered through a 0.2 μm polycarbonate filters to sterilize the water and were subsequently stored at 4 °C.

Dichloromethane (DCM) and toluene were OmniSolv ultra high purity obtained from EMD. HPLC solvent grade pentane and naphthalene were obtained from J.T. Baker. Titanium (IV) oxide (anatase, nanopowder, <25 nm, 99.7%), iron (III) oxide (<50 nm), fluorene, fluoroanthane,

anthracene, pyrene, and eicosane were obtained from Aldrich. Pentadecane, n-octacosane, n-docosane, n-tetracosane, and n-triacontane were from Alfa Aesar. Octane, nonane, decane, and dodecane were obtained from Fluka. Benzo[a]pyrene was obtained from Sigma. Microtox diluent, osmotic adjusting solution, reconstitution solution, and acute reagent were obtained from SDIX.

To reduce the hydrophobicity of the TiO_2 and Fe_2O_3 nanoparticles and to make them more readily disperse in the oil, the photocatalysts were coated with stearic acid. Stearic acid coating was achieved by sonicating the oxide in an ethanol solution of steric acid (0.353 mM). After sonication the sample was centrifuged, the ethanol was removed, and the coated oxide particles were dispersed in toluene.

Prior to exposure to simulated sunlight, 100 mg of crude oil was weighed and dissolved in a mixture of pentane and toluene (20:1). For samples treated with TiO_2 or Fe_2O_3 , the photocatalyst was added to the mixture instead if toluene. The mixture was then sonicated to fully disperse the oil and photocatalyst. The mixture was then poured onto the surface of 10 of mL Gulf water in a 150 mL water-jacketed beaker (5 cm i.d.). The sample was kept uncovered for 5 minutes to allow the pentane and toluene to evaporate. After drying the samples were exposed to 765 W/m^2 solar simulated light (Atlas Suntest CPS+ equipped with a 1500 W air cooled xenon arc lamp). Solar simulator intensity accounts for irradiations in the 300-800 nm range and not the full spectrum. During irradiation, the tops of the jacketed beakers were covered with a piece of quartz glass, and the samples were kept at 27°C by circulating thermostatic water through the jacketed beakers. After irradiation the samples were either extracted with DCM for GC-FID and fluorescence analysis, or the aqueous layer was taken for Microtox analysis.

Oil extracts were analyzed on a Hewlett-Packard Agilent 6890 GC coupled to an auto sampler with a flame ionization detector and a 30 m \times 0.32 mm (i.d.) AT-1 capillary column. The injector and detector temperatures were set to 300 °C and 350 °C, respectively, and the temperature programming was as follows: 80 °C held for 1 minute, ramp at 15 °C/min until a final temperature of 320 °C which was held for 15 minutes. To eliminate any variations in the GC's performance, dodecane was added as an internal standard to all samples.

Fluorescence excitation-emission matrices and synchronous scans were collected with a PerkinElmer LS 55 luminescence spectrometer. Synchronous scans on the diluted oil extracts were collected from 250 to 500 nm with a delta lambda of 25 nm and excitation and emission slits set to 2.5 and 5.0 nm, respectively. To determine the PAH emission wavelength ranges, DCM diluted samples of individual PAH were analyzed via synchronous scan. Excitation-emission matrix scans were collected with an emission range from 300 to 600 nm and with excitation starting at 200 nm and incrementing every 5 nm until 400 nm. Excitation and emission slits were both set to 5.0 nm.

Microtox analysis was performed using a Microtox 500 analyzer (SDIX). The protocol used to analyze the toxicity of the water exposed to the oil was the comparison test for marine and estuarine samples.^{216, 243} For each day Microtox was used, the basic test was run on phenol or zinc sulfate standards to ensure proper function of the Microtox analyzer and procedure.

Results and Discussion

The very low molecular weight alkanes (C13 and smaller) were absent from the GC-FID chromatograms. These compounds were most likely lost in weathering of the oil between its release from the well and its collection. The more volatile and more water soluble compounds either evaporated or were removed by dissolution in the Gulf of Mexico water.

The optical spectrum of the irradiation source in the solar simulator used in our studies was similar to the optical spectrum of the sun, with a slightly higher intensity. To standardize our instrument a calibrated Hamamatsu S1718 (National Renewable Energy Laboratory) solar cell was used to measure the intensity of the xenon arc lamp used. From the measured intensity, it was discovered that the output of our solar simulator 765 W/cm^2 is relatively equal to 1.26 suns. Since the sun's full intensity is only for 6 hours, this means our 6 hour irradiation is equal to 1.26 days of irradiation.

Crude oil was deposited onto the Gulf water to mimic the interactions of the components in the water with those of the oil and degradation products. 100 mg of the oil was used which produced a film of oil that was approximately $60 \text{ }\mu\text{m}$ thick. Photographs were taken before and after each irradiation to document the physical changes in the oil layer throughout irradiation and are presented in Figure 4.1. After 6 hours of irradiation the oil layer became leathery in appearance, and upon movement the oil layer cracked. The leathery appearance was likely due to loss of the lower molecular weight fractions from the oil layer. The oil sample irradiated for 12 hours was slightly lighter in color than the six hour irradiated sample. The 12 hour sample had a leathery appearance similar to the 6 hour sample; however, cracks were not apparent in the 12 hour sample due to a smaller extent of movement of the sample after irradiation. After 24 and 48 hours of irradiation, significant physical degradation of the oil was apparent.

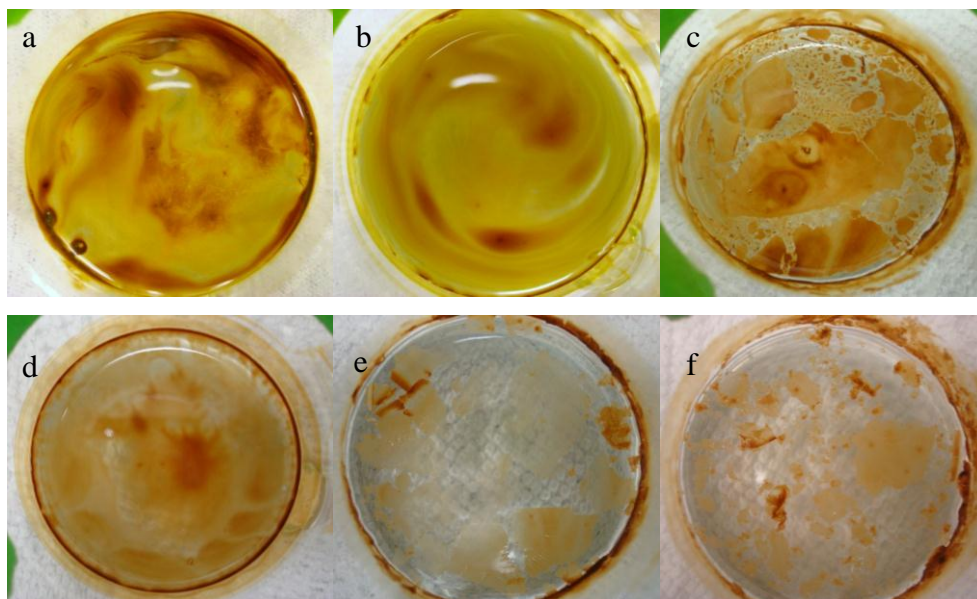


Figure 4.1. Appearance of oil as a function of irradiation time: (a) before irradiation, and after (b) 3 hours, (c) 6 hours, (d) 12 hours, (e) 5.4 days, and (f) 48 hours irradiation.

In comparison to other methods (e.g. liquid chromatography with UV diode array detection, gas chromatography/mass spectrometry), fluorescence has been shown to exhibit better detection limits for PAHs. However many PAHs have similar excitation and emission wavelengths, thus making the detection of individual compounds in multiple component systems impossible with conventional fluorescence without previous separation methods. To overcome this limitation, Lloyd introduced synchronous fluorescence scan (SFS) as a method to characterize complex mixtures without a separation step.²⁴⁴ Years later, Christian *et al.* designed a device for the simultaneous recording of the fluorescence data in a method called excitation-emission matrix (EEM).²⁴⁵

Synchronous scans were performed on the DCM extract and are presented in Figure 4.2a. In our studies we collected synchronous scan data from 250-500 nm, which slightly differs from the range of 300-700 nm used by Guedes *et al.*²⁴⁶ It was observed in their studies that after 100 hour of solar irradiation the total fluorescence intensity decreased 61% and 72% for Arabian and Columbian oil, respectively. D'Auria *et al.* observed synchronous scan fluorescence emission

spectrum ranges 300-550 nm for Centro Oil. In their studies the maximum emission peak was observed at 396 nm and the fluorescence intensity decrease 20% after 100 hours of irradiation with a high pressure mercury lamp.²⁰⁷ For our 3 hour irradiated samples the maximum emission intensity was at 306 nm and decreased by 28, 42, and 32% for no oxide, TiO₂, and Fe₂O₃, respectively after irradiation. The difference in the synchronous scan emission wavelength ranges of these previous studies and our studies is the result of the different location of the source oil, thus resulting in different chemical composition.

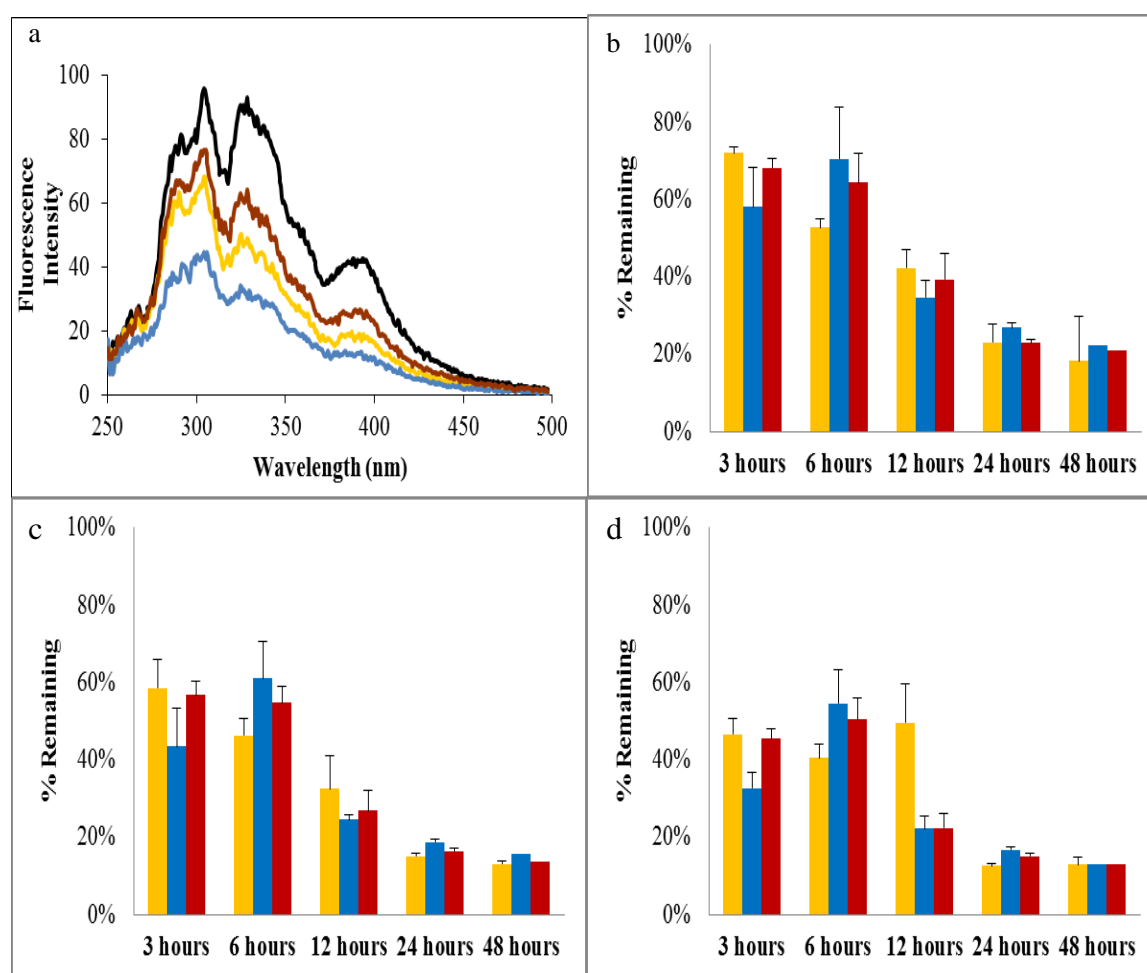


Figure 4.2. Synchronous scan of the (a) 3 hour dark (—) and no oxide (—), TiO₂ (—), and Fe₂O₃ (—) irradiated samples with $\Delta\lambda = 25$ nm. The percent remaining of PAH for (b) small (305 nm), (c) medium (326 nm) and (d) large (390 nm) molecules with no oxide (■), TiO₂ (■), and Fe₂O₃ (■).

Previous studies established that fluorescence synchronous scan data can be separated into different regions which represent different size PAHs; smaller PAH emissions are at lower wavelengths while larger PAH emissions occur at longer wavelengths.^{205, 247, 248} From the synchronous scans of known PAH and from previous literature, three wavelengths were chosen to represent the different molecular weight PAHs. The wavelength regions used were 305 nm (small), 326 nm (medium), and 390 nm (large).^{205, 207} Figures 4.2b-d show the observed decrease in fluorescence intensity for each of these regions for samples irradiated for various times. Concentrations of small and medium PAH decrease over irradiation times until 24 hours for irradiated samples without oxides. After 24 hours of irradiation no difference is observed in the percent remaining in comparison to the 48 hour irradiated samples. From the results it is evident that the larger the PAH the more readily degraded it is. This increase in the photolysis of the larger PAH is likely due ability of the larger PAHs to absorb light in the visible spectrum.

Samples containing Fe_2O_3 exhibited the same extent of degradation as the samples without the modifier present. Irradiated samples with TiO_2 present exhibited an increase in degradation after 3 hours of degradation in comparison to the no oxide and Fe_2O_3 samples; however after 6 hours of irradiation TiO_2 samples exhibit a decrease in the degradation rates in comparison to the no oxide. The difference in the initial oil degradation rates of samples with Fe_2O_3 compared to those with TiO_2 is likely due to the fact that Fe_2O_3 has a very short electron-hole recombination time, preventing effective reaction of the electrons and holes with oil, water, or oxygen present in the system.

Excitation-emission matrix fluorescence has been proven by previous researchers as a viable tool for the analysis of multiple components PAH samples, including crude oil.²⁴⁹⁻²⁵¹ EEM spectra were acquired for the DCM extracted oils, and the data are presented in Figure

4.3a. As a rough measure of percent degradation, we examined the peak intensity at the highest point, which has been done in previous studies.²⁵² The maximum of the EEM for the oil used in this study coincides with an excitation wavelength of 260 nm and an emission wavelength of 375 nm as shown in Figure 4.3b. From the results it is evident that after 3 hours of irradiation the TiO₂ doped samples exhibited an increase in degradation (45% removed) in comparison to the Fe₂O₃ and no oxide samples (25% and 27% removed, respectively). For the EEM data, Fe₂O₃ and no oxide samples had almost identical degradation patterns. The trends of the EEM data, increase in degradation for samples containing TiO₂ then those with no oxide and Fe₂O₃ and the identical degradation pattern with no oxide and Fe₂O₃ samples, are analogous to that of the synchronous scan data discussed above. After 12 hours of irradiation the TiO₂ degradation patterns start to mimic that of the no oxide and the Fe₂O₃. Trends of increased initial degradation rate followed by slowly decreasing rate are seen in both of the synchronous scan and EEM data sets. Decrease in the rate of degradation over time could be related to the decomposition of the photosensitizers that are initially present in the crude oil samples.

D'Auria, *et al.* discovered that linear alkanes did not undergo photochemical degradation after 100 hours of mercury lamp irradiation.²⁵³ Klein and Pilpel studied the photodegradation of n-alkanes in solution with 1-naphthol present.²⁵⁴ In their studies it was observed that the photodegradation of the n-alkanes increased with increasing amounts of photosensitizer present, whereas marginal degradation occurred in the samples without 1-naphthol. Rontani and Giral observed that the branched alkanes had were more susceptible to endure phototransformation than the linear alkanes.²¹² Hansen reported similar results that the branched alkanes are more readily decomposed than the n-alkanes.²²² Rontani and Giral later reported that the extent of degradation can be confirm by comparing the ratio of branched alkanes to n-alkanes.²¹³

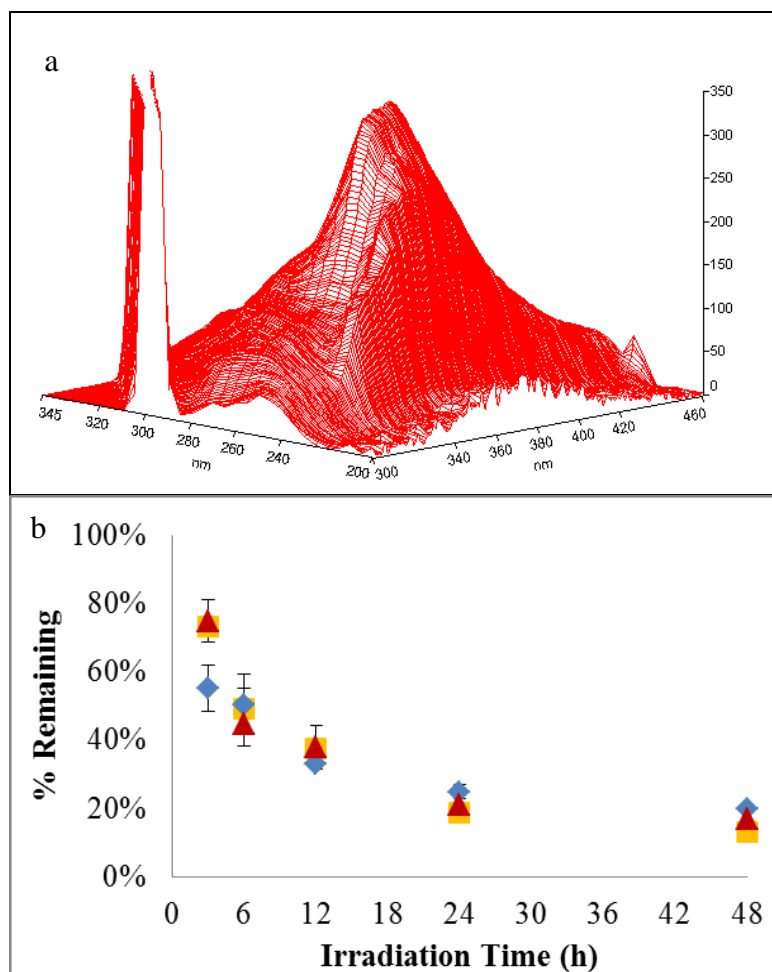


Figure 4.3. (a) EEM of the DCM diluted non-irradiated oil extracted. (b) The percent emission remaining for the oil after irradiation with no oxide (■), TiO_2 (◆), and Fe_2O_3 (▲). Excitation wavelength = 260 nm and emission wavelength = 375nm

The extent of loss of alkanes was studied via GC-FID. Data for these experiments are presented in Figure 4.4. Identification of the major peaks was accomplished by comparison to retention times of known n-alkane standards. All peaks were normalized to dodecane to eliminate possible injection and instrument variations. From the results it was observed that all samples which were exposed to simulated sunlight exhibited extensive reduction of C14-C17 alkanes. Minute differences in the loss of the lower molecular weight alkanes are observed between 3 and 12 hours of irradiation; however after 24 hours a substantial reduction in the C14-C17 alkanes is observed. To confirm the losses present in our samples are due to the

photodegradation of the alkanes, the ratio of n-heptadecane (n-C17) to pristane and n-octadecane (n-C18) to phytane is compared, Table 4.1 and 4.2. From the ratios of n-C17 to pristane and n-C18 to phytane it is evident that the disappearance in the lower molecular weight alkanes is not to photodegradation, but probably evaporation. C14-C17 alkanes are not that volatile, however upon irradiation the surface of the oil is heated from the light source. In addition, the samples in the solar simulator are exposed to a current of air that is used to cool the lamp. The heating and air current in the simulator is thought to be the source of the increase in the evaporation of the C14-C17 alkanes. The dark samples are placed in the water bath outside of the solar simulator during irradiation. Since the dark samples are not exposed to the same heating and evaporation as the irradiation samples, evaporation is not observed. To test this theory the temperature of the irradiated samples was taken after 65 and 100 minutes of irradiation. The average temperature of the oil's surface was recorded as 30.9°C, which indicated that irradiation of the oil caused an increase in the surface's temperature of 3.9°C. To study the evaporation of the lower molecular weight alkanes, the samples that were normally irradiated were wrapped in aluminum foil to block out the light. GC analysis of the evaporation study oil indicated a decrease in the C14-C17 alkanes similar to that of the irradiated samples, thus concluding that the loss of the n-alkanes is due to evaporation.

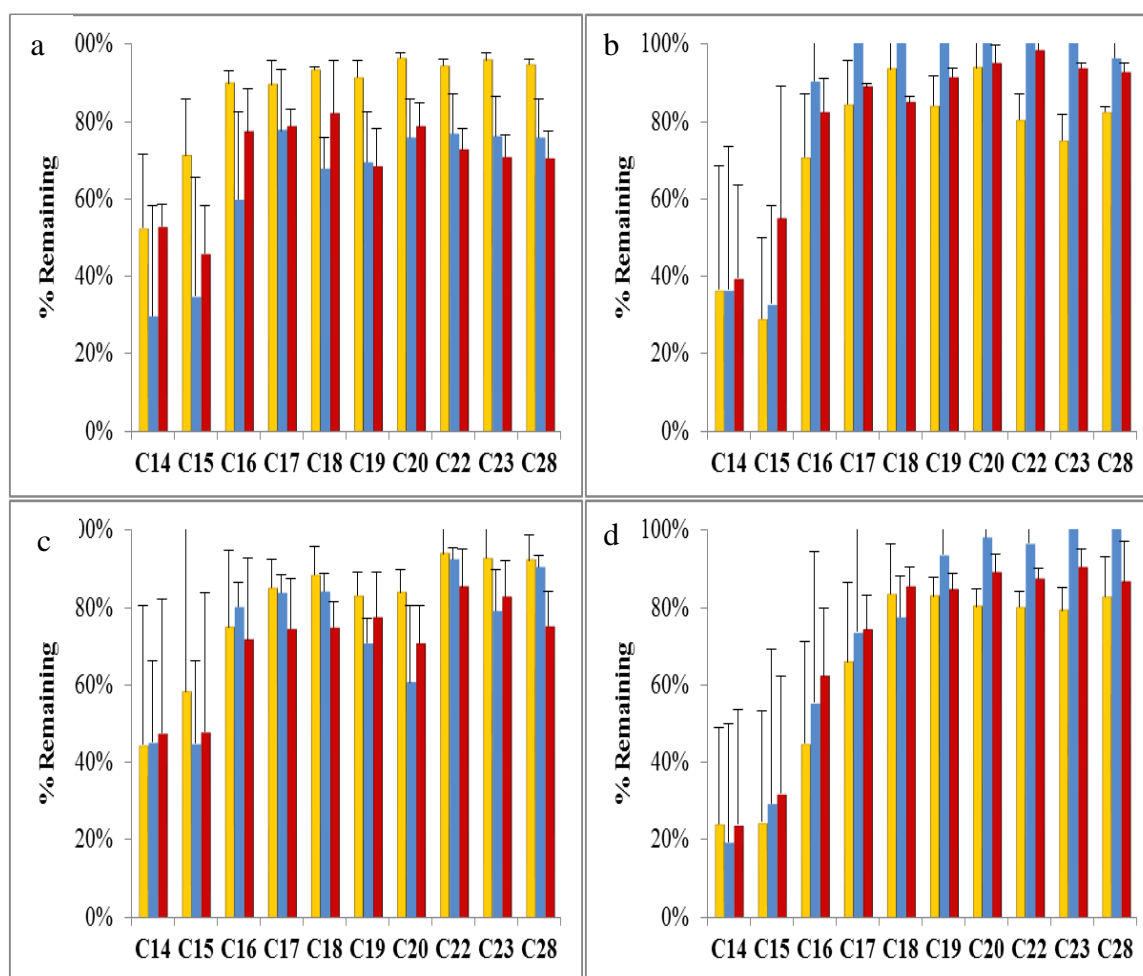


Figure 4.4. The GC-FID analysis of oil exposed to irradiation for (a) 3 hours, (b) 6 hours, (c) 12 hours, and (d) 24 hours with no oxide (■), TiO_2 (■), and Fe_2O_3 (■).

Table 4.1. The ratio of n-C17 to pristane and n-C18 to phytane over irradiation time in samples without photocatalyst

Time (hours)	n-C17:pristane		n-C18:phytane	
	Dark	Irradiated	Dark	Irradiated
3	0.52±0.01	0.53±0.04	0.40±0.00	0.40±0.01
6	0.60±0.03	0.63±0.01	0.52±0.15	0.37±0.03
12	0.50±0.16	0.50±0.09	0.47±0.18	0.49±0.11
24	0.61±0.00	0.58±0.03	0.38±0.04	0.40±0.04

Table 4.2. The ratio of n-C17 to pristane and n-C18 to phytane over irradiation time in samples containing photocatalyst

Time (hours)	n-C17:pristane				n-C18:phytane			
	TiO ₂		Fe ₂ O ₃		TiO ₂		Fe ₂ O ₃	
	Dark	Irradiated	Dark	Irradiated	Dark	Irradiated	Dark	Irradiated
3	0.63±0.00	0.60±0.01	0.63±0.01	0.57±0.06	0.34±0.00	0.36±0.04	0.42±0.04	0.40±0.01
6	0.65±0.00	0.63±0.01	0.57±0.01	0.62±0.02	0.35±0.00	0.37±0.03	0.39±0.01	0.48±0.00
12	0.60±0.01	0.60±0.01	0.61±0.03	0.61±0.00	0.39±0.03	0.39±0.02	0.37±0.01	0.42±0.04
24	0.59±0.01	0.61±0.01	0.61±0.00	0.59±0.03	0.37±0.00	0.42±0.04	0.39±0.02	0.41±0.03

The aqueous fraction of the irradiated sample was analyzed to evaluate the toxicity of the samples over time. To examine the toxicity of aqueous samples exposed to the oil with and without exposure to simulated sunlight, the emission intensity of the luminescent bacteria, *Vibrio fischeri*, was monitored. The toxicity of samples is reported as the % effect. The % effect correlates to the decrease in fluorescence of the bacteria that is exposed to the toxin which directly related to the amount of test bacteria killed. Ziolli *et al.* observed that the toxicity of the water soluble fraction of Brazilian crude oil samples with TiO₂ increased in comparison to samples that did not contain photocatalysts after 1 day of irradiation via high pressure mercury lamps.²¹⁶ The toxicity then decreased until 3 days when the samples were no longer toxic. The increase and subsequent decrease in the toxicity were attributed to the formation and destruction of degradation intermediates which were more toxic than the parent compounds. Our studies found that after exposing water to oil for 24 hours in the dark, no toxicity was observed for the water using Microtox analysis. The lack of toxicity is likely due to the fact that our oil was largely depleted of water soluble species. Consequently, during the 24 hours exposure, little of the oil dissolved in the water and no toxicity was observed. However, all irradiated samples showed substantial toxicity (Figure 4.5). These results contradict the findings of Ziolli *et al.* because we did not observe a decrease in the toxicity of the samples after 12 hours of irradiation, which would equal about 2.72 days of solar irradiation. The difference between the two studies can be attributed to two factors. First, Ziolli *et al.* used a mercury lamp which provided significantly more UV radiation than sunlight. Second Ziolli *et al.* used water soluble fractions which should be more readily degraded than the higher molecular weight species used in our studies. The crude oil in our studies was not depleted, allowing for continuous release of degradation products over the complete irradiation period. Thus the likelihood of the

intermediates being fully degraded during our exposures was highly improbable.

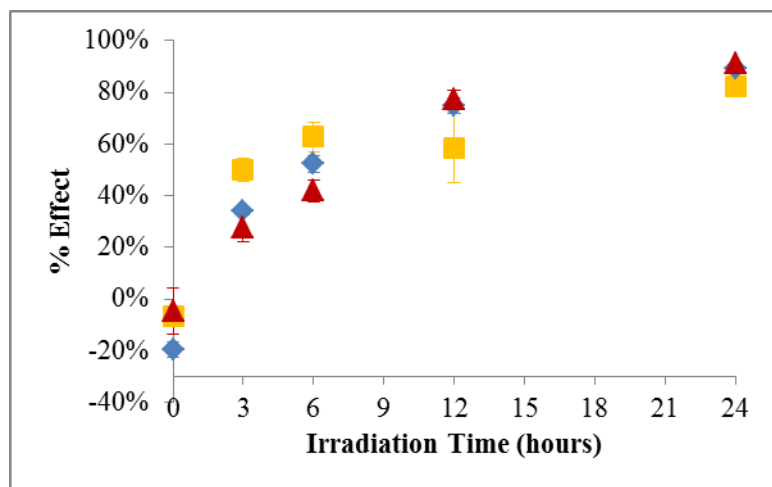


Figure 4.5. Microtox data of the toxicity of the aqueous layer of the irradiated samples with no oxide (■), TiO₂ (◆), and Fe₂O₃ (▲). % Effect represents the % of bacteria killed during incubation for 15min in the sample.

The increase in toxicity observed in our studies was expected due to the anticipated increase in solubility of the degradation products. Many studies have investigated the products during photodegradation of oil. Hansen *et al.* studied the photodegradation of thin films of crude oil fractions and found that the major products produced were primarily aliphatic and aromatic acids in addition to a less significant quantity of alcohols and phenols.²²² Tjessem and Aaberg observed substantial changes in the chemical and physical properties of photodegraded oil.²⁵³ Further investigations detected formation of ketones as degradation products.^{228, 254} Thominette and Verdu suggested that PAHs are important in radical propagation of chain reactions and that phase separation can occur due to insoluble, high molecular weight species formed by condensation and polymerization reactions.^{206, 255} These polymers were found to be linear or branched and not cross-linked. In other studies, photosensitized reactions involved in photochemical transformations were indicated to be of importance for the degradation of otherwise unreactive linear and branched alkanes.^{256, 257} Alkane degradation products were

identified to be mostly ketones and alcohols in these explorations. In more recent work, a number of benzothiophene photooxidation products were identified.²⁵⁸

Samples irradiated for 3 and 6 hours containing photocatalysts showed lower toxicity compared to the samples that contained no oxide. The fluorescence results for TiO_2 samples irradiated for 3 hour indicated an increase in the degradation rate in comparison to that of the no oxide and the Fe_2O_3 . With this in mind, it is theorized that the TiO_2 would have higher concentration of aqueous degradations products, thus the toxicity samples would be higher than that of the no oxide and the Fe_2O_3 , which is not observed. In addition, degradation of samples with Fe_2O_3 and no oxide are almost identical, thus the toxicities should be identical, which again is not observed. A plausible explanation for the differences in the patterns could be attributed to possible different degradation pathways. In addition, it is conceivable that the degradation products could be attaching to the photocatalysts in the oil layer, which will inhibit the number of degradation products in the aqueous phase. After the samples were exposed for 24 hours of irradiation, all the aqueous samples had similar toxicity.

Conclusion

The photolytic and photocatalytic degradation of surface oil from the Deepwater Horizon oil spill was studied in this chapter. PAH concentrations decreased over irradiation time up to 24 hours. In comparison to small and medium PAH, larger PAH exhibited an increase in degradation. Identical degradation rates were observed for Fe_2O_3 and no oxide samples. After 3 hours of irradiation, lower percent of PAH remaining was observed for samples containing TiO_2 ; however after 6 hours the same extent of degradation was observed for samples with and without photocatalyst. Loss of C14-C17 alkanes was observed over irradiation time; however the ratios of branched to linear alkanes indicate loss is not attributed to photodegradation. Further studies

concluded the loss of linear alkanes was due to evaporation. While the surface only samples was not toxic, the toxicity of the irradiated samples increased over irradiation time. After 3 and 6 hours of irradiation lower toxicities were observed for samples containing photocatalyst; however after 24 hours of irradiation equal toxicities were observed for all samples.

CHAPTER 5

PHOTOLYTIC AND PHOTOCATALYTIC DEGRADATION OF CHEMICALLY DISPERSED SURFACE OIL FROM THE DEEPWATER HORIZON OIL SPILL

Introduction

During the Deepwater Horizon oil spill, dispersants were employed in efforts to clean up the oil. It is reported that from May 15, 2010 to July 12, 2010 1.85 million gallons of dispersants were used.¹⁵⁶ Not only was this the largest application of dispersants to date, it was also the first application of dispersants applied to the oil at the well head. Over 0.77 million gallons of dispersant were applied at the well head and 1.07 million gallons were applied to the water surface. Of the 20 EPA approved dispersants, BP chose Corexit EC9527A and Corexit EC9500A.¹⁷¹ Corexit EC9527A was applied on the Gulf's surface, while Corexit EC9500A was applied both at the well head and on the surface. Both dispersants contain an anionic surfactant, dioctyl sodium sulfosuccinate, and propylene glycol.^{172, 173} The differences in the two dispersants is the solvent used: Corexit EC9500A contains hydrotreated light petroleum distillates while Corexit EC9527A contains 2-butoxyethanol, which has been shown to be an endocrine disruptor.²⁵⁹

Numerous studies have been conducted on the biodegradation of oil or components of oil containing dispersants.^{168, 169, 260} Fought *et al.* studied the biodegradation of sulfur heterocyclics and n-alkanes with Corexit EC9527A.^{202, 203} In their studies it was observed that the degradation was dependent on the dispersant concentration and the amount of nutrients available. Zahed *et*

al. studied the biodegradation of crude oil with Corexit EC9500A.¹⁹⁷ Their studies agreed with those of Foght that the degradation of crude oil decreased with low nutrient concentrations and the presence of dispersant. In addition they found that the biodegradation was inversely proportional to the initial oil concentration. Okpokwaski and Odokuma studied the microbial degradation of Corexit EC9257A and found that increases in the salinity will decrease the degradation rate of the dispersant.²⁶¹ Later studies by this group found that the biodegradability of dispersants is dependent on the dispersant composition and that Corexit EC9527A is readily biodegraded.²⁶² While many studies have been conducted on the effect of dispersants on the biodegradation of crude oil, there are no published studies to date that study the photodegradation of crude oil exposed to dispersants.

There is an abundance of studies that examine the photochemical degradation of crude oil; however, in most studies the researchers used mercury lamps. Yang *et al.* has compared the degradation of crude oil with both a mercury lamp and natural sunlight. In these studies it was observed that the mercury lamp degraded the crude oil at a faster rate due to the high intensity and the ability to emit light at lower wavelengths in the ultraviolet range.²⁶³ Additionally, similar results were reported by D'Auria *et al.* on the photodegradation of crude oil with mercury lamps and natural sunlight. Few studies have been conducted using natural sunlight or xenon lamps which have similar emission of light to that of the sun. Tjessem and Aaberg studied the changes in the oxygen uptake by petroleum residues in marine environments with exposure to natural sunlight.²⁶⁴ In their studies elemental analysis concluded that oxygen uptake by the oil residues drastically increased. Furthermore, Nicodem *et al.* studied the photodegradation of Brazilian intermediate crude oil by natural sunlight.²⁴³ After 100 hours of irradiation elemental

analysis indicated no increase in the oxygen content of the oil layer, however hydroxyl groups and carbonyl or carboxyl groups were observed in the infrared data of the aqueous layer.

This chapter examined the photodegradation of Deepwater Horizon surface oil with dispersants present. Photolysis studies were conducted with and without Corexit EC9527A and Corexit EC9500A. Similar to studies conducted in Chapter 4, dispersant-oil studies were carried out with and without the photocatalyst TiO_2 . Fluorescence and GC-FID analysis were used to evaluate the degree of PAH and alkane photodegradation. To evaluate the toxicity of the aqueous layer, Microtox analysis was utilized.

Experimental Materials and Methods

Crude oil and water samples were collected on May 26, 2010 at N 28° 48.316, W 89° 07.949, which is approximately 47 miles northwest of the Deepwater Horizon spill site. Oil samples collected were thick and dark brown. The water samples were collected from a nearby area in the Gulf of Mexico that was not visibly contaminated with oil. After collecting, the water samples were filtered through 0.2 μm polycarbonate filters to sterilize the water and were subsequently stored at 4 °C.

Dichloromethane (DCM) and toluene were OmniSolv ultra high purity obtained from EMD. HPLC solvent grade pentane was obtained from J.T. Baker. Titanium (IV) oxide (anatase, nanopowder, < 25 nm, 99.7%) was obtained from Aldrich. Corexit EC9500A and Corexit 9572 were obtained from Nalco. Microtox diluent, osmotic adjusting solution, reconstitution solution, and acute reagent were obtained from SDIX.

To reduce the hydrophilicity of the TiO_2 nanoparticles and to make them more readily disperse in the oil, the photocatalysts were coated with stearic acid. Stearic acid coating was achieved by sonicating the oxide in an ethanol solution of steric acid (0.353 mM). After

sonication the sample was centrifuged, the ethanol was removed, and the coated oxide particles were dispersed in toluene.

Prior to exposure to simulated sunlight, 100 mg of crude oil was weighed and dissolved in a mixture of pentane and toluene (20:1). For samples treated with TiO_2 and/or dispersant, the photocatalyst and/or dispersant were added to the resulting mixture. The mixture was then sonicated to fully distribute the oil, dispersant and photocatalyst. The mixture was then poured onto the surface of 10 of mL Gulf water in a 150 mL water-jacketed beaker (5 cm i.d.). The sample was kept uncovered for 5 minutes to allow the pentane and toluene to evaporate. After drying the samples were exposed to 765 W/m^2 solar simulated light (Atlas Suntest CPS+ equipped with a 1500 W air cooled xenon arc lamp). Solar simulator intensity accounts for irradiations in the 300-800 nm range and not the full spectrum. During irradiation, the tops of the jacketed beakers were covered with a piece of quartz glass, and the samples were kept at 27°C by circulating thermostated water through the jacketed beakers. After irradiation the samples were either extracted with DCM for GC-FID and fluorescence analysis, or the aqueous layer was taken for Microtox analysis.

Oil extracts were analyzed on a Hewlett-Packard Agilent 6890 GC coupled to an auto sampler with a flame ionization detector and a $30 \text{ m} \times 0.32 \text{ mm}$ (i.d.) AT-1 capillary column. The injector and detector temperatures were set to 300°C and 350°C , respectively, and the temperature programming was as follows: 80°C held for 1 minute, ramp at $15^\circ\text{C}/\text{min}$ until a final temperature of 320°C which was held for 15 minutes.

Fluorescence excitation-emission matrices and synchronous scans were collected with a PerkinElmer LS 55 luminescence spectrometer. Synchronous scans on the diluted oil extracts were collected from 250 to 500 nm with a delta lambda of 25 nm and excitation and emission

slits set to 2.5 and 5.0 nm, respectively. Excitation-emission matrix scans were collected with an emission range from 300 to 600 nm and with excitation starting at 200 nm and incrementing every 5 nm until 400 nm. Excitation and emission slits were both set to 5.0 nm.

Microtox analysis was performed using a Microtox 500 analyzer (SDIX). The protocol used to analyze the toxicity of the water exposed to the oil was the comparison test for marine and estuarine samples. For each day Microtox was used, the basic test was run on phenol or zinc sulfate standards to ensure proper function of the Microtox analyzer and procedure.

Results and Discussion

The physical changes of the surface oil were visually recorded over time, Figures 5.1 and 5.2. After the oil-dispersant mixture was dried on the gulf water surface, the oil film had a rippled appearance. These ripples were not observed in previous studies performed on the surface oil without Corexit present (Chapter 4). In addition, samples with dispersant present did not exhibit the leathery and cracked appearance that was seen previously until after 12 hours of exposure. However, after 24 hours of irradiation little oil was observed on the surface of the aqueous layer.

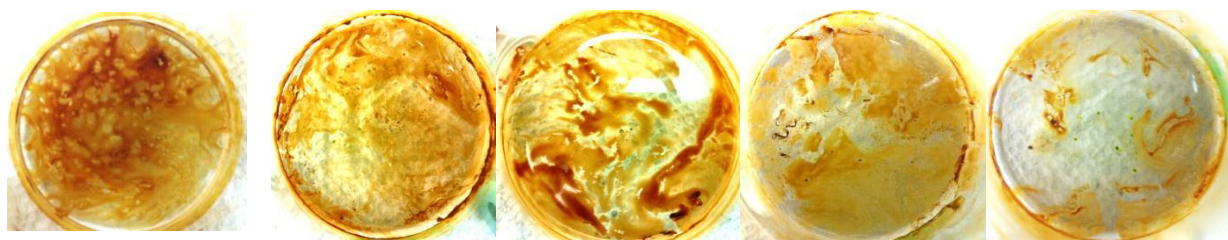


Figure 5.1. Appearance of surface oil with Corexit EC9500A as a function of irradiation time (from left to right): before irradiation, and after 3 hours, 6 hours, 12 hours, and 24 hours of irradiation

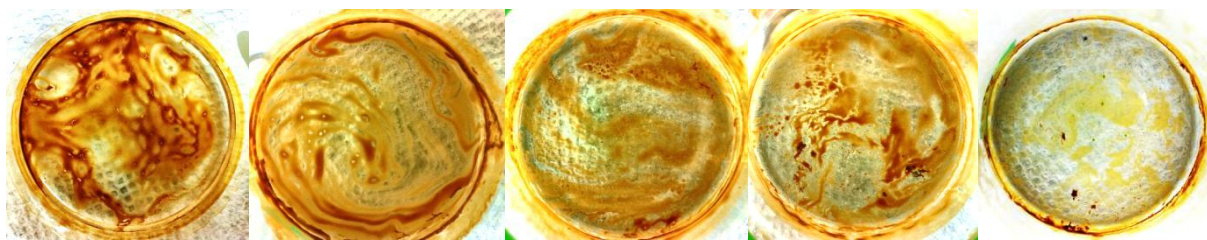


Figure 5.2. Appearance of surface oil with Corexit EC9527A as a function of irradiation time (from left to right): before irradiation, and after 3 hours, 6 hours, 12 hours, and 24 hours of irradiation

Trudel *et al.* have investigated the effectiveness of dispersants on different crude oils deposited on an aqueous surface.¹⁷⁶ In their studies the dispersibility of Corexit EC9500A was measured as the percent of oil recovered after 30 minutes of breaking wave action to mimic sea like conditions. To further confirm that the oil was being dispersed into the aqueous layer, the oil concentration and oil droplet size were measured in the aqueous layer. Trudel *et al.* studies concluded that the dispersants were only partially effective at viscosities of 2,500-18,690 cP and was ineffective at viscosities over 18,690 cP. In our studies oil was visually seen in the aqueous layer; however, the extent of the dispersed oil appeared minor. It is clear from the oil's thick molasses like texture that the surface oil that was used in our studies was of high viscosity, thus dispersant was not fully effective.

Fluorescence analysis of the DMC extracts of the irradiated oil samples was performed to analyze the change in the polycyclic aromatic hydrocarbon (PAH) concentration. Synchronous scans have been shown to be beneficial for the analysis of complex PAH mixtures.²⁶⁵ Previous studies on PAH mixtures have shown the advantages of synchronous scans, in particular the ability of wavelength regions to be sectioned based on the sizes of the PAH.^{205, 207} In general larger PAHs emit at longer wavelengths, while smaller PAH emit at shorter wavelengths. Based on this theory, the synchronous scan data has been separated and a wavelength has been chosen from each section as representative of the fluorescence for a range of PAH sizes. Figure 5.3 and 5.4 represent the degradation of the three different sizes of PAHs (small, medium and large) over

irradiation time. Studies conducted in Chapter 4 on the degradation of surface oil without dispersants indicated that large molecular weight PAHs degraded faster than smaller PAHs. With dispersants, only a slight increase in degradation was observed for the higher molecular weight PAH than the small PAHs. In contrast to our studies without dispersants, samples that contained dispersant had a decrease in the degradation of PAHs.

Synchronous scan data for most of the irradiated data indicate statistically equivalent degradation for samples with and without photocatalyst with their respective dispersant. There were only two deviations from uniform degradation: 12 hour irradiated Corexit EC9500A data and 6 hour Corexit EC9527 data. The TiO_2 Corexit EC9500A samples for the 12 hour irradiation exhibited an increase in degradation in comparison to the no oxide samples. In contrast increase in the degradation was observed for the no oxide Corexit EC9527A sample in comparison to TiO_2 samples after 6 hours of irradiation. Similar extents of degradation are observed after 3 hours of irradiation for both dispersant; however after 6 and 12 hours of irradiation increase in degradation of all sizes of PAHs are observed for Corexit EC9500A over Corexit EC9527A. In contrast, after 24 hours of irradiation lower percentages remaining are observed for Corexit EC9527A than Corexit EC9500A.

To measure the total PAH concentrations, the oil samples were analyzed via excitation-emission scans. To simplify the analysis of the excitation emission spectra, the largest peak from the 3-dimensional graph was chosen and the emission data were graphed over the course of the irradiation time, Figure 5.5. Degradation of the total PAHs emission was lower than our studies in Chapter 4 without dispersants present. This decrease is similar to the decrease that was observed in the synchronous scans. For both the samples without photocatalyst and samples with TiO_2 , there is a trend that Corexit EC9527A has a lower extent of degradation for the

samples irradiated for 3 hours than those for Corexit EC9527A. After 6 hours of irradiation the degradation pattern was reverse for the no oxide samples in that Corexit EC9527A had the lower percent remaining. After 12 hours of irradiation the total PAH concentration was similar for the 6 hours of irradiation for both of the dispersants. After 12 hours the degradation for the samples with and without photocatalyst was almost identical.

Overall, the photodegradation of PAHs decreased with dispersants present in comparison to our studies in Chapter 4 without dispersants. Possible reasons for this decrease may be due to the dispersants ability to increase the solubility of the PAH in the aqueous layer. This in turns changes the environment of the oil, thus in return changing the reactivity of the oil. In addition, dispersants added to the system can act as scavenger, thus reducing the PAH photooxidation.

Previous studies on alkane degradation suggest that n-alkanes are resistant to direct photolysis; therefore the photodegradation of n-alkanes must occur though indirect photolysis.²⁶⁶⁻²⁶⁸ Studies have found that n-alkanes will only undergo photodegradation when a photosensitizer is present^{238, 269}. Common photosensitizers in these studies were PAH alcohols and quinones, which are ordinary photooxidation products of PAHs. In addition, studies have found that alkyl-substituted alkane photodegradation is more probable than n-alkane photodegradation due to the added number of sites for oxidation.²¹³ In fact many studies have used the ratio of n-heptadecane to pristane and n-octadecane to phytane to detect the degree of oil weathering.

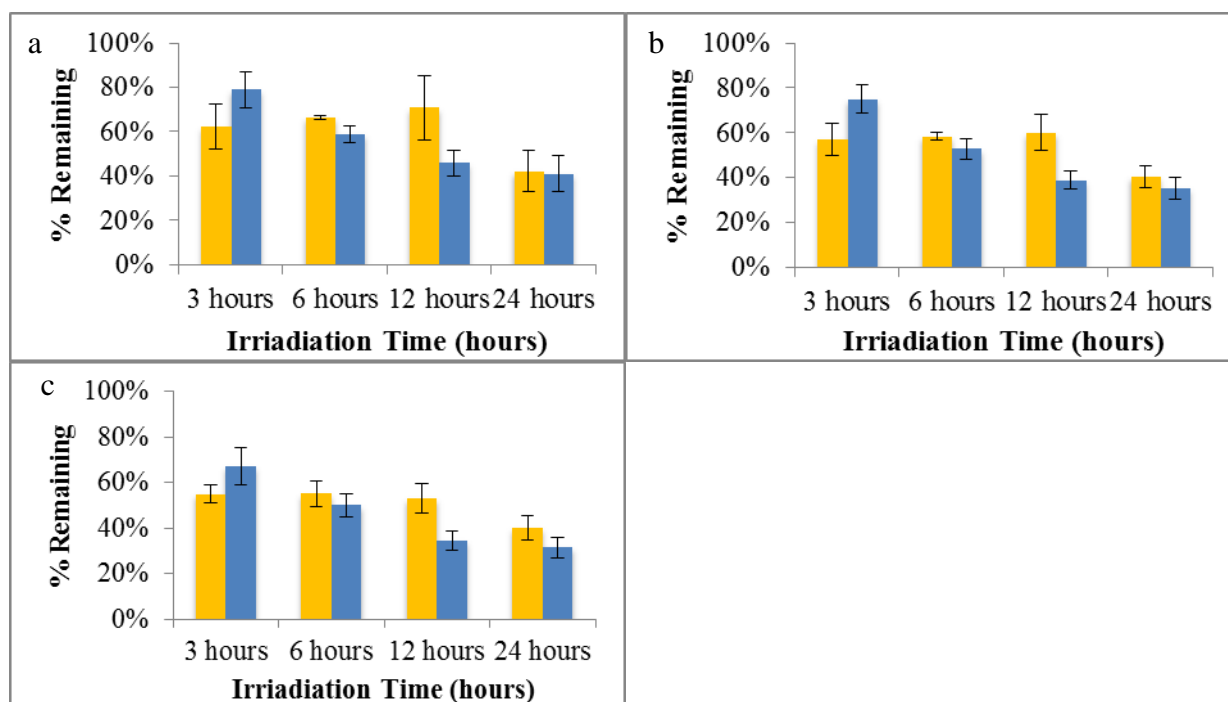


Figure 5.3. Synchronous scan of the irradiated samples containing Corexit EC9500A with $\Delta\lambda=25\text{nm}$. The percent remaining of PAH for (a) small (305 nm), (b) medium (326 nm) and (c) large (390 nm) molecules with no oxide (■) and TiO₂ (■).

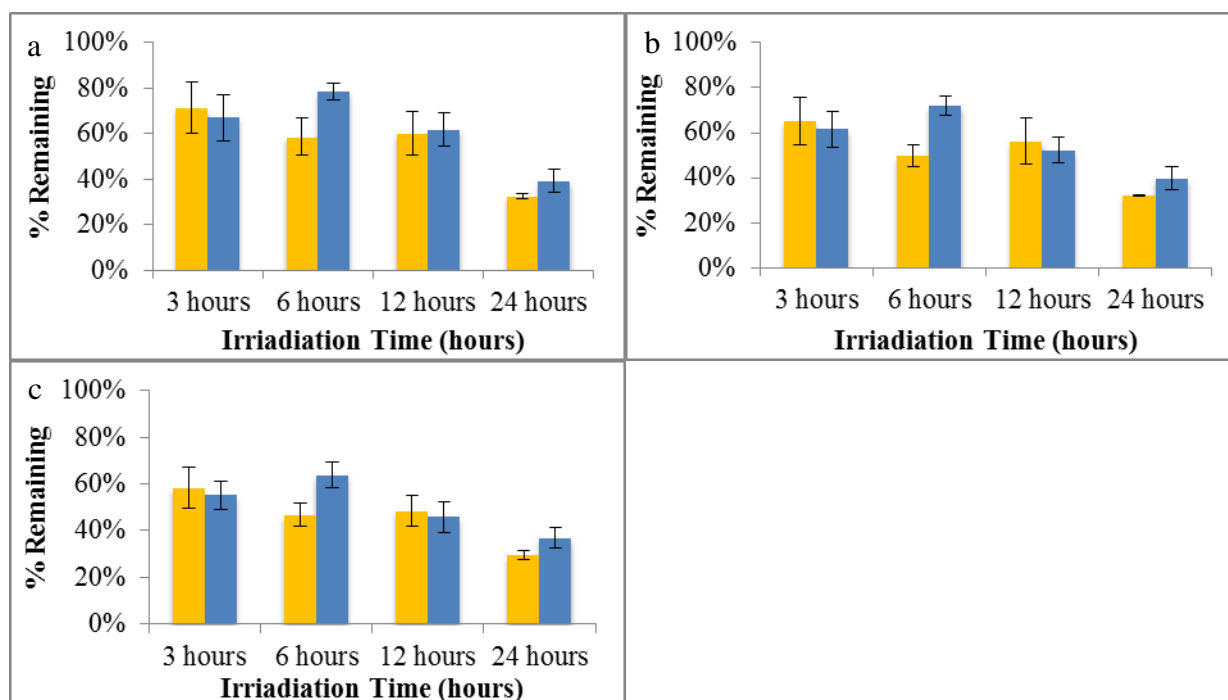


Figure 5.4. Synchronous scan of the irradiated samples containing Corexit EC9527A with $\Delta\lambda=25\text{nm}$. The percent remaining of PAH for (a) small (305 nm), (b) medium (326 nm) and (c) large (390 nm) molecules with no oxide (■) and TiO₂ (■).

two dispersants. Lower degradation intensities were seen for the TiO₂ samples after 3 hours and

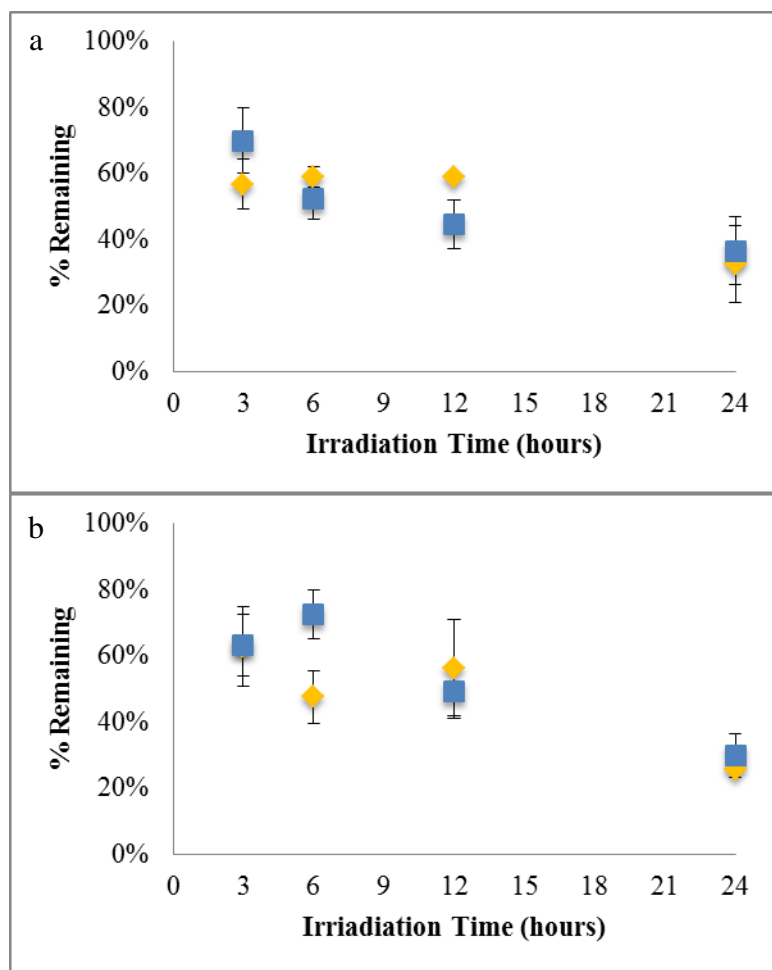


Figure 5.5. Percent remaining of total fluorescence of the DCM oil extracts after irradiation with (a) Corexit EC9500A and (b) Corexit EC9527A with no oxide (■) and TiO₂ (■). Excitation wavelength= 260 nm and emission wavelength = 375nm.

GC-FID analysis was performed on the DMC extract to monitor the changes in n-alkane concentration over irradiation time, Figures 5.6 and 5.7. It is evident from the graphs that the lower molecular weight n-alkanes decrease in concentration over time with respect to the dark control. However, consistent ratios of n-heptadecane to pristane and n-octadecane to phytane over degradation time suggest that photodegradation is not the reason for the decrease in the alkane concentrations, Tables 5.1 and 5.2. Similar to our study, Nicodem *et al.* studied the photochemical weathering of Brazilian crude oil by tropical sunlight.²⁴³ In their study n-heptadecane to pristane and n-octadecane to phytane ratio suggested that after 100 hours of

irradiation no photochemical transformation occurred to the alkane fraction. The most feasible explanation for the decrease in the alkane concentration in our studies is evaporation of the sample over time. In the solar simulator a current of air is used to cool the exposure chamber. This air current can aid in the evaporation of the samples. The loss was only evident in our irradiated samples because unlike our irradiated samples, the dark samples were not placed in the solar simulator.

Numerous studies have been conducted on the effects and toxicity of dispersants. Since the Deepwater Horizon oil studies have examined the effects of Corexit EC9500A on rats. Krajnak *et al.* reported an increase in heart rate and blood pressure and a decrease in responsiveness of tail arteries in rats after 1 day of inhalation exposure.²⁷⁰ Additionally, Sriram *et al.* observed significant neurological abnormalities in rats days after being exposed to 5 hours of inhalation of Corexit EC9500A.²⁷¹ However, Roberts *et al.* reported no pulmonary inflammation in rats after inhalation exposure to Corexit EC9500A.²⁷² Hemmer *et al.* compared the toxicity of 8 dispersants, including Corexit EC9500A, approved by the Environmental Protection Agency on mysid shrimp and inland silverside. In Hemmer's studies the toxicity of the dispersant, Louisiana sweet crude (LSC) oil, and a dispersant-LSC mixture was evaluated and it was reported that Corexit EC9500 was only slightly toxic to the mysid shrimp and was practically not toxic to the inland silverside.

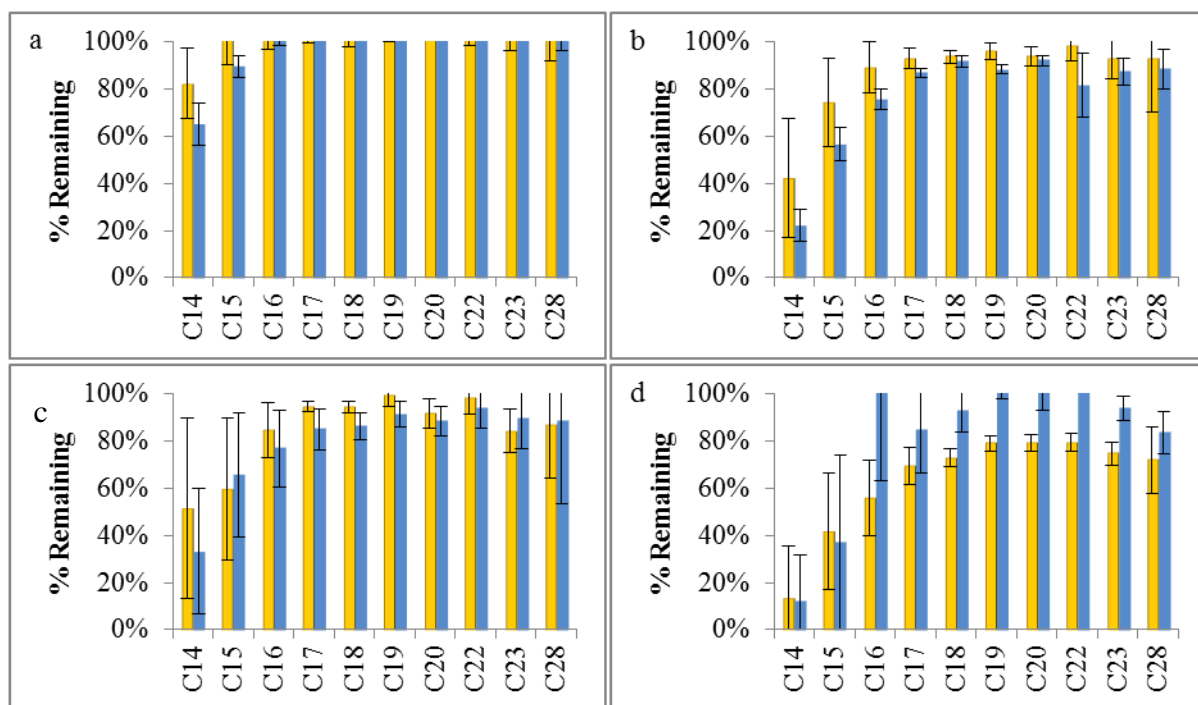


Figure 5.6. The GC-FID analysis of oil with Corexit EC9500A exposed to irradiation for (a) 3 hours, (b) 6 hours, (c) 12 hours, and (d) 24 hours with no oxide (■) and TiO₂ (■).

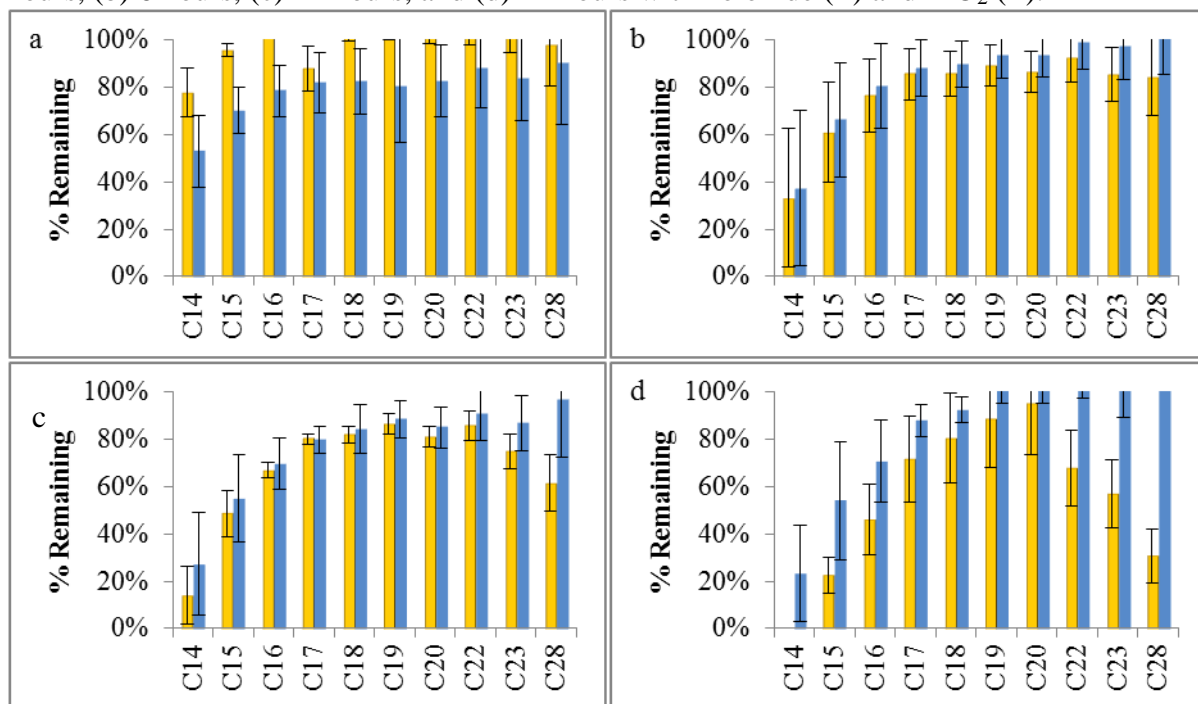


Figure 5.7. The GC-FID analysis of oil with Corexit EC9527A exposed to irradiation for (a) 3 hours, (b) 6 hours, (c) 12 hours, and (d) 24 hours with no oxide (■) and TiO₂ (■).

Table 5.1. The ratio of n-C17 to pristane and n-C18 to phytane over irradiation time in samples containing Corexit EC9527A

Time (hours)	n-C17:pristane				n-C18:phytane			
	No Oxide		TiO ₂		No Oxide		TiO ₂	
	Dark	Irradiated	Dark	Irradiated	Dark	Irradiated	Dark	Irradiated
3	0.78±0.03	0.65±0.08	0.68±0.11	0.67±0.08	0.46±0.01	0.46±0.01	0.45±0.00	0.46±0.01
6	0.76±0.04	0.68±0.09	0.69±0.12	0.63±0.08	0.45±0.02	0.46±0.00	0.47±0.00	0.47±0.01
12	0.79±0.02	0.61±0.02	0.61±0.00	0.67±0.08	0.47±0.00	0.46±0.01	0.45±0.00	0.46±0.01
24	0.68±0.07	0.73±0.03	0.63±0.04	0.71±0.11	0.46±0.03	0.46±0.01	0.46±0.00	0.47±0.00

Table 5.2. The ratio of n-C17 to pristane and n-C18 to phytane over irradiation time in samples containing Corexit EC9500A

Time (hours)	n-C17:pristane				n-C18:phytane			
	No Oxide		TiO ₂		No Oxide		TiO ₂	
	Dark	Irradiated	Dark	Irradiated	Dark	Irradiated	Dark	Irradiated
3	0.83±0.08	0.66±0.09	0.77±0.06	0.70±0.08	0.48±0.03	0.46±0.01	0.45±0.01	0.46±0.01
6	0.68±0.10	0.70±0.08	0.70±0.11	0.60±0.00	0.45±0.00	0.49±0.06	0.46±0.00	0.46±0.00
12	0.78±0.07	0.72±0.07	0.60±0.01	0.66±0.06	0.47±0.03	0.46±0.01	0.45±0.02	0.46±0.01
24	0.76±0.01	0.72±0.04	0.78±0.01	0.66±0.08	0.46±0.01	0.46±0.01	0.47±0.01	0.47±0.00

The toxicity of the photodegradation products were tested via Microtox analysis. Before the irradiated samples were tested, toxicity studies were conducted on the toxicity of irradiated dispersant samples without oil present, Figure 5.8. From the results it is evident that irradiation of the dispersants does not change toxicity, however the dispersants alone kill 35% of the test bacteria after 3 hours of exposure. After 6 hours of exposure to the dispersants, the toxicity of the gulf water are equal to the 3 hour irradiated samples for both the dark and irradiated samples.

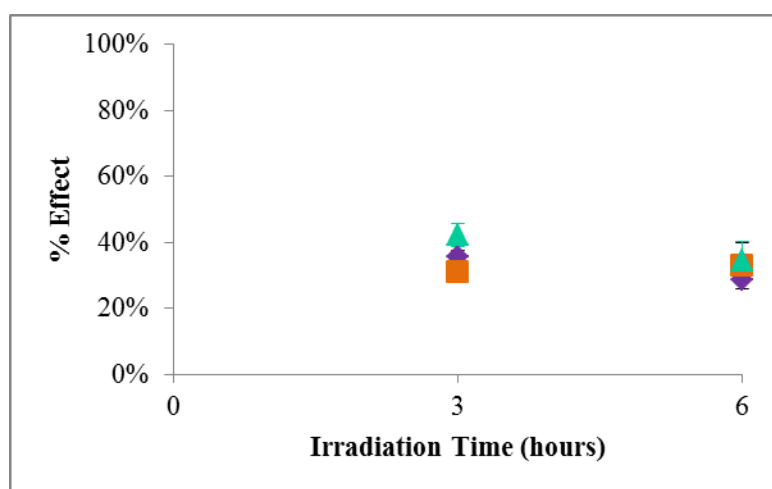


Figure 5.8. Microtox data of the toxicity of the aqueous layer of the dark (♦) and irradiated samples containing Corexit EC9500A (■) Corexit EC9527A (▲) without surface oil. Results displayed were outcome from the comparison test for marine samples

Figure 5.9 shows the toxicity of the irradiated surface oil samples with dispersants. Comparable to our previous studies in Chapter 4 without dispersant, the toxicity of the irradiated samples increased over time, which is due to the increase in toxic water soluble degradation products. In our previous studies without dispersant, toxicities after 3 hours of irradiation were 50% and 34% for the no oxide and TiO₂ samples, respectively. In our current studies with dispersants, after 3 hours of irradiation of oil with Corexit EC9527A, 80% of bacteria exposed to the aqueous fraction were killed and 75% were killed with TiO₂ present. For oil with Corexit EC9500A irradiated for 3 hours, 76% of bacteria exposed to the aqueous fraction were killed and

66% were killed with TiO_2 present. In contrast to our previous studies in Chapter 4, the no oxide and TiO_2 irradiated samples exhibited similar toxicities with both dispersants. After 24 hours of irradiation 100% of the test bacteria were killed with both dispersants, while an 82-91% effect was observed for studies without dispersant present. Differences in the values for the toxicity of the samples with and without dispersants are attributed to the dispersants' toxicity. The toxicity of the surface oil and dispersant were found not have an additive effect since the toxicity expected toxicity of the irradiated mixture was lower than sum of the toxicity of the oil and dispersant individually; however, the difference in the experimental value verses the expected value can be attributed to a small amount of the dispersants being confined in the oil film. These observations were similar to the findings in studies by Hemmer *et al.* in that the Louisiana sweet crude (LSC) oil was more toxic the Corexit EC9500A, however the Corexit EC9500A-LSC was less toxic than the and the LSC.^{178, 185}

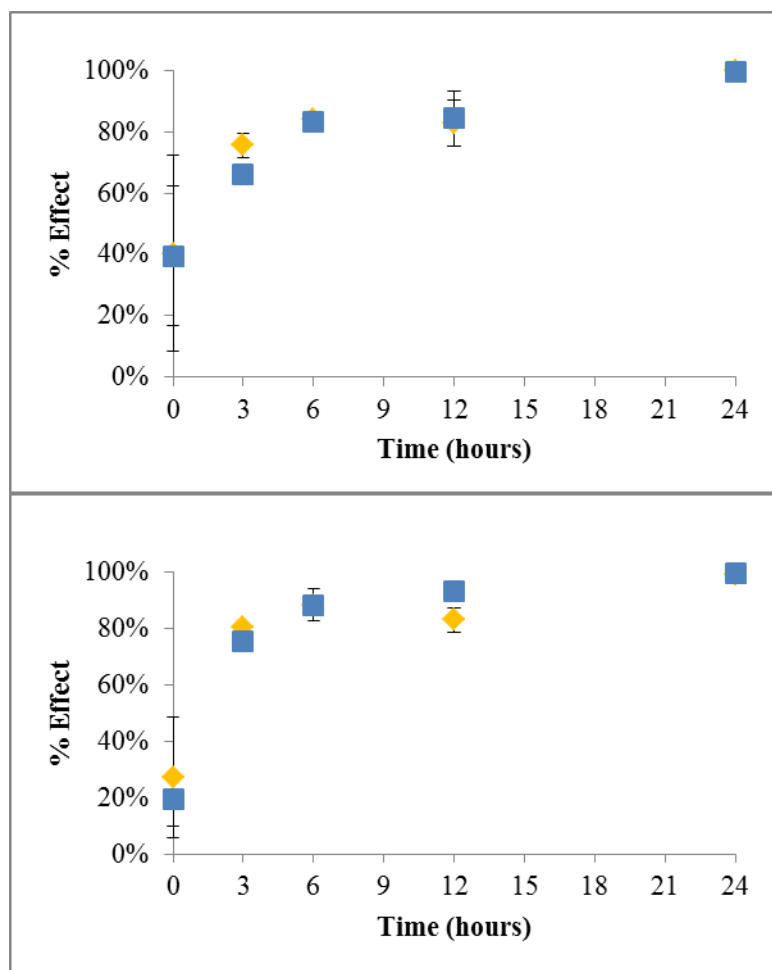


Figure 5.9. Microtox data of the toxicity of the aqueous layer of the surface oil irradiated samples containing (a) Corexit EC9500A and (b) Corexit EC9527A with no oxide (■) and TiO₂ (■). Results displayed were outcome from the comparison test for marine samples

Conclusion

Photodegradation of chemically dispersed Deepwater Horizon surface crude oil was studied. Unlike the results in Chapter 4, the larger PAH did not degrade faster than the small and medium PAH. In addition, chemically dispersed samples exhibited a lower extent of degradation in comparison to the non-dispersed samples in Chapter 4. Decreases in the degradation of the chemically dispersed oil in comparison to the non-dispersed oil were likely to be attributed to the increase in the solubility of the oil, thus changing the environment and the reactivity of the oil. Furthermore, the dispersant added can act as a scavenger of the reactive species thus reducing

degradation. PAH degradation of samples containing TiO_2 and Corexit EC9500A increase up to 12 hours; however minute changes were observed for the degradation of samples with Corexit EC9527A and no oxide samples with Corexit EC9500A up to 12 hours of irradiation. After 24 hours of irradiation, similar extents of degradation were observed for samples with and without photocatalyst. Similar to the surface only studies in Chapter 4, loss of C14-C18 alkanes was observed, however linear to branched alkane ratios indicate that the loss was not due to photodegradation but to evaporation. Toxicity studies found that dispersant alone killed 35% of the test bacteria. Increases in toxicities were observed over irradiation time for chemically dispersed surface oil, with 100% of the test bacteria killed after 24 hours of irradiation.

CHAPTER 6

PHOTOLYTIC AND PHOTOCATALYTIC DEGRADATION OF OIL FROM THE MACONDO WELLHEAD WITH AND WITHOUT DISPERSANTS

Introduction

Crude oil is a multicomponent mixture that varies depending on the geographical location of the oil source.¹⁶² Components of crude oil include hydrocarbons, metals, and polar compounds. Hydrocarbons are the most abundant portion of the oil and are comprised of paraffins, isoparaffins, cycloparaffins, aromatics, and olefins. Paraffins, isoparaffins, and cycloparaffins are classified as saturated hydrocarbons and account for a large portion of the oil. The aromatic portion consists of monocyclic and polycyclic aromatic hydrocarbons (PAHs). Depending on the source of the oil, PAHs can constitute 0-60% of the oil's components. Polar fractions include hydrocarbons that contain sulfur, oxygen, or nitrogen. These fractions and the metal fraction account for only a minute portion of the oil.

There are many physical processes that occur during the weathering of oil released into the environment, including dissolution, mixing, absorption, and evaporation. In addition, oil released into the environment undergoes chemical transformations via biodegradation and photodegradation. Previous studies on the biodegradation of crude oil have been shown to be beneficial to the degradation of alkanes.^{168, 202, 234} However, studies have observed that the rate of biodegradation is dependent on the availability of the nutrients in the surrounding environments.^{200, 201, 203} Nutrient deficient waters such as the Gulf of Mexico are limited by the

nutrient availability, thus biodegradation of contaminated sites can be very lengthy. Furthermore, larger molecular weight compounds, including PAHs and alkanes, are resistant to biodegradation, thus alternative methods are needed for degradation to occur.

Photodegradation has shown promise for degradation of compounds resistant to biotransformation. Numerous studies have been conducted on the photodegradation of crude oil.^{205, 243, 273} In some of these studies the oil was fractionated before exposure, which limited the interactions with other chemical species.^{213, 216, 240} Additionally, studies have been conducted using improper irradiation sources, such as mercury lamps.^{210, 222, 274} These irradiation sources do not accurately represent the solar spectrum. Studies have identified that spectral limitations and increased irradiation intensities have resulted in different rates of photodegradation in comparison to natural solar irradiation.^{238, 275}

To enhance the photodegradation of oil, photocatalysts have been added. Previous studies have examined the photodegradation of oils using titanium dioxide (TiO₂) as a photocatalyst.^{239, 242, 276} Studies by Nair *et al.* observed that without a photocatalyst, only PAHs that absorb in the near UV and visible ranges were degraded.²¹⁷ When a photocatalyst was added to the system, not only was an increase in degradation of the PAHs was observed, but also degradation of the oxidative products produced during photodegradation was observed. Ziolli *et al.* examined the photodegradation of the oil's water soluble fraction with and without TiO₂.^{216, 220} In these studies increase in photodegradation was reported with a photocatalyst present. In addition, complete removal of the aromatic fraction was reported after 6 hours of irradiation with TiO₂.

In this chapter, we investigated the photolysis of oil collected directly from the Macondo wellhead. Similar to studies conducted in Chapter 5 on surface oil, studies were conducted with

source oil that was chemically dispersed with the dispersants used in the Deepwater Horizon oil spill, Corexit EC9500A and Corexit EC9527A. Comparable to the surface oil of studies of Chapter 4, the aforementioned studies were conducted with and without TiO_2 as photocatalyst. To quantitate the degradation over irradiation time, GC and fluorescence were used. Additionally, Microtox was utilized to measure the toxicity of the aqueous layer of the irradiated samples.

Experimental Materials and Methods

Crude oil for irradiations was acquired from British Petroleum (BP). The oil obtained was collected from the Deepwater Horizon wellhead. Water samples were collected September 9, 2011 by Dr. Thomas Soniat from the Gulf of Mexico (Lake Jean Robin) at N 29° 43.801, W 89° 36.248. After collection the water samples were filtered through 0.2 μm polycarbonate filters to sterilize the water and were subsequently stored at 4 °C.

Dichloromethane (DCM) and toluene were OmniSolv ultra high purity obtained from EMD. HPLC solvent grade pentane was obtained from J.T. Baker. Titanium (IV) oxide (anatase, nanopowder, < 25 nm, 99.7%) was obtained from Aldrich. Corexit EC9500A and Corexit 9572 were obtained from Nalco. Microtox diluent, osmotic adjusting solution, reconstitution solution, and acute reagent were obtained from SDIX.

Prior to exposure to simulated sunlight, 120 μL of crude oil was added to 10 mL of sea water in a 150 mL water-jacketed beaker (5 cm i.d.). For samples treated with TiO_2 and/or dispersant, the photocatalyst and/or dispersant were added to the oil prior to depositing on the sea water and 125 μL of the mixture was added to the sea water. After depositing the sample on the water, the samples were exposed to 765 W/m^2 solar simulated light (Atlas Suntest CPS+ equipped with a 1500 W air cooled xenon arc lamp). Solar simulator intensity accounts for

irradiations in the 300-800 nm range and not the full spectrum. During irradiation, the tops of the jacketed beakers were covered with a piece of quartz glass, and the samples were kept at 27 °C by circulating thermostated water through the jacketed beakers. After irradiation the samples were either extracted with DCM for GC-FID and fluorescence analysis, or the aqueous layer was taken for Microtox analysis.

Oil extracts were analyzed on a Hewlett-Packard Agilent 6890 GC coupled to an auto sampler with a flame ionization detector and a 30 m × 0.32 mm (i.d.) HP-1 capillary column. The injector and detector temperatures were set to 300 °C and 350 °C, respectively, and the temperature programming was as follows: 80 °C held for 1 minute, ramp at 15 °C/min until a final temperature of 320 °C which was held for 8 minutes.

Fluorescence excitation-emission matrices and synchronous scans were collected with a PerkinElmer LS 55 luminescence spectrometer. Synchronous scans on the diluted oil extracts were collected from 250 to 500 nm with a delta lambda of 25 nm and excitation and emission slits set to 2.5 and 5.0 nm, respectively. Excitation-emission matrix scans were collected with an emission range from 300 to 600 nm and with excitation starting at 200 nm and incrementing every 5 nm until 400 nm. Excitation and emission slits were both set to 5.0 nm.

Microtox analysis was performed using a Microtox 500 analyzer (SDIX). The protocol used to analyze the toxicity of the water exposed to the oil was the comparison test for marine and estuarine samples. For each day that Microtox analysis was performed, the basic test was run on phenol or zinc sulfate standards to ensure proper function of the Microtox analyzer and procedure.

Results and Discussion

The composition of the source crude oil obtained by BP was different than the oil that was collected from the surface of the Gulf of Mexico used in our previous studies. Physically the oil that was obtained from the surface in Chapter 4 and Chapter 5 was thicker and had a molasses like fluidity. The source oil from BP was almost as fluid as water and in comparison to the surface oil had a stronger, pungent smell. The source oil formed a uniform layer without solvents when deposited on the surface of water; however, the surface oil clumped on the surface and would not form a layer unless solvents were added. Additionally, when the dispersants were added to the samples, the source oil mixed freely without any additional agitation. In comparison, the surface oil stayed together as a large mass when dispersants were added to the surface and little oil was visually dispersed into the aqueous layer. Dispersion of the source oil into the aqueous fraction reduced the amount of oil on the surface. Reduction in the amount of the source oil on the surface resulted in an increase in the evaporation of the water that would otherwise be covered by an intact oil film. Complete evaporation of the aqueous phase was observed for the 24 hour samples with photocatalyst, thus these samples were eliminated from this study.

During the extraction procedure, the unirradiated source oil samples did not form emulsions when mixed with DCM, however all samples of the surface oil did form emulsions during extraction with DCM. Previous studies have observed emulsification of weathered oil samples as oxidation products are produced.^{187, 188} The formation of the emulsions with the dark samples suggests that the surface oil samples were weathered prior to collection and that oxidation had already occurred prior to collection of the surface oil samples.

In addition to the differences in physical characteristics, some differences were also observed for the chemical compositions. Comparison of the fluorescence data between the two oils indicates that the PAH components did not change during the weathering processes. These results were expected since the PAH are not likely to undergo dissolution or biodegradation processes. Evaporation of the aromatics fractions does occur, but fluorescence of the volatile compounds are minor in comparison to highly fluorescent PAHs like pyrene. PAHs readily undergo phototransformations, however lack of differences in the PAH components suggest little to no photodegradation of the collected samples occur. In addition, differences were observed in the GC-FID chromatograms, Figure 6.1. The source oil contained peaks from 1.5 minutes to 5.8 minutes that were not present in the surface oil samples. Peaks in this region of the chromatogram were likely lost due to evaporation of the sample as it traveled to the collection site. Previous laboratory studies have confirmed the loss of alkanes up to C15 due to evaporation.^{191, 192} In addition to the loss of the lower molecular weight alkanes, increases in the humped portion of the chromatograph, also known as the unresolved complex mixture (UCM), were observed. Increases in the UCM have been previously reported for weathered crude oils.²⁰⁵

Previous studies have analyzed non-fractionated crude oil via fluorescence. In these studies synchronous scans were utilized to analyze the different molecular weight PAHs in a single fluorescence scan.^{248, 265, 277-279} Different ranges in the synchronous scans have been identified to correlate to the different size PAHs with the smaller PAHs emitting at shorter wavelengths and the larger PAHs emitting at longer wavelengths.^{205, 207} Based on these reports the synchronous scans were sectionalized and a wavelength was taken from each section to represent the small, medium, and large PAHs. Figures 6.2-6.4 show the synchronous scan data of the source oil samples. Higher extent of degradation was observed for the larger molecular

weight PAHs without dispersant present, Figure 6.2. Similar to our observations, Saeed *et al.* reported increase in the degradation of higher molecular weight PAHs in comparison to lower molecular weight PAHs at similar irradiation intensities.²⁸⁰ With the no dispersant samples, degradation without TiO₂ increased over the irradiation time; however, with TiO₂ present, no further degradation was observed during the 6 to 24 hour irradiation period. After 3 hours of irradiation, percent remaining differences were not observed between the no oxide and TiO₂ samples; however after 6 hours of irradiation the TiO₂ showed a slight decrease in the percent remaining in comparison to the no oxide samples. This pattern is reversed after 24 hours of irradiation in that the no oxide samples have a lower percent remaining.

In contrast to the no dispersant samples, larger PAHs did not degrade faster than the smaller and medium PAHs for samples with Corexit EC9500A present, Figure 6.3. A decrease in the percent remaining was observed over the irradiation times for both the no oxide and TiO₂ containing samples. Samples with TiO₂ exhibited increased degradation compared to the no oxide samples after 3 hours of irradiation; however, after 6 hours of irradiation similar extent of degradation was observed with or without the oxide present. Similar to the no dispersant samples, for samples containing Corexit EC9527A, larger PAHs showed more degradation than smaller PAHs. Minute differences in the percent remaining were observed for samples containing both TiO₂ and Corexit EC9527A over irradiation times, however over the irradiation time increases in degradation was observed for samples without photocatalyst up to 12 hours. Between 12 and 24 hours of irradiation little difference in degradation was evident in no oxide samples.

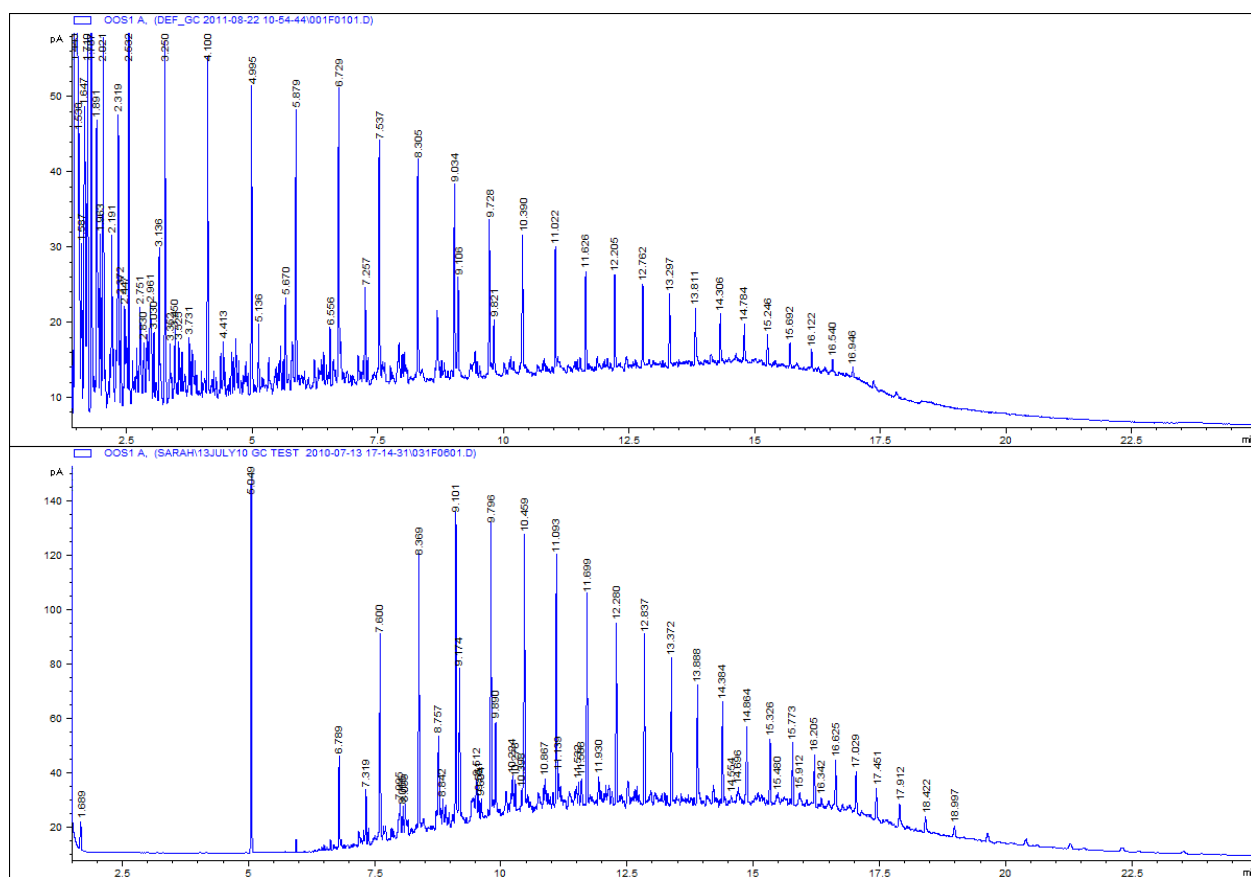


Figure 6.1. Gas chromatogram of (a) source and (b) surface oils. Surface oil sample was spiked with dodecane as an internal standard.

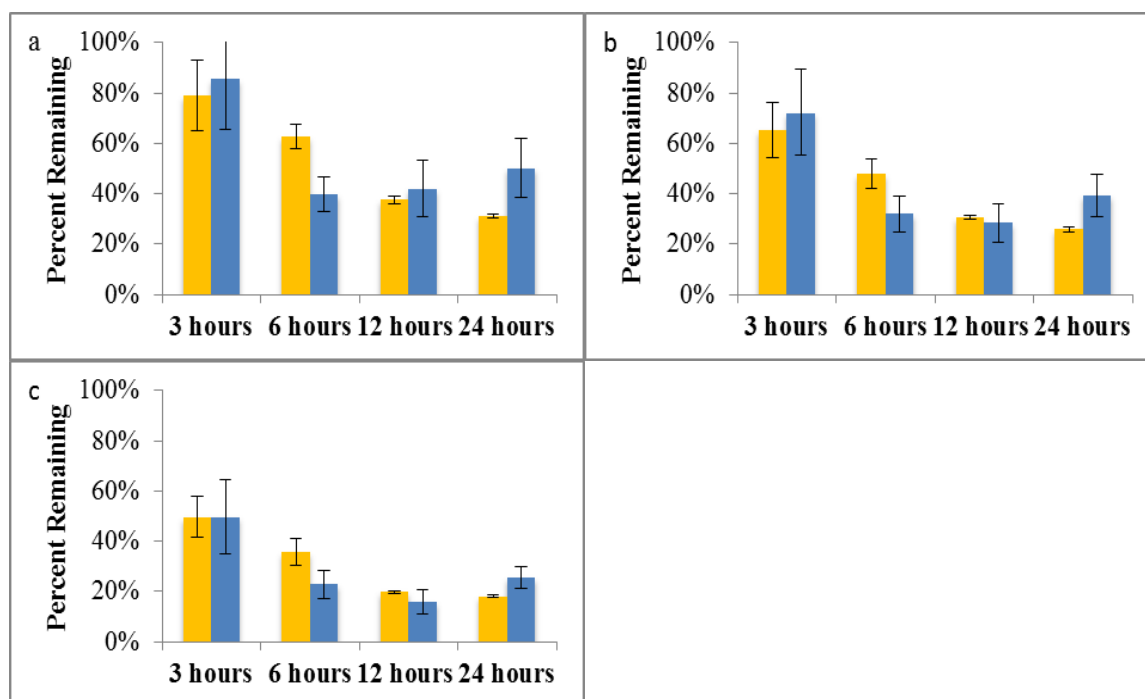


Figure 6.2. Synchronous scan of the irradiated samples containing no dispersant with $\Delta\lambda = 25\text{nm}$. The percent remaining of PAH for (a) small (305 nm), (b) medium (326 nm) and (c) large (390 nm) molecules with no oxide (■) and TiO₂ (■).

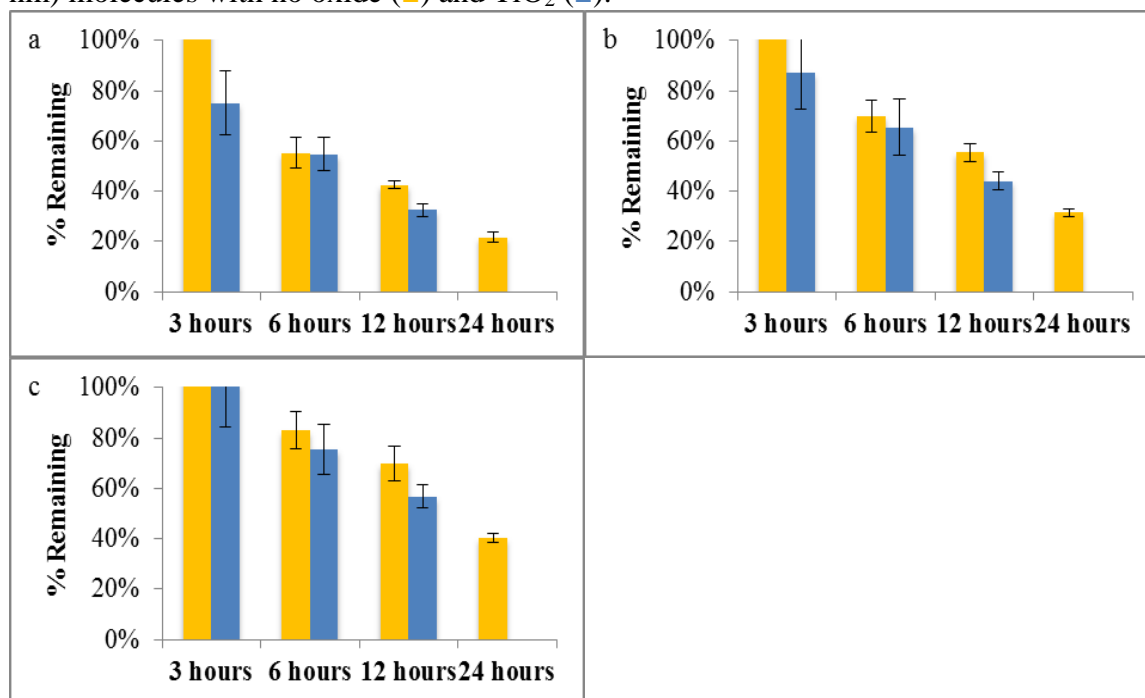


Figure 6.3. Synchronous scan of the irradiated samples containing Corexit EC9500A with $\Delta\lambda = 25\text{nm}$. The percent remaining of PAH for (a) small (305 nm), (b) medium (326 nm) and (c) large (390 nm) molecules with no oxide (■) and TiO₂ (■). TiO₂ samples for 24 hour irradiation were not reported due to evaporation of the aqueous layer.

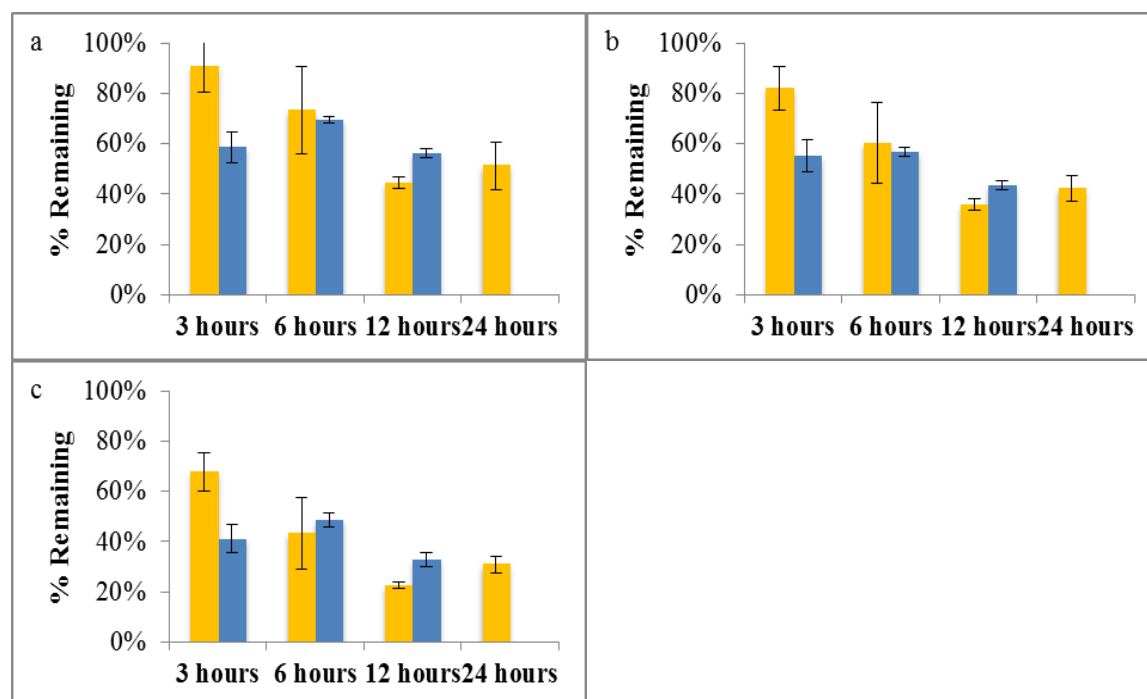


Figure 6.4. Synchronous scan of the irradiated samples containing Corexit EC9527A with $\Delta\lambda=25\text{nm}$. The percent remaining of PAH for (a) small (305 nm), (b) medium (326 nm) and (c) large (390 nm) molecules with no oxide (■) and TiO₂ (■). TiO₂ samples for 24 hour irradiation were not reported due to evaporation of the aqueous layer.

Similar to the non-dispersed surface oil samples in Chapter 4, increase in the photodegradation of large molecular weight PAHs was observed for the non-dispersed source oil samples. In comparison to surface oil samples, source oil no oxide non-dispersed samples have a higher percent remaining for the small and medium molecular weight PAHs and similar percent remaining for larger PAHs. Higher percent remaining was observed for the non-dispersed TiO₂ source oil samples than surface oil samples in Chapter 4. Higher percent remaining for the source oil can be attributed to the source oil having more components in the oil, some that may be more photochemically active. Surface oil samples studied in Chapter 5 containing Corexit EC9500A and no oxide had higher initial rates of degradation than the source oil samples; however after 24 hours of irradiation similar depletion of PAHs were observed. For source oil samples with both photocatalyst and Corexit EC9500A, lower rates of degradation were observed. Source oil samples with Corexit EC9527A but no oxide had a higher percent

remaining than the surface oil samples in Chapter 5 for the small and medium PAHs, though similar percent remaining were observed for larger PAHs. Source oil samples containing both TiO_2 and Corexit EC9527A had higher degradation rates than surface oil samples with TiO_2 and Corexit EC9527A.

In addition to the synchronous scans, excitation emission matrix scans were collected to analyze the total fluorescence of each sample.²⁴⁹⁻²⁵¹ With an excitation emission matrix, 3 dimensional graphs of the emission of the sample over different excitation wavelengths were constructed. Similar to previous studies, one excitation and emission wavelength was chosen to represent the overall fluorescence of the sample.²⁵² Excitation and emission wavelengths were chosen that corresponded to the highest peak of the 3 dimensional graph. Total fluorescence of the source oil with no oxide decreased over irradiation time for samples with and without dispersant added, Figure 6.5. After 6 hours of irradiation, no changes were observed in degradation for the samples containing TiO_2 without dispersants. A decrease in the total fluorescence was observed for samples containing Corexit EC9500A with and without photocatalyst as a function of irradiation time. In comparison to TiO_2 samples, increase in photodegradation was observed for no oxide samples containing Corexit EC9527A; however little difference in the percent remaining was detected for TiO_2 samples. After 24 hours of irradiation, lower total fluorescence was observed for no oxide samples that were non-dispersed in comparison to dispersed oil samples. The higher percent remaining for these samples is due to the increase solubility of the PAHs in the aqueous phase, thus changing the reactivity of oil. In addition, decrease in the degradation is attributed to the scavenging effects of the dispersants. After 24 hours of irradiation, the total fluorescence for the source oil without oxide with and without dispersants were similar to the respective surface oil samples. While the minute

differences were observed in the 24 hour irradiated samples, initial degradation occurred at a slower rate for the source oil samples in comparison to the surface oil samples in Chapter 4 and Chapter 5. For the no oxide source oil samples without dispersants, a lower percent of fluorescence was observed after 3 hours of degradation in comparison to the surface oil samples. After 6 hours of irradiation, fluorescence for the different oil sources were essentially identical; however after 12 hours of irradiation source oil samples exhibited a lower percent remaining than the surface oil samples. For source oil samples with Corexit EC9500A and Corexit EC9527A, higher fluorescence was observed after 3 and 6 hours of irradiation than the surface oil samples, however after 12 hours of irradiation fluorescence of the different oils were statically indistinguishable.

With the exception of the 6 hours samples, the total fluorescence of samples containing TiO_2 and no dispersant were higher in comparison to surface oil samples from Chapter 4. Like the no oxide samples, source oil samples containing TiO_2 and Corexit EC9500A had a higher percent remaining than the corresponding surface oil in Chapter 5 after 3 hours of irradiation, but the fluorescence intensity was equal to that of the surface oil after 12 hours of irradiation in comparison to the surface oil samples. Lower percent remaining was observed for all irradiation times for source oil than surface oil samples with TiO_2 and Corexit EC9527A.

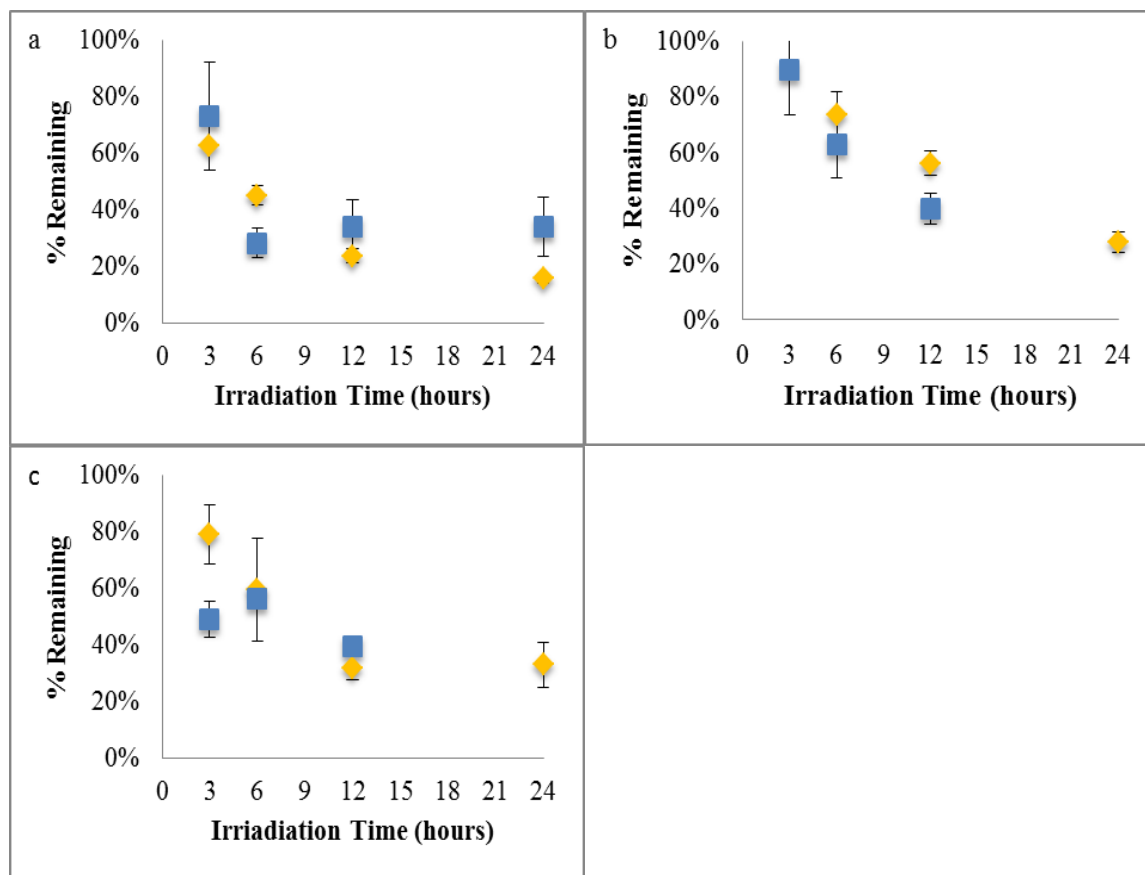


Figure 6.5. The percent remaining of the DCM oil extracts after irradiation of (a) no dispersant, (b) Corexit EC9500A and (c) Corexit EC9527A containing samples with no oxide (♦) and TiO₂ (■). Excitation wavelength= 260 nm and emission wavelength = 375nm. Chemically dispersed TiO₂ samples for 24 hour irradiation were not reported due to evaporation of the aqueous layer.

Previous studies examine the photodegradation of alkanes. In these studies alkane photodegradation was not observed.²⁴⁰ However, studies have reported photodegradation of alkanes with photosensitizers present in the pollutant matrix.^{213, 269, 281, 282} Additional studies on alkanes found that branched alkanes undergo photodegradation more readily than linear alkanes, and a ratio comparison can be made of the two to indicate the extent of photodegradation. Alkane degradation was analyzed via GC-FID, Figures 6.6-6.8. For all samples with and without dispersants, loss of lower molecular weight alkanes was observed over irradiation time. For samples with dispersants, higher percent remaining were observed for the lower molecular

weight alkanes in comparison to samples without dispersant present. These trends in the alkane disappearance are similar to that of the surface oil samples.

To determine if the loss of the samples was due to photodegradation, the ratios of n-heptadecane (n-C17) to pristane and n-octadecane (n-C18) to phytane was compared, Tables 6.1-6.3. For most of the irradiations the ratio of the linear alkanes to the branched alkanes were not statistically different, which suggests that photodegradation was not occurring. In some circumstances the ratios between the dark and the irradiated samples were statistically different. A decrease in the ratio of n-heptadecane to pristane was observed for the no dispersant samples irradiated for 24 hours. Decrease in the irradiation ratio represents a decrease in the pristane concentration which suggests photodegradation is occurring. Statistical differences were also observed for several of the TiO₂ containing samples. For these samples, increases in the ratios were observed for the irradiated samples over the dark samples. Increasing ratios suggest that the linear alkanes were degrading more than the branched alkanes. Alkanes are not readily photodegraded due to the lack of ability to absorb light; however photocatalyst in the system absorb the light. The light absorbed by the photocatalyst produces an electron-hole pair that can react with water to produce hydroxyl radical or with oxygen to produce a superoxide radical. The hydroxyl radical and superoxide radicals can react with the alkanes to produce oxidized species. The increase in the n-C17/pristane and n-C18/phytane ratios for the TiO₂ samples and not the no oxide samples suggest that photocatalytic degradation is occurring. Linear to branched alkane ratio statistical differences were not observed for all of the TiO₂ samples. Crude oil contains an assortment of compound in the system that are each activated differently by photolysis. Variations in the branched to linear alkane ratios suggest different photochemical processes are occurring.

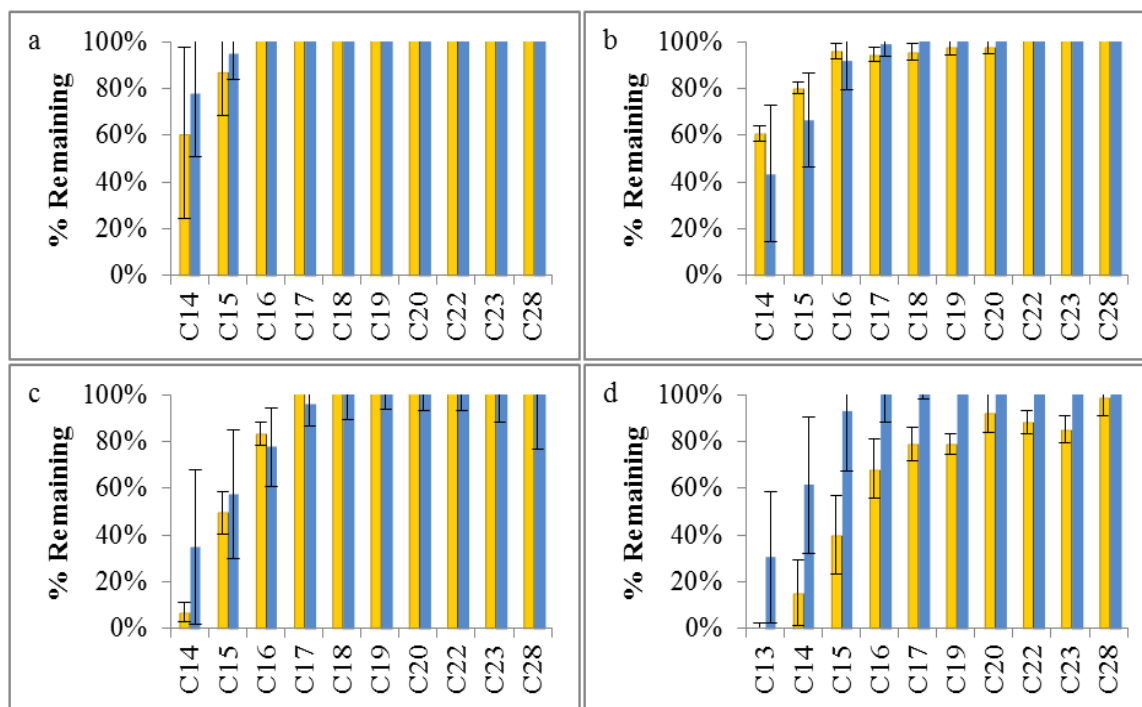


Figure 6.6. The GC-FID analysis of oil without dispersant exposed to irradiation for (a) 3 hours, (b) 6 hours, (c) 12 hours, and (d) 24 hours with no oxide (■) and TiO_2 (■).

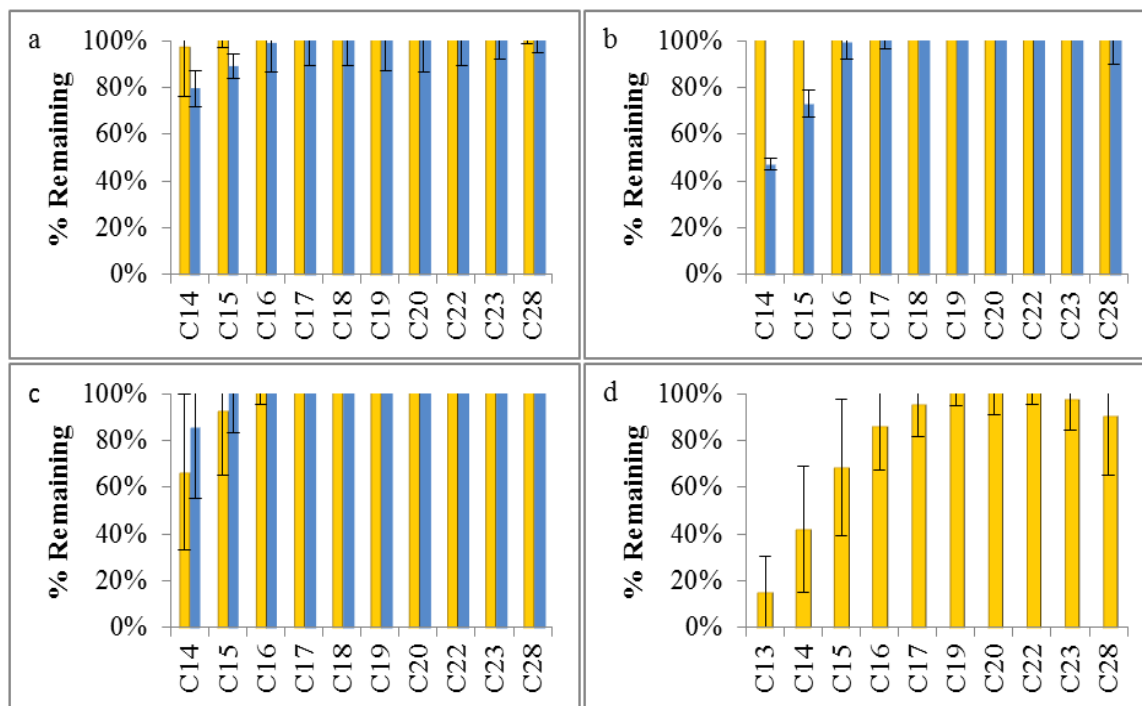


Figure 6.7. The GC-FID analysis of oil with Corexit EC9500A exposed to irradiation for (a) 3 hours, (b) 6 hours, (c) 12 hours, and (d) 24 hours with no oxide (■) and TiO_2 (■). TiO_2 samples for 24 hour irradiation were not reported due to evaporation of the aqueous layer.

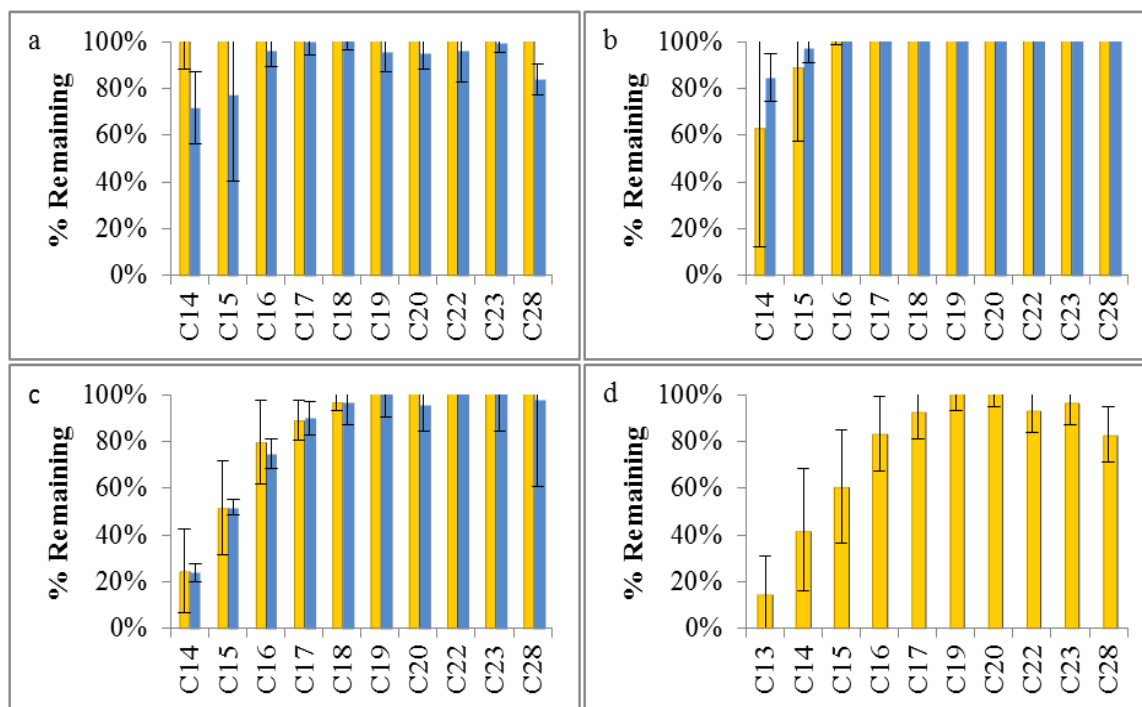


Figure 6.8. The GC-FID analysis of oil with Corexit EC9500A exposed to irradiation for (a) 3 hours, (b) 6 hours, (c) 12 hours, and (d) 24 hours with no oxide (■) and TiO_2 (■). TiO_2 samples for 24 hour irradiation were not reported due to evaporation of the aqueous layer.

Table 6.1. The ratio of n-C17 to pristane and n-C18 to phytane over irradiation time in samples without dispersant

Time (hours)	n-C17:pristane				n-C18:phytane			
	No Oxide		TiO ₂		No Oxide		TiO ₂	
	dark	irradiated	dark	irradiated	dark	irradiated	dark	irradiated
3	0.77 ± 0.13	0.76 ± 0.16	0.62 ± 0.03	0.71 ± 0.14	0.45 ± 0.05	0.48 ± 0.00	0.43 ± 0.00	0.48 ± 0.01
6	0.71 ± 0.13	0.69 ± 0.12	0.59 ± 0.00	0.75 ± 0.11	0.45 ± 0.02	0.49 ± 0.00	0.42 ± 0.01	0.48 ± 0.01
12	0.78 ± 0.24	0.63 ± 0.03	0.65 ± 0.05	0.73 ± 0.10	0.47 ± 0.02	0.49 ± 0.01	0.46 ± 0.01	0.48 ± 0.01
24	0.87 ± 0.01	0.68 ± 0.08	0.57 ± 0.04	0.65 ± 0.10	0.48 ± 0.01	0.48 ± 0.00	0.40 ± 0.06	0.48 ± 0.01

Table 6.2. The ratio of n-C17 to pristane and n-C18 to phytane over irradiation time in samples with Corexit EC 9500A

Time (hours)	n-C17:pristane				n-C18:phytane			
	No Oxide		TiO ₂		No Oxide		TiO ₂	
	dark	irradiated	dark	irradiated	dark	irradiated	dark	irradiated
3	0.56 ± 0.05	0.59 ± 0.06	0.56 ± 0.03	0.58 ± 0.04	0.45 ± 0.05	0.41 ± 0.02	0.39 ± 0.02	0.40 ± 0.04
6	0.61 ± 0.07	0.66 ± 0.09	0.57 ± 0.00	0.63 ± 0.08	0.45 ± 0.02	0.47 ± 0.01	0.37 ± 0.00	0.45 ± 0.01
12	0.55 ± 0.04	0.65 ± 0.09	0.56 ± 0.01	0.60 ± 0.01	0.47 ± 0.02	0.46 ± 0.01	0.38 ± 0.02	0.45 ± 0.01
24	0.66 ± 0.08	0.71 ± 0.10		0.47 ± 0.01	0.47 ± 0.01			

Table 6.3. The ratio of n-C17 to pristane and n-C18 to phytane over irradiation time in samples with Corexit EC 9527A

Time (Hours)	n-C17:pristane				n-C18:phytane			
	No Oxide		TiO ₂		No Oxide		TiO ₂	
	dark	irradiated	dark	irradiated	dark	irradiated	dark	irradiated
3	0.58 ± 0.01	0.62 ± 0.03	0.57 ± 0.02	0.56 ± 0.03	0.45 ± 0.05	0.46 ± 0.02	0.38 ± 0.02	0.38 ± 0.03
6	0.59 ± 0.00	0.61 ± 0.03	0.58 ± 0.01	0.63 ± 0.07	0.45 ± 0.02	0.46 ± 0.03	0.38 ± 0.02	0.44 ± 0.00
12	0.60 ± 0.04	0.60 ± 0.01	0.59 ± 0.01	0.59 ± 0.01	0.47 ± 0.02	0.47 ± 0.01	0.42 ± 0.04	0.44 ± 0.02
24	0.71 ± 0.10	0.66 ± 0.10			0.48 ± 0.01	0.47 ± 0.00		

Previous studies have identified an array of oxidative products produced through photodegradation including alcohols, ketones, aldehydes, carboxylic acids, esters, epoxides, phenols, and quinones.^{205, 221} These oxidative products are known to have increased water solubility in comparison to crude oil. Studies have reported that the increased solubility of the degradation products increases the number of components in the aqueous phase, thus producing increases in the toxicity of the aqueous phase.^{268, 283, 284} Microtox analysis was employed to determine the toxicity of the irradiated samples. Microtox utilizes fluorescent bacteria, *Vibrio fischeri*, to determine the toxicity of the samples. The toxicity of a sample is reported as the % Effect which correlates to the decrease in the fluorescence of the bacteria that has been exposed to a potentially toxic sample. The higher the reported % Effect the more test bacteria that have been killed and the increase in toxicity of the samples.

Minute differences were observed for the toxicity of the dark samples of source oil with and without dispersants present which indicates that the dispersants did not increase nor decrease the toxicity of source oil, Figure 6.9. These results contradict previously reported results that the mixture of dispersant and oil are less toxic than the oil samples alone.^{178, 185} For the non-dispersed samples, toxicity increase for both the no oxide and TiO₂ samples over irradiation time. After 6 hours of irradiation, the TiO₂ samples were slightly less toxic than the no oxide sample, but after 24 hours of irradiation equal toxicity was observed, in that 100% of the test bacteria are killed. The no oxide Corexit EC9500A samples increase toxicity over irradiation time, resulting in 100% of the test bacteria killed after 24 hours of irradiation. Only slight increases in the toxicity were observed over irradiation time for samples containing Corexit EC9500A and TiO₂. Fluorescence of these samples decreased over irradiation time which proposes that either (1) the products produced with TiO₂ present are less toxic than the products

without photocatalyst or (2) degradation of the photodegradation products. Previous studies have observed higher toxicity of photodegraded oil samples with TiO_2 after 1 day of irradiation compared to samples without catalyst; however after 2 days irradiation no toxicity was observed for the TiO_2 samples.²¹⁶ The increase in toxicity followed by a drastic decrease suggests that with TiO_2 present caused an increase in the degradation rates of the photodegradation products. Differences in the toxicity of Corexit EC9527A with and without photocatalyst samples were not observed until 12 hours after irradiation and these samples exhibited equal toxicities for all irradiated samples. After 24 hours of irradiation the no oxide, Corexit E9527A containing samples killed only 92% of the test bacteria. A decrease in the toxicity of these samples in comparison to the non-dispersed and Corexit EC9500A samples can be possibly attributed to the degradation of the photooxidation products.

Corexit EC9527A contains 2-butanoxylethanol as a solvent. Previous studies have found 2-butanoxylethanol to be an endocrine disruptor. Since this compound is absent in Corexit EC9500A one would expect that samples with Corexit EC9500A would be less toxic than samples with Corexit EC9527A. In contrast to this prediction, source oil with Corexit EC9500A samples were found to be more toxic than source oil with Corexit EC9527A. Decrease in the toxicity can be contributed to the lower photodegradation rates with Corexit EC9527A. The lower degradation rates decreases the number of products released, thus decreasing the overall toxicity of the samples.

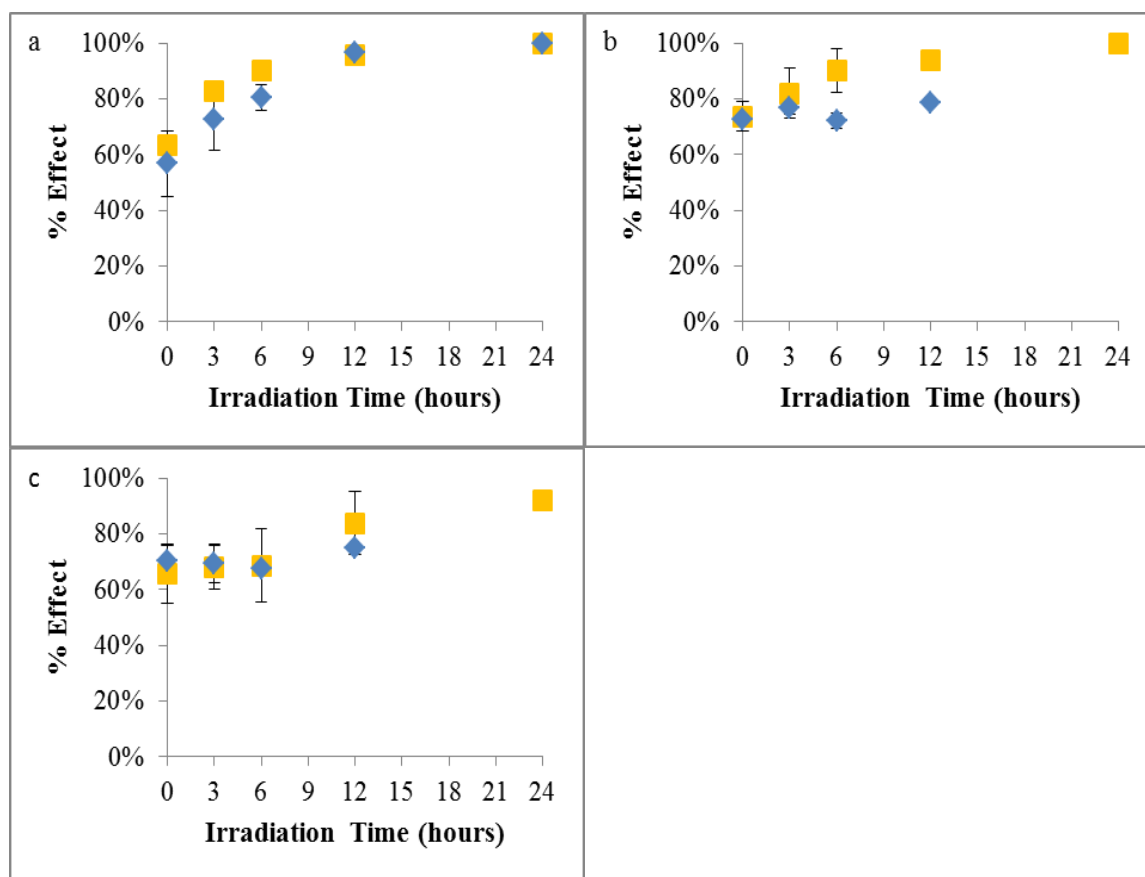


Figure 6.9. Microtox data of the toxicity of the aqueous layer of the irradiated samples containing (a) no dispersant, (b) Corexit EC9500A and (c) Corexit EC9527A with no oxide (■) and TiO_2 (◆). Results displayed were outcome from the comparison test for marine samples. Chemically dispersed TiO_2 samples for 24 hour irradiation were not reported due to evaporation of the aqueous layer.

Higher toxicity was observed for the source oil dark samples in comparison to the surface oil samples previously studied in Chapter 4 and Chapter 5. Toxicity of the unirradiated surface oil samples was not observed due to the fact that the oil samples underwent weathering before collection, which depleted the more water soluble and hence more toxic fractions of the oil. When the source oil samples were exposed to the aqueous layer, the polar fractions were released to the water, thus increasing the toxicity of the unirradiated source oil samples compared to the surface oil samples. In comparison to their corresponding surface oil samples, higher toxicities were observed for the source oil samples with no oxide only samples and Corexit EC9500A samples with and without photocatalyst; however, after 24 hours of irradiation 100% of the test

bacteria were killed in both systems. After 3 hours of irradiation higher toxicity was observed for Corexit EC9500A TiO_2 source oil samples than their respective surface oil sample, but in these same samples lower toxicities were observed after 6 hours of irradiation. In comparison to the correlating surface oil samples, decreased toxicity of the source oil samples was observed for Corexit EC9527A samples with and without photocatalyst present.

Conclusion

In this chapter, the photodegradation of source oil from the Macondo wellhead was studied. Similar to the Chapter 4 and Chapter 5 the surface oil studies, higher extent of degradation was observed for the larger PAHs in comparison to the small and medium PAHs for the non-dispersed and Corexit EC9527A samples. Additionally, lower extent of PAH degradation was observed for the chemically dispersed source oil in comparison to the chemically dispersed surface oil. Decreases in PAH concentrations were observed for the no oxide samples with and without dispersant over irradiation time up to 12 hours of irradiation, whereas decrease was only observed for the TiO_2 samples with Corexit EC9500A. Similar to the surface oil studies in Chapter 4 and Chapter 5, loss of the C14-C17 alkanes as observed. Comparisons of the linear to branched alkanes indicate that most samples did not undergo photodegradation. Unlike the surface oil studies, degradation of the branched alkanes was observed for non-dispersed samples without photocatalyst after 24 hours of irradiation. Additionally, degradation was also observed for linear alkanes with TiO_2 present which reflect the importance of the photocatalyst in the degrading compounds resistant to photochemical transformations. Toxicity studies of the non-irradiated source oil samples killed 60% of the bacteria. Addition of dispersants to the non-irradiated source oil samples killed 70% of the bacteria. Similar to the surface oil samples in Chapter 4 and Chapter 5, the toxicity of the

irradiated non-dispersed samples and no oxide samples with Corexit EC9500A increased over time. Chemically dispersed samples containing TiO_2 exhibited no increase in toxicity over irradiation time.

Chapter 7

CHEMICAL AND PHYSIOLOGICAL MEASURES ON OYSTERS FROM OIL-EXPOSED SITES IN LOUISIANA

Introduction

The Deepwater Horizon oil spill devastated the Gulf of Mexico ecosystem. To fully understand the effects of the oil spill, short term and long term studies are needed. Short term studies have been conducted on the embryotoxicity of weathered Deepwater Horizon oil.²⁸⁵ This study observed lethal effects for fertilized duck eggs after 4 days of exposure. Milroy *et al.* monitored macrofauna PAH concentrations in the Mississippi Sound after the Deepwater Horizon oil spill.²⁸⁶ Six weeks after the capping of the well head, macrofauna PAH concentrations in the Mississippi Sound were found to be as high as 42,620 ppb. Additionally, the National Oceanic and Atmospheric Administration (NOAA) monitored the number of stranded cetaceans during and after the oil spill.²⁸⁷ In comparison to averages from 2002-2009, cetacean strandings have risen 469% during the spill (April-July 2010) and 449% after the spill (August 2010-August 2011). Furthermore, the number of stranded premature, still born, and neonatal bottle nose dolphins intensely increased during February (36) and March (30) in comparison to pre-spill records (1 and 11, respectively). In addition to the surge in stranded cetaceans, NOAA has observed an increase in the number of stranded sea turtles in 2011.²⁸⁸

Of the marine species, bivalves are thought to be keystone to understanding the pollution in marine environments.^{289, 290} Filter feeding allows for contaminant to bioaccumulate in the organisms. Moreover, due the immobility, oysters have been the focus of many studies to fully

comprehend the level of contamination. A previous study compared the level of oil pollutants in oysters with those of the surrounding soil.²⁹¹ That study observed that the pollutant concentrations were lower than detectable limits in the soil, while the oyster samples indicated high levels of contaminants. In addition, Kumar *et al.* observed that in some contaminated sites the total polycyclic aromatic hydrocarbon (PAH) concentration in oysters was 15 times higher than the surrounding soil.²⁹² Luna-Acosta *et al.* studied the effects of oil and chemically dispersed oil on oysters.²⁹³ In their studies they observed a PAH body burden of 2.7 times higher for oysters exposed to an oil-dispersant mixture compared to those exposed to oil only.

In this research we have studied the physical and chemical effects of oyster samples 6 months after the capping of the Deepwater Horizon well head. This study has been completed in collaboration with Dr. Thomas Soniat and Megan Thorne from the University of New Orleans Biology Department. Dr. Soniat has monitored the physiological changes and has studied the presence of *Perkinsus marinus* (Dermo) infection in the oyster collected. Our participation in the project was to monitor the PAH concentrations in the collected oysters. The physiological and chemical results were compared to correlate the data.

Experimental Materials and Methods

Samples were collected by Dr. Soniat from Lake Borgne and Mississippi Sound in Louisiana on January 4, 2011. Position and depth were determined using a Garmin 440S Chartplotter/Fishfinder. Shelton and Hunter observed hypoxia in oil contaminated soil samples and an increase in hypoxia with thermohaline stratification.²⁹⁴ To assess if hypoxia conditions are present, top and bottom temperatures, salinities, and oxygen concentrations were measured (Yellow Springs Instrument Model 85 T/S/O meter), Table 7.1.

Table 7.1. Environmental conditions at oyster collection sites. Area 1 includes the un-oiled sites (1-3), whereas Area 2 includes the oiled sites (4-6).²⁹⁵

Area	Site	Bottom Temp (°C)	Bottom Salinity (ppt)	Bottom Oxygen (ppm)	Top Temp (°C)	Top Salinity (ppt)	Top Oxygen (ppm)	Depth (m)
1	1	10.5	9.0	10.2	10.5	8.9	9.9	2.9
1	2	10.4	12.8	9.5	10.5	9.7	10.15	2.9
1	3	10.5	15.0	9.4	10.4	12.1	10.21	3.2
2	4	10.9	17.8	9.64	11.3	17.5	9.84	4.3
2	5	10.6	25.3	9.23	10.6	24.8	9.27	2.3
2	6	11.2	28.4	9.08	11.1	27.6	8.98	2.8

Figure 7.1 is the areas sampled for this study. There were two areas sampled – an un-oiled area in Lake Borgne (area 1, stations 1-3) and an oiled area in Mississippi Sound (area 2, stations 4-6). Studies by NOAA indicated that the Mississippi Sound was moderately contaminated throughout the duration of the oil spill, Figure 7.1b, and trace levels of oil are still currently being detected. For each station a minimum of 3 or more dredge samples were taken until 15 adult sized oysters were retrieved. The oysters were kept refrigerated overnight. The next day 3 or 4 of the oysters from each site were shucked and the shell length and oysters weight was recorded, Table 7.2. The oysters were then homogenized and frozen until PAH analysis.

For the PAH analysis, the thawed oysters were extracted using the Agilent QuEChERS method. For the QuEChERS method, 15 mL of acetonitrile (EMD, HPLC grade) was added to 5 g of the homogenized oysters and vortexed for 1 minute. The QuEChERS salt packet (6 g MgSO₄, 1.5 g NaC₂H₃O₂) was then added and the mixture was vortex for an additional minute. The sample was then centrifuged for 10 minutes at 3000 rpm. The supernatant was then filtered with a 0.2 µm PTFE filter and stored at 4°C until analysis.

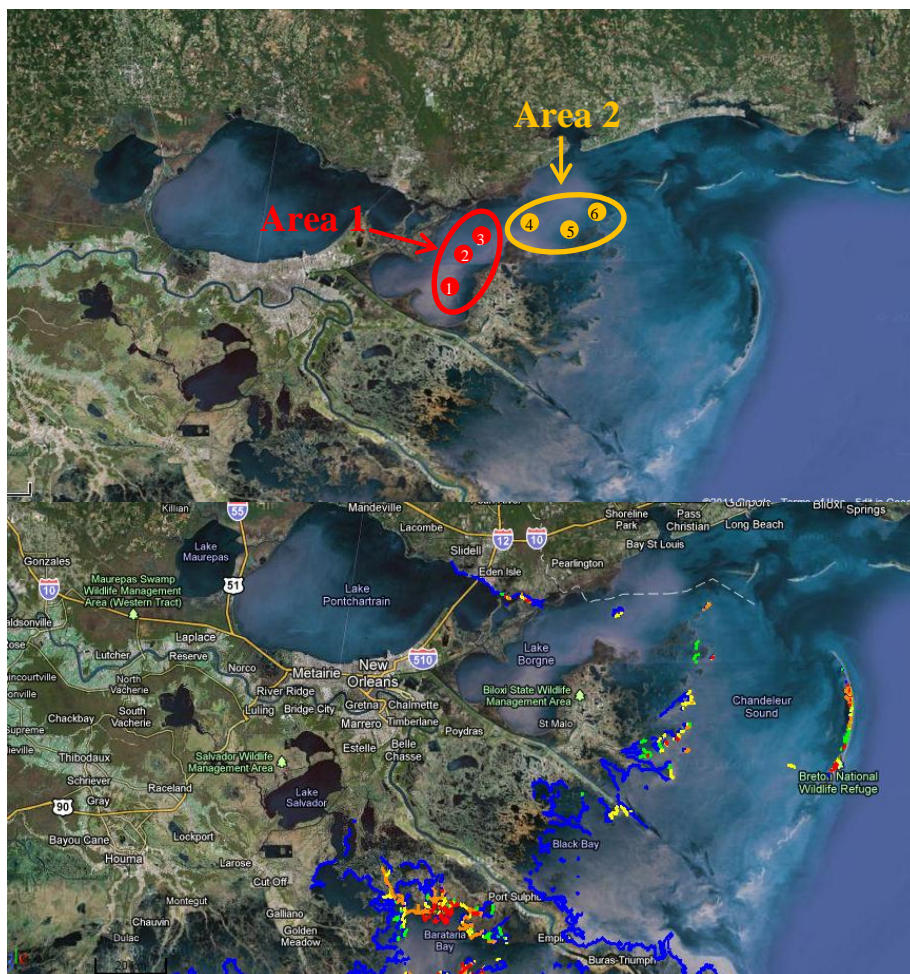


Figure 7.1. (a) Map of collection sites. Area 1: site 1, 2, 3 (un-contaminated sites) and Area 2: sites 4, 5, 6 (contaminated sites). (b) The 08-May-11 SCAT oiling ground observations. Oil contamination is reported as follows: heavy (●), moderate (●), light (●), very light (●), no oil found (●), trace <1% (July 22, 2010).¹⁵⁹

Before analysis the extracts were diluted 1:1 with water. The samples were then analyzed using an Agilent 1100 high performance liquid chromatograph with a Zorbax Eclipse PAH analytical column (4.6 x 50 mm 1.8 μ m) coupled to a HP 1046A fluorescence detector. The flow rate was 0.8 mL/min and the LC and fluorescence parameters are listed in Tables 7.3 and 7.4. Fluorescence scan experiments were conducted on a PerkinElmer LS 55 luminescence spectrometer. Excitation wavelength for the full fluorescence scans was 260 nm with emissions collected from 300-500 nm and the excitation and emission wavelengths of 5 nm.

Table 7.2. Weight and shell length of the oysters used for PAH analysis

Area 1				Area 2			
Site	Oyster	Shell height (mm)	Meat weight (g)	Site	Oyster	Shell Height (mm)	Meat Weight (g)
1	1	69.61	7.57	4	1	104.25	21.83
	2	69.18	10.45		2	85.47	16.62
	3	73.73	10.71		3	101.37	25.83
	4	70.50	7.89				
2	1	97.83	17.27	5	1	93.58	17.26
	2	99.44	15.08		2	96.57	15.99
	3	87.35	14.52		3	106.02	19.70
	4	93.58	23.13		4	93.58	18.50
3	1	104.29	21.83	6	1	93.93	22.97
	2	85.47	16.62		2	99.13	24.76
	3	101.37	25.83		3	97.47	26.71
	4	120.06	31.63		4	101.95	23.99

Table 7.3. Mobile phase parameters for PAH analysis

Time (min)	% Acetonitrile	% Water
0	60	40
1.5	60	40
7	90	10
13	100	0
30	100	0
30.01	60	40
35	60	40

Table 7.4. Fluorescence parameters for PAH analysis

Time (min)	λ_{ex} (nm)	λ_{em} (nm)	PMT-Gain
0	260	352	13
5.5	260	420	13
15.25	260	460	13

Results and Discussion

Extraction methods were verified by spiking store bought oysters (Motivatit Seafoods) with a 16 QTM PAH mixture (Supleco). Calibration curves were constructed and the percent recoveries for each PAH was calculated, Table 7.5. Detection limits for the PAHs were 15ng/g of wet oyster weight. For the 16 PAHs, 13 were observed with a similar recovery as reported by Gratz *et al.*²⁹⁶ In addition, 11 of the 13 PAH recoveries were 75% or above, which is acceptable

with biological samples. Recoveries of 74.3% and 57.6% were observed for benzo[a]pyrene and benzo[g,h,i]perylene which are known to be challenging to extract from biological samples.

Table 7.5. Percent recoveries of the PAHs monitored

PAH	% Recovery
naphthalene	104.7
acenaphthene	107.2
fluorene	89.1
phenanthrene	87.2
anthracene	82.2
fluoranthene	96.0
pyrene	95.8
benz[a]anthracene	81.3
chrysene	93.3
benzo[b]fluoranthene	76.1
benz[a]pyrene	74.3
dibenz[a,h]anthracene	76.0
benzo[g,h,i]perylene	57.6

Oyster samples from oiled and un-oiled sites were analyzed for PAH content, Figure 7.2. It is evident from the chromatogram that 12 of the 13 PAHs monitored were not found in either of the oyster samples. A peak at 12 minutes coincided with the retention time of benzo[a]pyrene; however, this peak was also observed in the uncontaminated and reference oyster samples. To further study this peak, the compound was collected and analyzed using fluorescence spectroscopy, Figure 7.3. From the spectra it is obvious that the 12 minute peak observed in the oyster extracts was not benzo[a]pyrene. Since the peak was observed in all the oyster samples, it is concluded to be a component of the oysters.

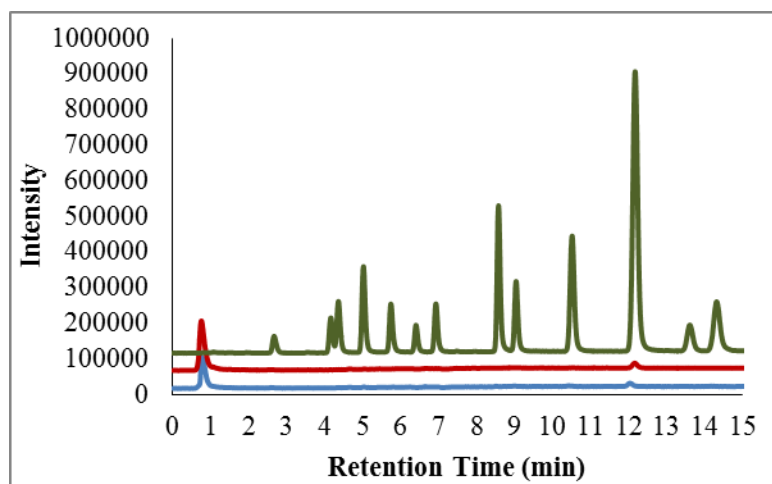


Figure 7.2. LC-FLD chromatogram of the PAH standard (—), un-oiled (—) and oiled samples (—).

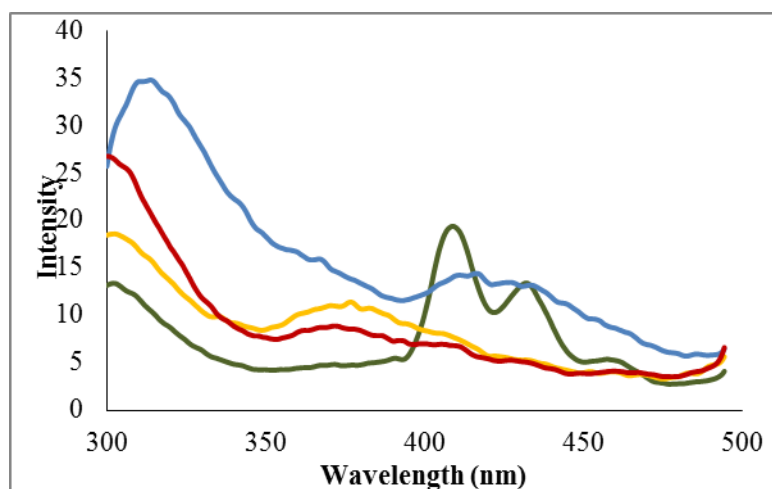


Figure 7.3. Fluorescence scan of the 12 minute peak: benzo[a]pyrene (—), purchased oyster (—), un-oiled oyster (—), and oiled oyster (—).

Michael *et al.* studied the PAH concentrations in oysters in El Salvador after a small shallow oil spill in which dispersants were used.²⁹⁷ In that study, high concentrations of PAHs from the source oil were observed 7 days after the spill. After 28 days, the concentration of PAHs decreased 94-98%. Six months after the spill low levels of PAH were still detected, but identification data suggested PAH sources other than the oil spill. In contrast, Neff *et al.* monitored the PAHs in oysters for 27 months after the *Amoco Cadiz* oil spill.²⁹⁸ PAHs were detected 27 months after the spill; however, it is suspected that the oysters were recontaminated

23 months after the spill from a storm induced resuspension of the contaminated sediment. Kelly *et al.* observed PAH concentration in oyster to range from 20.2 to 484µg/kg dry weight 10 months after the Jiyeh oil spill.²⁹⁹ A key factor to consider during the comparison of PAH concentration to those previously reported is that most reported detectable PAH concentrations are given in dry weight values. For our study, we have reported the wet weight concentrations which can be 2 to 15 times lower than dry weight values. In addition, some studies do not identify that the PAHs detected are those of the source oil. Therefore, it is possible that the PAH detected could be contributed from other oil sources or other PAH sources (i.e. pyrogenic sources).

Barszcz *et al.* studied the physiological changes to oysters that were chronically exposed to low levels of oil. In their studies they found that oil exposure led to reduced food intake and an emaciated appearance.³⁰⁰ In addition, they observed that the oyster tissues were clear and the connective tissue was swollen. To evaluate the health of the oysters, Dr. Soniat calculated the condition index of 10 oysters collected from each site, Table 7.6. To calculate the condition index the oyster's wet meat weight was divided by the shell weight and the resulting value was multiplied by 100. From the data it is evident that the condition index of the oiled oysters rival that of the un-oiled oysters, thus suggesting that the oysters were relatively healthy.

Table 7.6. Reproductive, condition and disease metrics based on composites of 10 oysters. Area 1 includes the un-oiled sites (1-3), whereas Area 2 includes the oiled sites (4-6). GI = Gonadal Index, CI = Condition index, PF = Percent female, WP = Weighted prevalence, II = Infection intensity, and PI = Percent infection.²⁹⁵

Area	Site	GI	CI	PF	WP	II	PI
1	1	6.38	8.58	60	0	0	0
1	2	5.35	10.24	50	0	0	0
1	3	5.15	9.43	60	0	0	0
2	4	7.17	11.05	60	0	0	0
2	5	7.61	8.46	80	0.33	0.56	60
2	6	8.75	8.86	80	0.6	0.86	70

Dermo disease prevalence was measured for the collected oysters. Samples collected from un-oiled sites did not exhibit Dermo disease; however, most samples from 2 of the 3 oiled sites were infected. Wilson *et al.* observed a significant increase in Dermo disease in oysters exposed to PAHs.³⁰¹ In addition, studies have established that infection intensities increase in salinities above 20 ppt.^{302, 303} In our study, PAH contamination was not detected in any of the oyster samples. Consequently, Dermo infection is due to the high salinities at sites 5 and 6.

Conclusions

Approximately six months after the capping of the Macondo wellhead, no PAH contamination was found in oysters from oil and un-oiled sites. Differences in the Dermo infection, condition, and reproductive state were observed in oiled sites versus un-oiled sites. These variations were concluded to be due to natural differences in the salinities of the two sites and not to PAH contamination.

Chapter 8

Summary and Future Work

Toxic pollutants pose severe risk to the environment and species depending on the environment for survival. To alleviate the toxicity risks, remediation of polluted areas is needed. The research presented in this dissertation focused on two different methods of remediation for two classes of pollutants: Fenton degradation of TNT and photolytic degradation of oil from the Deepwater Horizon oil spill. In addition to these studies, oil contaminated oysters were analyzed for PAH accumulations.

The first study presented in this dissertation was the Fenton degradation of TNT. These experiments were conducted at near neutral pHs with varying iron concentrations. In these studies a maximum of 44% of the TNT was removed with 0.75 and 1 mM of iron. After the reaction proceeded for 1.5 minutes, degradation of TNT ceased due to the precipitation of iron at the near neutral pHs. Higher iron concentration resulted in the decrease in degradation rate due to the surplus of iron acting as a radical scavenger. When β -cyclodextrin and carboxymethyl- β -cyclodextrin were added to the reaction, an increase in degradation was observed; however, at lower iron concentrations inhibition of TNT degradation was observed. The increase in the degradation of TNT at higher iron concentration is the result of the formation of binary and ternary complexes and to the formation of secondary radicals that are more efficient at degrading the TNT. Addition of the hydroxyl radical scavenger diethyl ether to the cyclodextrin systems, did not result in a decrease in the degradation rate as was previously observed in other studies with different pollutants. In fact, the diethyl ether caused enhanced degradation of TNT. Since diethyl ether is not environmentally friendly, studies were conducted on polyethylene glycol (MW = 200, 400, 600 g/mol), diethylene glycol, diethyl ether, dipropyl ether, ethanol, ethyl

acetate, or methanol. In comparison to water only reactions, increases in degradation rates were observed in reactions with all organic modifiers but methanol. Further investigation of polyethylene glycol (PEG) at different iron concentrations displayed similar results as seen with the cyclodextrins: lower iron concentration led to a inhibition in degradation while higher iron concentration resulted in an increase in degradation in comparison to water systems. Pseudo first order rate constants were compared and the enhancement of TNT degradation in the presence of organic modifiers followed the trend: PEG 600 ~ PEG 400 > β -CD ~ PEG 200 > CM- β -CD.

Studies were conducted on the mechanism of Fenton degradation with PEG present via comparing the rate constants of Fenton degradation of other nitrotoluenes and monitoring the production of nitrate and ammonium. Pseudo first order rate constants for 2-nitrotoluene was almost 10 times that for TNT without PEG present; however with PEG present, TNT's rate constants was 10 time larger than 2-nitrotoluene. Since 2-nitrotoluene is much more readily oxidized than TNT and TNT is much more readily reduced than 2-nitrotoluene, it is evident that Fenton degradation of TNT with PEG proceeds through a reductive pathway. Analysis of ionic products of the Fenton reactions showed that without PEG present only nitrate was produced. When PEG was present nitrate production decreased and ammonium was produced. The productions of ammonium in the reactions with PEG indicate that when PEG is present in the system a reductive pathway is occurring.

Studies presented in this dissertation have observed increases in the Fenton degradation of TNT with a series of organic modifiers. Studies have proven that Fenton degradation in the presence of PEG proceeds though a reductive pathway. Future work will investigate Fenton degradation with PEG on other readily reduced pollutants such as polychlorinated biphenyls. In

addition experiments will be conducted to examine the degradation interferences from natural organic matter, such as fulvic and humic acids.

The second topic presented in this dissertation was the photolytic degradation of oil from the Deepwater Horizon oil spill. These studies were conducted on weathered oil collected from the Gulf of Mexico surface and source oil collected from the Macondo wellhead. In addition to using different oil samples, studies were conducted with and without photocatalyst (TiO_2 and Fe_2O_3) and with and without dispersants (Corexit EC9500A and Corexit EC9527A). Degradation in the studies was determined by monitoring the changes in PAH and alkane concentration over time. In addition, toxicity of the photodegradation products were monitored over time.

Visually, the dispersants had little effect on the surface oil, however rapid mixing was observed for source oil samples with dispersants. With all samples the oil was physically diminished over the irradiation time. Decrease in the PAH concentration was observed with irradiation for all samples. Identical rates of PAH degradation were observed for Fe_2O_3 and no oxide samples for the surface oil samples. For non-dispersed and Corexit EC9527A samples increase in the degradation of large molecular weight PAH in comparison to the lower molecular weight PAHs was observed. Almost all samples exhibited a decrease in degradation when dispersants were present. This decreased can be attributed to two mechanisms. The first is the increase in water solubility of the oil, which changes the reactivity of the oil due to the change in the environmental interactions, oil matrix in direct contact with air verses oil dissolved in water. The second reason for the decrease in degradation is that the dispersant can scavenge reactive intermediates so that they cannot react with the oil components.

Alkane analysis indicated a loss in lower molecular weight alkanes during irradiation. Heptadecane to pristane and octadecane to phytane ratios indicated that in surface oil samples photodegradation was not occurring. Further studies determined that loss of the lower molecular weight alkanes was due to evaporation. Similar loss was observed for source oil samples, but the linear to branched alkane ratios indicated that after 24 hours of irradiation branched alkanes did undergo some degradation for the no oxide samples without dispersant. Additionally, increases in the ratios were observed for the TiO_2 which suggest that the linear alkanes were degrading in the systems with TiO_2 present.

Increases in the toxicity were observed for all samples over irradiation time. Unirradiated surface oil samples were found to be relatively nontoxic. Lower toxicities were observed after 3 and 6 hours for non-dispersed irradiated surface oil samples with photocatalyst. Dispersants alone were found to kill 35% of test bacteria, however in comparison to the dispersant only samples slight decreases in toxicity were observed in the dispersed oil samples. Indistinguishable toxicities were observed for dispersed oil samples with and without TiO_2 . Dark source oil killed roughly 60% of the test bacteria. Increases in the toxicity of the source oil in comparison to the surface oil are due to the presence of the water soluble polar products, which were previously depleted in the surface oil. Non-dispersed TiO_2 samples exhibited slightly less toxicity than the no oxide samples for 3 and 6 hours. Adding dispersants to the source oil increased the unirradiated source oil sample toxicity to 70 percent. Similar toxicities were observed for Corexit EC9527A samples with and without photocatalyst, however for Corexit EC9500A with TiO_2 samples showed lower toxicities for 6 and 12 hour irradiated samples in comparison to the no oxide samples. After 24 hours of irradiation, all samples exhibited indistinguishable toxicities whether or not photocatalyst were present in the system. After 24 hours of irradiation, non-

dispersed surface oil samples killed 82% and 89% of the test bacteria for no oxide and TiO₂, respectively and no oxide Corexit EC9527A samples killed 92% of the test bacteria. In all other studies 100% of the test bacteria was killed after 24 hours.

Future research on the oil project will study the mechanism of photodegradation and the photodegradation products. To study the mechanism a variety of different methods will be employed. To analyze the kinetics of alkane photodegradation, the oil will be separated into different fractions and analyzed via GC-FID and GC-MS. Additionally, studies will be conducted with a series of scavengers to better understand the role that hydroxyl radical, singlet oxygen, and triplet oxygen play during the photodegradation of oil. To study the products of photodegradation, HPLC-MS studies will be conducted on the aqueous portion of the reaction system. The aforementioned studies will be conducted with and without photocatalyst present. In addition to the TiO₂ nanoparticles previously studied, ZnO nanoparticles, TiO₂ nanotubes and ZnO nanotubes will be studied. Furthermore, the above studies will be conducted with chemically dispersed oil.

References

1. Yinon, J., *Toxicity and Metabolism of Explosives*. CRC Press: Boca Raton, 1990; p 176.
2. Patterson, J.; Shapira, N. I.; Brown, J.; Duckert, W.; Polson, J. *State-of-the-art Military Explosives and Propellants Production Industry. Volume I. The military explosives and propellants industry*; Am. Def. Prep. Assoc.: 1976; p 96 pp.
3. Meyer, R., *Explosives*. 3rd ed.; VCH Verlagsgesellschaft: Weinheim, New York, 1987.
4. Akhavan, J., *The chemistry of Explosives, Second Edition*. Royal Society of Chemistry: 2004; p 180 pp.
5. Wilbrand, J., Notiz über Trinitrotoluol. *Annalen der Chemie und Pharmacie* **1863**, 128 (2), 178-179.
6. Beilstein, F.; Kuhlberg, A., Untersuchungen über Isomerie in der Benzoëreihe. Dreizehnte Abhandlung. Ueber einige Derivate des Aethylbenzols. *Justus Liebigs Annalen der Chemie* **1870**, 156 (2), 206-215.
7. Claus; Becker, Ueber Trinitrotoluol und das flüssige Dinitrotoluol. *Berichte* **1883**, 16, 1596.
8. McConnell, W. J.; Flinn, R. H., Summary of twenty-two trinitrotoluene fatalities in World War II. *J. Ind. Hyg. Toxicol.* **1946**, 28, 76-86.
9. Brown, G. I., *The Big Bang: A History of Explosives*. Sutton England, 2005; p 256.
10. Navy, U.S. EXPLOSIVE ORDNANCE, OP 1664. ORDNANCE, B. O., Ed. Navy: Washington, D.C., 1947; Vol. 1, p 581.
11. Haythorn, S. R., Experimental trinitrotoluene poisoning. *J. Ind. Hyg.* **1920**, 2, 298-318.
12. McGee, L. C.; McCausland, A.; Preston, J. F., Jr.; Houff, L. A., Metabolic disturbances in workers exposed to trinitrotoluene. *Gastroenterology* **1945**, 4, 72-84.
13. Levine, B. S.; Rust, J. H.; Barkley, J. J.; Furedi, E. M.; Lish, P. M., Six month oral toxicity study of trinitrotoluene in beagle dogs. *Toxicology* **1990**, 63, 233-44.
14. Dilley, J. V.; Tyson, C. A.; Spanggord, R. J.; Sasmore, D. P.; Newell, G. W.; Dacre, J. C., Short-term oral toxicity of 2,4,6-trinitrotoluene in mice, rats, and dogs. *J. Toxicol. Environ. Health* **1982**, 9, 565-85.
15. Levine, B. S.; Furedi, E. M.; Gordon, D. E.; Lish, P. M.; Barkley, J. J., Subchronic toxicity of trinitrotoluene in Fischer 344 rats. *Toxicology* **1984**, 32, 253-65.
16. Levine, B. S.; Furedi, E. M.; Gordon, D. E.; Barkley, J. J.; Lish, P. M., Toxic interactions of the munitions compounds TNT and RDX in F344 rats. *Fundam. Appl. Toxicol.* **1990**, 15, 373-80.
17. Dilley, J. V.; Tyson, C. A.; Spanggord, R. J.; Sasmore, D. P.; Newell, G. W.; Dacre, J. C., Short-term oral toxicity of a 2,4,6-trinitrotoluene and hexahydro-1,3,5-trinitro-1,3,5-triazine mixture in mice, rats, and dogs. *J. Toxicol. Environ. Health* **1982**, 9, 587-610.
18. Army, Mammalian Toxicity of munitions compounds: Summary of toxicity of nitrotoluenes. Contract no. DAMD 17-74-C-4073. Frederick, MD, 1980.
19. Hassman, P.; Hassmanova, V., Exposure tests in trinitrotoluene workers. *Sb. Ved. Pr., Lek. Fak. Karlovy Univ. Hradci Kralove* **1976**, 19, 51-60.
20. Hassman, P.; Hassmanova, V.; Borovska, D.; Preiningeroval, O.; Hanus, H.; Juran, J.; Sverak, J., Neurological and psychiatric health status of workers processing trinitrotoluene for long periods of time. *Cesk. Neurol. Neurochir.* **1978**, 41, 372-9.
21. Hassmanova, V.; Hulek, P.; Nozicka, J., Toxic impairment of the liver with trinitrotoluene. *Prac. Lek.* **2002**, 54, 186-189.

22. Moore, B., *The causation and prevention of tri-nitrotoluene (T.N.T.) poisoning*. 1917.
23. Barnes, J. A., Special Discussion on the Origin, Symptoms, Pathology, Treatment, and Prophylaxis of Toxic Jaundice observed in Munition Workers. *Proc R Soc Med* **1917**, *10*, 84-7.
24. Voegtlin, C.; Hooper, C. W.; Johnson, J. M., Trinitrotoluene poisoning. *Public Health Rep.* **1919**, *34*, 1307-13.
25. Neal, P. A.; Von, O. W. F.; Snyder, R. K., Absorption of TNT through the intact skin of human subjects. *U. S. Pub. Health Bull.* **1944**, No. 285, 55.
26. Hundal, L. S.; Shea, P. J.; Comfort, S. D.; Powers, W. L.; Singh, J., Long-term TNT sorption and bound residue formation in soil. *J. Environ. Qual.* **1997**, *26*, 896-904.
27. 2,4,6-Trinitrotoluene. <http://www.epa.gov/iris/subst/0269.htm> (accessed November 20, 2011).
28. ATSDR, Toxicology Profile of 2,4,6-Trinitrotoluene. ATSDR: 1995.
29. Lewis, T. A.; Newcombe, D. A.; Crawford, R. L., Bioremediation of soils contaminated with explosives. *Journal of Environmental Management* **2004**, *70* (4), 291-307.
30. Townsend, D. M.; Myers, T. E. *Recent developments in formulating model descriptors for subsurface transformation and sorption of TNT, RDX, and HMX. Final report*; AD-A--305176/0/XAB; WES/TR/IRRP--96-1; TRN: TRN: 61980083 United States TRN: TRN: 61980083 Mon Feb 04 19:51:20 EST 2008 GRA; SCA: 540220; 450100; PA: GRA-96:80083; EDB-96:122653; SN: 96001621662; TVI: 9617English; 1996; p Medium: P; Size: 38 p.
31. Pennington, J. C.; Patrick, W. H., Jr., Adsorption and desorption of 2,4,6-trinitrotoluene by soils. *J. Environ. Qual.* **1990**, *19*, 559-67.
32. Comfort, S. D.; Shea, P. J.; Hundal, L. S.; Li, Z.; Woodbury, B. L.; Martin, J. L.; Powers, W. L., TNT transport and fate in contaminated soil. *J. Environ. Qual.* **1995**, *24*, 1174-82.
33. Krumholz, L. R.; Li, J.; Clarkson, W. W.; Wilber, G. G.; Suflita, J. M., Transformations of TNT and related aminotoluenes in groundwater aquifer slurries under different electron-accepting conditions. *J. Ind. Microbiol. Biotechnol.* **1997**, *18*, 161-169.
34. Sheremata, T. W.; Thiboutot, S.; Ampleman, G.; Paquet, L.; Halasz, A.; Hawari, J., Fate of 2,4,6-Trinitrotoluene and Its Metabolites in Natural and Model Soil Systems. *Environ. Sci. Technol.* **1999**, *33*, 4002-4008.
35. Stucki, H., Toxicity and Degradation of Explosives. *CHIMIA International Journal for Chemistry* **2004**, *58* (6), 409-413.
36. Brannon, J. M.; Price, C. B.; Hayes, C., Abiotic transformation of TNT in montmorillonite and soil suspensions under reducing conditions. *Chemosphere* **1998**, *36* (6), 1453-1462.
37. Myers, T. E.; Brannon, J. M.; Pennington, J. C.; Davis, W. M.; Myers, K. F.; Townsend, D. M.; Ochman, M. K., Laboratory Studies of Soil Sorption/Transformation of TNT, RDX, and HMX. Engineers, U. A. C. o., Ed. Washington DC, 1998.
38. Selim, H. M.; Iskandar, I. K. *Sorption-desorption and transport of TNT and RDX in soils*; Cold Regions Res. Eng. Lab.: 1994; p 32 pp.
39. Selim, H. M.; Xue, S. K.; Iskandar, I. K., Transport of 2,4,6-trinitrotoluene and hexahydro-1,3,5-trinitro-1,3,5-triazine in soils. *Soil Sci.* **1995**, *160*, 328-39.
40. Xue, S. K.; Iskandar, I. K.; Selim, H. M., Adsorption-desorption of 2,4,6-trinitrotoluene and hexahydro-1,3,5-trinitro-1,3,5-triazine in soils. *Soil Sci.* **1995**, *160*, 317-27.
41. Haderlein, S. B.; Weissmahr, K. W.; Schwarzenbach, R. P., Specific Adsorption of Nitroaromatic Explosives and Pesticides to Clay Minerals. *Environmental Science & Technology* **1996**, *30* (2), 612-622.

42. Vasilyeva, G. K.; Kreslavski, V. D.; Shea, P. J., Catalytic oxidation of TNT by activated carbon. *Chemosphere* **2002**, *47*, 311-317.
43. Saupe, A.; Garvens, H. J.; Heinze, L., Alkaline hydrolysis of TNT and TNT in soil followed by thermal treatment of the hydrolyzates. *Chemosphere* **1998**, *36*, 1725-1744.
44. McCutcheon, S. C.; Medina, V. F.; Larson, S. L. In *Proof of phytoremediation for explosives in water and soil*, John Wiley & Sons, Inc.: 2003; pp 429-480.
45. Vanek, T.; Nepovim, A.; Podlipna, R.; Zeman, S.; Vagner, M., Phytoremediation of Selected Explosives. *Water, Air, Soil Pollut.: Focus* **2003**, *3*, 259-267.
46. Baek, K.-H.; Chang, J.-Y.; Chang, Y.-Y.; Bae, B.-H.; Kim, J.; Lee, I.-S., Phytoremediation of soil contaminated with cadmium and/or 2,4,6-trinitrotoluene. *J. Environ. Biol.* **2006**, *27*, 311-316.
47. Lee, I.; Baek, K.; Kim, H.; Kim, S.; Kim, J.; Kwon, Y.; Chang, Y.; Bae, B., Phytoremediation of soil co-contaminated with heavy metals and TNT using four plant species. *J. Environ. Sci. Health, Part A: Toxic/Hazard. Subst. Environ. Eng.* **2007**, *42*, 2039-2045.
48. Popescu, J. T.; Singh, A.; Zhao, J.-S.; Hawari, J.; Ward, O. P., Metabolite production during transformation of 2,4,6-trinitrotoluene (TNT) by a mixed culture acclimated and maintained on crude oil-containing media. *Applied Microbiology and Biotechnology* **2004**, *65* (6), 739-746.
49. Haidour, A.; Ramos, J. L., Identification of Products Resulting from the Biological Reduction of 2,4,6-Trinitrotoluene, 2,4-Dinitrotoluene, and 2,6-Dinitrotoluene by *Pseudomonas* sp. *Environ. Sci. Technol.* **1996**, *30*, 2365-2370.
50. Banerjee, H. N.; Verma, M.; Hou, L. H.; Ashraf, M.; Dutta, S. K., Cytotoxicity of TNT and its metabolites. *Yale J Biol Med.* **1999**, *72* (1), 1-4.
51. Hwang, H. M.; Slaughter, L. F.; Cook, S. M.; Cui, H., Photochemical and microbial degradation of 2,4,6-trinitrotoluene (TNT) in a freshwater environment. *Bull Environ Contam Toxicol* **2000**, *65*, 228-35.
52. Hwang, S.; Batchelor, C. J.; Davis, J. L.; MacMillan, D. K., Sorption of 2,4,6-trinitrotoluene to natural soils before and after hydrogen peroxide application. *J. Environ. Sci. Health, Part A: Toxic/Hazard. Subst. Environ. Eng.* **2005**, *40*, 581-592.
53. Chen, W.-S.; Juan, C.-N.; Wei, K.-M., Decomposition of dinitrotoluene isomers and 2,4,6-trinitrotoluene in spent acid from toluene nitration process by ozonation and photo-ozonation. *J. Hazard. Mater.* **2007**, *147*, 97-104.
54. Dillert, R.; Nahen, M.; Fels, G.; Bahnemann, D. In *Photocatalytic treatment of TNT-polluted water*, Papierflieger Verlag: 1996; pp Paper 40, pp. 6.
55. Son, H.-S.; Lee, S.-J.; Cho, I.-H.; Zoh, K.-D., Kinetics and mechanism of TNT degradation in TiO₂ photocatalysis. *Chemosphere* **2004**, *57*, 309-317.
56. Schmelling, D. C.; Gray, K. A. In *Photocatalytic transformations and degradation of 2,4,6-trinitrotoluene (TNT) in TiO₂ slurries*, American Society of Civil Engineers: 1994; pp 751-5.
57. Schmelling, D. C.; Gray, K. A., Photocatalytic transformation and mineralization of 2,4,6-trinitrotoluene (TNT) in TiO₂ slurries. *Water Res.* **1995**, *29*, 2651-62.
58. Wang, Z.; Kutal, C., Photocatalytic mineralization of 2,4,6-trinitrotoluene in aqueous suspensions of titanium dioxide. *Chemosphere* **1995**, *30*, 1125-36.
59. Schmelling, D. C.; Gray, K. A., Photocatalytic transformations of TNT in titania slurries: an analysis of the role of interfacial nitrogen reduction utilizing γ -radiolysis. *Chem. Oxid.* **1997**, *4*, 173-183.

60. Dillert, R.; Huppatz, J.; Renwranzt, A.; Siebers, U.; Bahnemann, D., Light-induced degradation of nitroaromatic compounds in aqueous systems: Comparison between titanium dioxide photocatalysis and photo-Fenton reactions. *J. Adv. Oxid. Technol.* **1999**, *4*, 85-90.
61. Halasz, A.; Groom, C.; Zhou, E.; Paquet, L.; Beaulieu, C.; Deschamps, S.; Corriveau, A.; Thiboutot, S.; Ampleman, G.; Dubois, C.; Hawari, J., Detection of explosives and their degradation products in soil environments. *J. Chromatogr., A* **2002**, *963*, 411-418.
62. Chen, W.-S.; Liang, J.-S., Electrochemical destruction of dinitrotoluene isomers and 2,4,6-trinitrotoluene in spent acid from toluene nitration process. *J. Hazard. Mater.* **2009**, *161*, 1017-1023.
63. Rabanal, M. E.; Martinez, M. A.; Criado, A. J.; Braojos, N.; Perez, d. D. A., TNT destruction by electrochemical way. *Int. Annu. Conf. ICT* **1997**, *28th*, 100.1-100.6.
64. Doppalapudi, R. B.; Sorial, G. A.; Maloney, S. W., Electrochemical reduction of simulated munitions wastewater in a bench-scale batch reactor. *Environ. Eng. Sci.* **2002**, *19*, 115-130.
65. Fenton, H. J. H., Oxidation of tartaric acid in presence of iron. *J. Chem. Soc., Trans.* **1894**, *65*, 899-910.
66. Fenton, H. J. H., On a new reaction of tartaric acid. *Chem News* **1876**, *33*, 190.
67. Haber, F.; Weiss, J., The catalysis of hydrogen peroxide. *Naturwissenschaften* **1932**, *20*, 948-50.
68. Barb, W. G.; Baxendale, J. H.; George, P.; Hargrave, K. R., Reactions of ferrous and ferric ions with hydrogen peroxide. *Nature (London, U. K.)* **1949**, *163*, 692-4.
69. Barb, W. G.; Baxendale, J. H.; George, P.; Hargrave, K. R., Reactions of ferrous and ferric ions with hydrogen peroxide. II. Ferric-ion reaction. *Trans. Faraday Soc.* **1951**, *47*, 591-616.
70. Barb, W. G.; Baxendale, J. H.; George, P.; Hargrave, K. R., Reactions of ferrous and ferric ions with hydrogen peroxide. I. Ferrous-ion reaction. *Trans. Faraday Soc.* **1951**, *47*, 462-500.
71. Wells, C. F.; Salam, M. A., Hydrolysis of ferrous ions: a kinetic method for the determination of the Fe(II) species. *Nature (London, U. K.)* **1965**, *205*, 690-2.
72. Wells, C. F.; Salam, M. A., Effect of pH on the kinetics of the reaction of iron-(II) with hydrogen peroxide in perchlorate media. *J. Chem. Soc., A* **1968**, 24-9.
73. Sun, Y.; Pignatello, J. J., Activation of hydrogen peroxide by iron(III) chelates for abiotic degradation of herbicides and insecticides in water. *J. Agric. Food Chem.* **1993**, *41*, 308-12.
74. Wells, C. F.; Salam, M. A., Complex formation between iron(II) and inorganic anions. I. Effect of simple and complex halide ions on the iron(II) + hydrogen peroxide reaction. *Trans. Faraday Soc.* **1967**, *63*, 620-9.
75. Wells, C. F.; Salam, M. A., Complex formation between iron(II) and inorganic anions. II. The effect of oxyanions on the reaction of iron(II) with hydrogen peroxide. *J. Chem. Soc. A* **1968**, 308-15.
76. Francis, K. C.; Cummins, D.; Oakes, J., Kinetic and structural investigations of ethylenediaminetetraacetatoiron(1-) catalyzed decomposition of hydrogen peroxide. *J. Chem. Soc., Dalton Trans.* **1985**, 493-501.
77. Lindsey, M. E.; Tarr, M. A., Inhibited hydroxyl radical degradation of aromatic hydrocarbons in the presence of dissolved fulvic acid. *Water Res.* **2000**, *34*, 2385-2389.
78. Lindsey, M. E.; Tarr, M. A., Inhibition of Hydroxyl Radical Reaction with Aromatics by Dissolved Natural Organic Matter. *Environ. Sci. Technol.* **2000**, *34*, 444-449.

79. Buxton, G. V.; Greenstock, C. L.; Helman, W. P.; Ross, A. B., Critical Review of rate constants for reactions of hydrated electrons, hydrogen atoms and hydroxyl radicals ($\cdot\text{OH}$ / $\cdot\text{O}$) in Aqueous Solution. *Journal of Physical and Chemical Reference Data* **1988**, 17 (2), 513-886.
80. Anbar, M.; Meyerstein, D.; Neta, P., The Reactivity of Aromatic Compounds toward Hydroxyl Radicals. *The Journal of Physical Chemistry* **1966**, 70 (8), 2660-2662.
81. Przado, D.; Kafarski, P.; Steininger, M., Studies on degradation of polychlorinated biphenyls by means of Fenton's reagent. *Pol. J. Environ. Stud.* **2007**, 16, 881-887.
82. Teel, A. L.; Warberg, C. R.; Atkinson, D. A.; Watts, R. J., Comparison of mineral and soluble iron Fenton's catalysts for the treatment of trichloroethylene. *Water Res* **2001**, 35, 977-84.
83. Teel, A. L.; Watts, R. J., Degradation of carbon tetrachloride by modified Fenton's reagent. *Journal of Hazardous Materials* **2002**, 94 (2), 179-189.
84. Li, Z. M.; Shea, P. J.; Comfort, S. D., Fenton oxidation of 2,4,6-trinitrotoluene in contaminated soil slurries. *Environ. Eng. Sci.* **1997**, 14, 55-66.
85. Li, Z. M.; Peterson, M. M.; Comfort, S. D.; Horst, G. L.; Shea, P. J.; Oh, B. T., Remediating TNT-contaminated soil by soil washing and Fenton oxidation. *Sci. Total Environ.* **1997**, 204, 107-115.
86. Li, Z. M.; Comfort, S. D.; Shea, P. J., Destruction of 2,4,6-trinitrotoluene by Fenton oxidation. *J. Environ. Qual.* **1997**, 26, 480-487.
87. Matta, R.; Hanna, K.; Chiron, S., Fenton-like oxidation of 2,4,6-trinitrotoluene using different iron minerals. *Sci. Total Environ.* **2007**, 385, 242-251.
88. Matta, R.; Hanna, K.; Kone, T.; Chiron, S., Oxidation of 2,4,6-trinitrotoluene in the presence of different iron-bearing minerals at neutral pH. *Chem. Eng. J. (Amsterdam, Neth.)* **2008**, 144, 453-458.
89. Hess, T. F.; Renn, T. S.; Watts, R. J.; Paszczynski, A. J., Studies on nitroaromatic compound degradation in modified Fenton reactions by electrospray ionization tandem mass spectrometry (ESI-MS-MS). *Analyst (Cambridge, U. K.)* **2003**, 128, 156-160.
90. Oh, S. Y.; Cha, D. K.; Chiu, P. C.; Kim, B. J., Enhancing oxidation of TNT and RDX in wastewater: pre-treatment with elemental iron. *Water Sci. Technol.* **2003**, 47, 93-99.
91. Oh, S.-Y.; Chiu, P. C.; Kim, B. J.; Cha, D. K., Enhancing Fenton oxidation of TNT and RDX through pretreatment with zero-valent iron. *Water Res.* **2003**, 37, 4275-4283.
92. Barreto-Rodrigues, M.; Silva, F. T.; Paiva, T. C. B., Optimization of Brazilian TNT industry wastewater treatment using combined zero-valent iron and fenton processes. *J. Hazard. Mater.* **2009**, 168, 1065-1069.
93. Barreto-Rodrigues, M.; Silva, F. T.; Paiva, T. C. B., Combined zero-valent iron and fenton processes for the treatment of Brazilian TNT industry wastewater. *J. Hazard. Mater.* **2009**, 165, 1224-1228.
94. Kitayama, T.; Sano, Y.; Matsumoto, M.; Nagaishi, T.; Nagayasu, N.; Harada, Y., Degradation of waste water from TNT manufacturing. *Sci. Technol. Energ. Mater.* **2006**, 67, 62-67.
95. Liou, M.-J.; Lu, M.-C.; Chen, J.-N., Oxidation of explosives by Fenton and photo-Fenton processes. *Water Res.* **2003**, 37, 3172-3179.
96. Liou, M.-J.; Lu, M.-C.; Chen, J.-N., Oxidation of TNT by photo-Fenton process. *Chemosphere* **2004**, 57, 1107-1114.

97. Chen, W.-S.; Liang, J.-S., Decomposition of nitrotoluenes from trinitrotoluene manufacturing process by Electro-Fenton oxidation. *Chemosphere* **2008**, 72, 601-607.
98. Chen, W.-S.; Lin, S.-Z., Destruction of nitrotoluenes in wastewater by Electro-Fenton oxidation. *J. Hazard. Mater.* **2009**, 168, 1562-1568.
99. Villiers, A., Fermentation of starch by the butyric ferment. *Compt. rend.* **1891**, 112, 536-8.
100. Schardinger, F., Over thermophilic bacteria from different meals and milk, as well as over some reaction products the same in carbohydrate-containing nutrient solutions, among them crystallized polysaccharides (dextrins) from strength. [machine translation]. *Z. Unters. Nahr.-Genussm.* **1903**, 6, 865-80.
101. Schardinger, F., Bacillus Macerans, an Acetone of Forming Red Bacillus. [machine translation]. *Centr.-Bl. f. Bakter. u. Parasitenk. II.* **1905**, 14, 772-81.
102. Schardinger, F., The Formation of Crystallin Polysaccharides (Dextrins) from Starch Paste by Micro.organisms. *Centr. Bakt. Parasitenk.* **1911**, II Abt.;29, 188-97.
103. Freudenberg, K.; Rapp, W., Starch and the Schardinger dextrins. *Ber. Dtsch. Chem. Ges. B* **1936**, 69B, 2041-5.
104. Freudenberg, K.; Meyer-Delius, M., The Schardinger dextrins from starch. *Ber. Dtsch. Chem. Ges. B* **1938**, 71B, 1596-1600.
105. Freudenberg, K.; Boppel, H.; Meyer-Delius, M., Starch. *Naturwissenschaften* **1938**, 26, 123-4.
106. Freudenberg, K.; Blomqvist, G.; Ewald, L.; Soff, K., Hydrolysis and acetolysis of starch and of the Schardinger dextrins. *Ber. Dtsch. Chem. Ges. B* **1936**, 69B, 1258-66.
107. Freudenberg, K.; Cramer, F., Constitution of the Schardinger dextrins α , β , and γ . *Z. Naturforsch.* **1948**, 3b, 464.
108. Connors, K. A., The Stability of Cyclodextrin Complexes in Solution. *Chem. Rev. (Washington, D. C.)* **1997**, 97, 1325-1357.
109. Harata, K., The structure of the cyclodextrin complex. III. The crystal structure of the α -cyclodextrin-sodium benzenesulfonate complex. *Bull. Chem. Soc. Jpn.* **1976**, 49, 2066-72.
110. Alvira, E.; Mayoral, J. A.; Garcia, J. I., A model for the interaction between β -cyclodextrin and some acrylic esters. *Chem. Phys. Lett.* **1995**, 245, 335-42.
111. Lichtenthaler, F. W.; Immel, S., Molecular modeling of saccharides. 11. Towards understanding formation and stability of cyclodextrin inclusion complexes: computation and visualization of their molecular lipophilicity patterns. *Starch/Staerke* **1996**, 48, 145-154.
112. Ivanov, P. M.; Jaime, C., Modeling of the inclusion process of α -, β -, and γ -cyclodextrin with 1-bromoadamantane. A comparative molecular mechanics study accounting for the solvent. *J. Mol. Struct.* **1996**, 377, 137-47.
113. Lu, T.; Zhang, D.; Dong, S., Molecular-mechanical study of cyclodextrin and its inclusion complexes. *J. Chem. Soc., Faraday Trans. 2* **1989**, 85, 1439-45.
114. Fotiadu, F.; Fathallah, M.; Jaime, C., Molecular mechanics calculations on the differentiation of diastereomeric complexes of cis-decalin with β -cyclodextrin. *J. Inclusion Phenom. Mol. Recognit. Chem.* **1993**, 16, 55-62.
115. Fathallah, M.; Fotiadu, F.; Jaime, C., Cyclodextrin Inclusion Complexes. MM2 Calculations Reproducing Bimodal Inclusions. *J. Org. Chem.* **1994**, 59, 1288-93.
116. Tabushi, I.; Kiyosuke, Y.; Sugimoto, T.; Yamamura, K., Approach to the aspects of driving force of inclusion by α -cyclodextrin. *J. Am. Chem. Soc.* **1978**, 100, 916-19.

117. Tabushi, I.; Mizutani, T., Nature of force field operating in molecular recognition by cyclodextrins. Contribution of nonpolar and polar interactions. *Tetrahedron* **1987**, *43*, 1439-47.
118. Arnold, E. N.; Lillie, T. S.; Beesley, T. E., Molecular modeling of cyclodextrin-guest molecule interactions. *J. Liq. Chromatogr.* **1989**, *12*, 337-43.
119. Amato, M. E.; Djedaini, F.; Pappalardo, G. C.; Perly, B.; Scarlata, G., Molecular modeling of β -cyclodextrin complexes with nootropic drugs. *J. Pharm. Sci.* **1992**, *81*, 1157-61.
120. Wojcik, J. F., Binding to cyclodextrins: an interpretive model. *Bioorg. Chem.* **1984**, *12*, 130-40.
121. Ohashi, M.; Kasatani, K.; Shinohara, H.; Sato, H., Molecular mechanics studies on inclusion compounds of cyanine dye monomers and dimers in cyclodextrin cavities. *J. Am. Chem. Soc.* **1990**, *112*, 5824-30.
122. Fornasier, R.; Parmagnani, M.; Tonellato, U., Induced circular dichroism and UV spectra of inclusion complexes of N-alkyldihydronicotinamides with cyclomaltoheptose and heptakis(2,6-di-O-methyl)cyclomaltoheptose. *J. Inclusion Phenom. Mol. Recognit. Chem.* **1991**, *11*, 225-31.
123. Kobayashi, N.; Osa, T., Complexation of aromatic carboxylic acids with heptakis(2,6-di-O-methyl)cyclomaltoheptaose in chloroform and water. *Carbohydr. Res.* **1989**, *192*, 147-57.
124. Tee, O. S.; Mazza, C.; Lozano-Hemmer, R.; Giorgi, J. B., Ester Cleavage by Cyclodextrins in Aqueous Dimethyl Sulfoxide Mixtures. Substrate Binding versus Transition State Binding. *J. Org. Chem.* **1994**, *59*, 7602-8.
125. Aboutaleb, A. E.; Abdel, R. A. A.; Samy, E. M., Studies of cyclodextrin inclusion complexes. II. Inclusion complexes between α -cyclodextrin and N-demethyldiazepam and chlordiazepoxide. *J. Pharm. Belg.* **1988**, *43*, 437-44.
126. Ueno, A.; Tomita, Y.; Osa, T., Association of naphthalene-appended γ -cyclodextrin with β -cyclodextrin. *J. Chem. Soc., Chem. Commun.* **1983**, 1515-16.
127. Liao, Y.; Bohne, C., Alcohol Effect on Equilibrium Constants and Dissociation Dynamics of Xanthone-Cyclodextrin Complexes. *J. Phys. Chem.* **1996**, *100*, 734-43.
128. Zheng, W.; Tarr, M. A. In *Evidence of formation of aqueous ternary Fe(II)-cyclodextrin-guest complexes from fluorescence techniques*, American Chemical Society: 2003; pp ANYL-159.
129. Zheng, W.; Tarr, M. A., Evidence for the Existence of Ternary Complexes of Iron, Cyclodextrin, and Hydrophobic Guests in Aqueous Solution. *J. Phys. Chem. B* **2004**, *108*, 10172-10176.
130. Zheng, W.; Tarr, M. A., Assessment of ternary iron-cyclodextrin-2-naphthol complexes using NMR and fluorescence spectroscopies. *Spectrochim. Acta, Part A* **2006**, *65A*, 1098-1103.
131. Cai, Y.; Tarr, M. A.; Xu, G.; Yalcin, T.; Cole, R. B., Dication induced stabilization of gas-phase ternary beta-cyclodextrin inclusion complexes observed by electrospray mass spectrometry. *J. Am. Soc. Mass Spectrom.* **2003**, *14*, 449-459.
132. Ko, S.-O.; Jee, S.-H.; Park, J.-W.; Min, J.-E.; Cho, S.; Shin, W.; Kim, Y. In *Effects of surfactants on the Fenton degradation of PAH compounds in contaminated sediments*, Battelle Press: 2005; pp C2.11/1-C2.11/7.
133. Yardin, G.; Chiron, S., Photo-Fenton treatment of TNT contaminated soil extract solutions obtained by soil flushing with cyclodextrin. *Chemosphere* **2006**, *62*, 1395-1402.
134. Sheremata, T. W.; Hawari, J., Cyclodextrins for Desorption and Solubilization of 2,4,6-Trinitrotoluene and Its Metabolites from Soil. *Environ. Sci. Technol.* **2000**, *34*, 3462-3468.

135. Jarand, C. W. Complexation of Organic Guests and Coordination of Metal Ions by Cyclodextrins: Role of Cyclodextrins in Metal-Guest Interactions. University of New Orleans, New Orleans, 2010.
136. Kaplan, D. L.; Kaplan, A. M., 2,4,6-Trinitrotoluene-surfactant complexes: decomposition, mutagenicity and soil leaching studies. *Environ. Sci. Technol.* **1982**, *16*, 566-71.
137. Gray, K., Bioremediating explosives-contaminated soil. *BioCycle* **1999**, *40*, 48-49.
138. Bin, A. K.; Machniewski, P.; Sakowicz, R.; Ostrowska, J.; Zielinski, J., Degradation of nitroaromatics (MNT, DNT and TNT) by AOPs. *Ozone: Sci. Eng.* **2001**, *23*, 343-349.
139. Kroeger, M.; Fels, G., Combined biological-chemical procedure for the mineralization of TNT. *Biodegradation* **2007**, *18*, 413-425.
140. Liu, X. H.; Fu, Y. B.; Wang, H. Y.; Zhong, Z. J.; Xu, Y. S., Photocatalytic degradation of 2,4,6-trinitrotoluene. *Sci. China, Ser. B: Chem.* **2008**, *51*, 1009-1013.
141. Approaches for the Remediation of Federal Facility Sites Contaminated with Explosives or Radioactive Waste. In *EPA-625/R-93/013*, Agency, U. S. E. P., Ed. Office of Research and Development: 1993; pp 1-4.
142. Van Dillewijn, P.; Caballero, A.; Paz, J. A.; Maria, G.-P. M.; Oliva, J. M.; Ramos, J. L., Bioremediation of 2,4,6-Trinitrotoluene under Field Conditions. *Environ. Sci. Technol.* **2007**, *41*, 1378-1383.
143. Oh, B. T.; Alvarez, P. J., Removal of explosives using an integrated iron-microbial treatment in flow-through columns. *Bull. Environ. Contam. Toxicol.* **2004**, *73*, 1-8.
144. Johnson, R. L.; Thoms, R. B.; Johnson, R. O. B.; Krug, T., Field evidence for flow reduction through a zero-valent iron permeable reactive barrier. *Ground Water Monit. Rem.* **2008**, *28*, 47-55.
145. Pignatello, J. J.; Oliveros, E.; MacKay, A., Advanced oxidation processes for organic contaminant destruction based on the Fenton reaction and related chemistry. *Crit. Rev. Environ. Sci. Technol.* **2006**, *36*, 1-84.
146. Kazarian, S. G.; Chan, K. L. A., "Chemical Photography" of Drug Release. *Macromolecules* **2003**, *36*, 9866-9872.
147. Lindsey, M. E.; Xu, G.; Lu, J.; Tarr, M. A., Enhanced Fenton degradation of hydrophobic organics by simultaneous iron and pollutant complexation with cyclodextrins. *Sci. Total Environ.* **2003**, *307*, 215-229.
148. Fan, Z.; Diao, C.-H.; Yu, M.; Jing, Z.-L.; Chen, X.; Deng, Q.-L., An Investigation of the Inclusion Complex of β -Cyclodextrin with 8-Nitro-Quinoline in the Solid State. *Supramol. Chem.* **2006**, *18*, 7-11.
149. Fan, Z.; Diao, C.-H.; Guo, M.-J.; Du, R.-J.; Song, Y.-F.; Jing, Z.-L.; Yu, M., An investigation of the inclusion complex of β -cyclodextrin with p-nitrobenzoic acid in the solid state. *Carbohydr. Res.* **2007**, *342*, 2500-2503.
150. Quaranta, A.; Zhang, Y.; Wang, Y.; Edge, R.; Navaratnam, S.; Land, E. J.; Bensasson, R. V., Single and double reduction of C60 in 2:1 γ -cyclodextrin/[60]fullerene inclusion complexes by cyclodextrin radicals. *Chem. Phys.* **2008**, *354*, 174-179.
151. Liou, M.-J.; Lu, M.-C., Catalytic degradation of nitroaromatic explosives with Fenton's reagent. *J. Mol. Catal. A: Chem.* **2007**, *277*, 155-163.
152. Li, Z. M.; Shea, P. J.; Comfort, S. D., Nitrotoluene destruction by UV-catalyzed Fenton oxidation. *Chemosphere* **1998**, *36*, 1849-1865.

153. Chen, W.-S.; Juan, C.-N.; Wei, K.-M., Mineralization of dinitrotoluenes and trinitrotoluene of spent acid in toluene nitration process by Fenton oxidation. *Chemosphere* **2005**, *60*, 1072-1079.
154. Jarand, C. W.; Chen, K.; Cole, R. B.; Pham, D.-T.; Lincoln, S. F.; Tarr, M. A. In *Degradation products of TNT after Fenton oxidation*, American Chemical Society: 2009; pp ENV-228.
155. Gilbert, B. C.; Lindsay, S. J. R.; Taylor, P.; Ward, S.; Whitwood, A. C., Free-radical reactions of carbohydrate moieties in macromolecular structures. EPR evidence for the importance of steric and stereoelectronic effects and for the influence of inclusion in cyclodextrins. *Perkin 2* **2000**, 2001-2007.
156. Restore the Gulf. <http://www.restorethegulf.gov/> (accessed July 26, 2011).
157. Cavnar, B., *Disaster on the Horizon: High Stakes, High Risk, and the Story Behind the Deepwater Horizon Blowout*. Chelsea Green Publishing: White River Junction, Vermont, 2010.
158. Price, A. R. G.; Downing, N.; Fowler, S. W.; Hardy, J. T.; Le Tissier, M.; Mathews, C. P.; McGlade, J. M.; Medley, P. A. H.; Oregioni, B.; Readman, J. W.; Roberts, C. M.; Wrathall, T. J., The 1991 Gulf War: Environmental Assessments of IUCN and Collaborators. Resources, I. U. f. C. o. N. a. N., Ed. International Union for Conservation Gland, Switzerland, 1994.
159. Environmental Response Management Application. <http://gomex.erma.noaa.gov/> (accessed September 9, 2011).
160. Klasnes, F.; Sholly, K.; Pfeiffenberge, J., Exxon Valdez Oil Spill and Kenai Fjords National Park - 20th Anniversary Questions and Answers. Interior, U. S. D. o. t., Ed. 2009.
161. Stigter, J. B.; de Haan, H. P. M.; Guicherit, R.; Dekkers, C. P. A.; Daane, M. L., Determination of cadmium, zinc, copper, chromium and arsenic in crude oil cargoes. *Environmental Pollution* **2000**, *107* (3), 451-464.
162. Fingas, M., *The Basics of Oil Spill Cleanup*. Second ed.; Lewis Publishers: Boca Raton, 2001; p 233.
163. Q4000 Virtual Oil Summary. British Petroleum: 2011.
164. Lindblom, G. P., Oil Spill Control Chemicals- A Current View. In *Chemical Dispersants for the Control of Oil Spills*, McCarthy, L. T.; Lindblom, G. P.; Walter, H. F., Eds. American Society for Testing and Materials: Baltimore, 1978; pp 127-140.
165. Venosa, A. D.; Holder, E. L., Biodegradability of dispersed crude oil at two different temperatures. *Mar. Pollut. Bull.* **2007**, *54*, 545-553.
166. Jahan, K.; Ahmed, T.; Maier, W. J., Phenanthrene mineralization in soil in the presence of nonionic surfactants. *Toxicological & Environmental Chemistry* **1997**, *64* (1-4), 127-143.
167. Jahan, K.; Ahmed, T.; Maier, W. J., Factors Affecting the Nonionic Surfactant-Enhanced Biodegradation of Phenanthrene. *Water Environment Research* **1997**, *69* (3), 317-325.
168. Bruheim, P.; Bredholt, H.; Eimhjellen, K., Effects of surfactant mixtures, including Corexit 9527, on bacterial oxidation of acetate and alkanes in crude oil. *Appl. Environ. Microbiol.* **1999**, *65*, 1658-1661.
169. Bruheim, P.; Bredholt, H.; Eimhjellen, K., Bacterial degradation of emulsified crude oil and the effect of various surfactants. *Can. J. Microbiol.* **1997**, *43*, 17-22.
170. Kujawinski, E. B.; Kido, S. M. C.; Valentine, D. L.; Boysen, A. K.; Longnecker, K.; Redmond, M. C., Fate of dispersants associated with the deepwater horizon oil spill. *Environ. Sci. Technol.* **2011**, *45*, 1298-1306.
171. Environmental Protection Agency. www.epa.gov (accessed January 15, 2012).
172. Corexit EC9527A; MSDS; Nalco Company; Naperville, I. O., 2008.

173. Corexit EC9500A; MSDS; Nalco Company; Naperville, I. J., 2005.
174. Belore, R. C.; Trudel, K.; Mullin, J. V.; Guarino, A., Large-scale cold water dispersant effectiveness experiments with Alaskan crude oils and Corexit 9500 and 9527 dispersants. *Mar. Pollut. Bull.* **2009**, 58, 118-128.
175. Moles, A.; Holland, L.; Short, J., Effectiveness in the Laboratory of Corexit 9527 and 9500 in Dispersing Fresh, Weathered, and Emulsion of Alaska North Slope Crude Oil under Subarctic Conditions. *Spill Science & Technology Bulletin* **2002**, 7 (5–6), 241-247.
176. Trudel, K.; Belore, R. C.; Mullin, J. V.; Guarino, A., Oil viscosity limitation on dispersibility of crude oil under simulated at-sea conditions in a large wave tank. *Mar. Pollut. Bull.* **2010**, 60, 1606-1614.
177. *Deep Water The Gulf Oil Disaster and the Future of Offshore Drilling*; National Commission on the BP Deepwater Horizon Oil Spill and Offshore Drilling: 2011; p 398.
178. Hemmer, M. J.; Barron, M. G.; Greene, R. M., Comparative toxicity of eight oil dispersants, Louisiana sweet crude oil (LSC), and chemically dispersed LSC to two aquatic test species. *Environ. Toxicol. Chem.* **2011**, 30, 2244-2252.
179. Scarlett, A.; Galloway, T. S.; Canty, M.; Smith, E. L.; Nilsson, J.; Rowland, S. J., Comparative toxicity of two oil dispersants, superdispersant-25 and corexit 9527, to a range of coastal species. *Environmental Toxicology and Chemistry* **2005**, 24 (5), 1219-1227.
180. Judson, R. S.; Martin, M. T.; Reif, D. M.; Houck, K. A.; Knudsen, T. B.; Rotroff, D. M.; Xia, M.; Sakamuru, S.; Huang, R.; Shinn, P.; Austin, C. P.; Kavlock, R. J.; Dix, D. J., Analysis of Eight Oil Spill Dispersants Using Rapid, In Vitro Tests for Endocrine and Other Biological Activity. *Environ. Sci. Technol.* **2010**, 44, 5979-5985.
181. Atlas, R. M.; Hazen, T. C., Oil Biodegradation and Bioremediation: A Tale of the Two Worst Spills in U.S. History. *Environ. Sci. Technol.* **2011**, 45, 6709-6715.
182. Camilli, R.; Reddy, C. M.; Yoerger, D. R.; Van, M. B. A. S.; Jakuba, M. V.; Kinsey, J. C.; McIntyre, C. P.; Sylva, S. P.; Maloney, J. V., Tracking Hydrocarbon Plume Transport and Biodegradation at Deepwater Horizon. *Science (Washington, DC, U. S.)* **2010**, 330, 201-204.
183. NOAA - National Oceanic and Atmospheric Administration www.noaa.gov (accessed July 22, 2011).
184. Ramachandran, S. D.; Hodson, P. V.; Khan, C. W.; Lee, K., Oil dispersant increases PAH uptake by fish exposed to crude oil. *Ecotoxicology and Environmental Safety* **2004**, 59 (3), 300-308.
185. Hemmer, M. J.; Barron, M. G.; Greene, R. M., Comparative Toxicity of Louisiana Sweet Crude Oil (LSC) and Chemically Dispersed LSC to Two Gulf of Mexico Aquatic Test Species. Development, U. S. E. P. A. O. o. R. a., Ed. 2010.
186. Shaw, S. Office of Research and Development. <http://www.meriresearch.org/Portals/0/Documents/Susan%20Shaw%20Statement%20Re%20EPA%20Report%20August%2013.pdf> (accessed January 26, 2012).
187. Atwood, D. K.; Ferguson, R. L., An example study of the weathering of spilled petroleum in a tropical marine environment: IXTOC-1. *Bull. Mar. Sci.* **1982**, 32 (1), 1-13.
188. Lee, R. F., Photo-oxidation and Photo-toxicity of Crude and Refined Oils. *Spill Sci. Technol. Bull.* **2003**, 8, 157-162.
189. Boehm, P. D.; Fiest, D. L.; Mackay, D.; Paterson, S., Physical-chemical weathering of petroleum hydrocarbons from the IXTOC I blowout: chemical measurements and a weathering model. *Environ. Sci. Technol.* **1982**, 16 (8), 498-505.

190. Payne, J. R.; Clayton Jr., J. R.; McNabb Jr., G. D.; Kirstein, B. E., Exxon Valdez Oil Weathering Fate and Behavior: Model Predictions and Field Observations. In *1991 Oil Spill Conference*, American Petroleum Institute: Washington, D.C., 1991; pp 641-654.
191. Douglas, G. S.; Owens, E. H.; Hardenstine, J.; Prince, R. C., The OSSA II Pipeline Oil Spill: the Character and Weathering of the Spilled Oil. *Spill Sci. Technol. Bull.* **2002**, 7, 135-148.
192. Prince, R. C.; Stibrany, R. T.; Hardenstine, J.; Douglas, G. S.; Owens, E. H., Aqueous Vapor Extraction: A Previously Unrecognized Weathering Process Affecting Oil Spills in Vigorously Aerated Water. *Environmental Science & Technology* **2002**, 36 (13), 2822-2825.
193. Wong, C. S.; Whitney, F. A.; Cretney, W. J.; Lee, K.; McLaughlin, F.; Wu Tianbao Fu, J.; Zhuang, D., An experimental marine ecosystem response to crude oil and corexit 9527: Part 1—Fate of chemically dispersed crude oil. *Marine Environmental Research* **1984**, 13 (4), 247-263.
194. Mille, G.; Almallah, M.; Bianchi, M.; Wambeke, F.; Bertrand, J. C., Effect of salinity on petroleum biodegradation. *Fresenius' Journal of Analytical Chemistry* **1991**, 339 (10), 788-791.
195. Hazen, T. C.; Dubinsky, E. A.; De, S. T. Z.; Andersen, G. L.; Piceno, Y. M.; Singh, N.; Jansson, J. K.; Probst, A.; Borglin, S. E.; Fortney, J. L.; Stringfellow, W. T.; Bill, M.; Conrad, M. E.; Tom, L. M.; Chavarria, K. L.; Alusi, T. R.; Lamendella, R.; Joyner, D. C.; Spier, C.; Baelum, J.; Auer, M.; Zemla, M. L.; Chakraborty, R.; Sonnenthal, E. L.; D'Haeseleer, P.; Holman, H.-Y. N.; Osman, S.; Lu, Z.; Van, N. J. D.; Deng, Y.; Zhou, J.; Mason, O. U., Deep-Sea Oil Plume Enriches Indigenous Oil-Degrading Bacteria. *Science (Washington, DC, U. S.)* **2010**, 330, 204-208.
196. Andreoni, V.; Gianfreda, L., PAH Bioremediation by Microbial Communities and Enzymatic Activities. In *Handbook of Green Chemistry*, Wiley-VCH Verlag GmbH & Co. KGaA: 2010.
197. Zahed, M. A.; Aziz, H. A.; Isa, M. H.; Mohajeri, L., Effect of Initial Oil Concentration and Dispersant on Crude Oil Biodegradation in Contaminated Seawater. *Bull. Environ. Contam. Toxicol.* **2010**, 84, 438-442.
198. Zahed, M. A.; Aziz, H. A.; Isa, M. H.; Mohajeri, L., Response Surface Analysis to Improve Dispersed Crude Oil Biodegradation. *Clean: Soil, Air, Water* **2012**, 40, 262-267.
199. Zahed, M. A.; Abdul, A. H.; Isa, M. H.; Mohajeri, L.; Mohajeri, S.; Kutty, S. R. M., Kinetic modeling and half life study on bioremediation of crude oil dispersed by Corexit 9500. *J. Hazard. Mater.* **2011**, 185, 1027-1031.
200. Macnaughton, S. J.; Swannell, R.; Daniel, F.; Bristow, L., Biodegradation of Dispersed Forties Crude and Alaskan North Slope Oils in Microcosms Under Simulated Marine Conditions. *Spill Science & Technology Bulletin* **2003**, 8 (2), 179-186.
201. Wrenn, B. A.; Sarnecki, K. L.; Kohar, E. S.; Lee, K.; Venosa, A. D., Effects of nutrient source and supply on crude oil biodegradation in continuous-flow beach microcosms. *J. Environ. Eng. (Reston, VA, U. S.)* **2006**, 132, 75-84.
202. Foght, J. M.; Westlake, D. W. S., Effect of the dispersant Corexit 9527 on the microbial degradation of Prudhoe Bay oil. *Can. J. Microbiol.* **1982**, 28, 117-22.
203. Foght, J. M.; Fedorak, P. M.; Westlake, D. W. S., Effect of the dispersant Corexit 9527 on the microbial degradation of sulfur heterocycles in Prudhoe Bay oil. *Can. J. Microbiol.* **1983**, 29, 623-7.
204. Davidson, R. S., Mechanisms of photo-oxidation reactions. *Pesticide Science* **1979**, 10 (2), 158-170.

205. Berthou, F.; Ducreux, J.; Bodennec, G., Analysis of water-soluble acidic compounds derived from spilled oil in a controlled marine enclosure. *Int. J. Environ. Anal. Chem.* **1985**, *21*, 267-82.
206. ThomINETTE, F.; Verdu, J., Photooxidative behavior of crude oils relative to sea pollution. Part II. Photo-induced phase separation. *Mar. Chem.* **1984**, *15*, 105-15.
207. D'Auria, M.; Emanuele, L.; Racioppi, R.; Velluzzi, V., Synchronous fluorescence spectroscopy and gas chromatography to determine the effect of UV irradiation on crude oil. *J. Photochem. Photobiol., A* **2008**, *198*, 156-161.
208. Plata, D. L.; Reddy, C. M., Photochemical degradation of select polycyclic aromatic hydrocarbons: First order disappearance rates and primary degradation mechanisms in oil-contaminated coastal zones. *Prepr. Ext. Abstr. ACS Natl. Meet., Am. Chem. Soc., Div. Environ. Chem.* **2005**, *45*, 274-279.
209. Plata, D. L.; Sharpless, C. M.; Reddy, C. M., Photochemical Degradation of Polycyclic Aromatic Hydrocarbons in Oil Films. *Environ. Sci. Technol.* **2008**, *42*, 2432-2438.
210. Schutt, W. S.; Feng, K.; Bousman, K. S.; Gao, N.; Li, Y., Photoinduced degradation of environmental pollutants in the presence of O₂-free ozone. *J. Adv. Oxid. Technol.* **1997**, *2*, 401-407.
211. Fasnacht, M. P.; Blough, N. V., Mechanisms of the Aqueous Photodegradation of Polycyclic Aromatic Hydrocarbons. *Environ. Sci. Technol.* **2003**, *37*, 5767-5772.
212. Rontani, J. F.; Giral, P. J. P., Photosensitized oxidation of pristane in sea water: effect of photochemical reactions on tertiary carbons. *J. Photochem. Photobiol., A: Chemistry* **1987**, *40* (1), 107-120.
213. Rontani, J. F.; Giral, P. J. P., Significance of photosensitized oxidation of alkanes during the photochemical degradation of petroleum hydrocarbon fractions in seawater. *Int. J. Environ. Anal. Chem.* **1990**, *42*, 61-8.
214. Considine, D. M., *Van Nostrand Reinhold encyclopedia of chemistry* 4th ed.; Van Nostrand Reinhold: New York, 1984; p 1082.
215. Gaya, U. I.; Abdullah, A. H., Heterogeneous photocatalytic degradation of organic contaminants over titanium dioxide: A review of fundamentals, progress and problems. *J. Photochem. Photobiol., C* **2008**, *9*, 1-12.
216. Ziolli, R. L.; Jardim, W. F., Photocatalytic decomposition of seawater-soluble crude-oil fractions using high surface area colloid nanoparticles of TiO₂. *J. Photochem. Photobiol., A* **2002**, *147*, 205-212.
217. Nair, M.; Luo, Z.; Heller, A., Rates of photocatalytic oxidation of crude oil on salt water on buoyant, cenosphere-attached titanium dioxide. *Ind. Eng. Chem. Res.* **1993**, *32*, 2318-23.
218. Pernyeszi, T.; Dekany, I., Photocatalytic degradation of hydrocarbons by bentonite and TiO₂ in aqueous suspensions containing surfactants. *Colloids Surf., A* **2003**, *230*, 191-199.
219. Zhang, H.; Chen, G.; Bahnemann, D. W., Photoelectrocatalytic materials for environmental applications. *J. Mater. Chem.* **2009**, *19*, 5089-5121.
220. Ziolli, R. L.; Jardim, W. F., Photochemical transformations of water-soluble fraction (WSF) of crude oil in marine waters. A comparison between photolysis and accelerated degradation with TiO₂ using GC-MS and UVF. *J. Photochem. Photobiol., A* **2003**, *155*, 243-252.
221. Ehrhardt, M.; Weber, R. R., Formation of low molecular weight carbonyl compounds by sensitized photochemical decomposition of aliphatic hydrocarbons in seawater. *Fresenius. J. Anal. Chem.* **1991**, *339*, 772-6.

222. Hansen, H. P., Photochemical degradation of petroleum hydrocarbon surface films on sea water. *Mar. Chem.* **1975**, *3*, 183-95.
223. Burwood, R.; Speers, G. C., Photo-oxidation as a factor in the environmental dispersal of crude oil. *Estuarine Coastal Mar. Sci.* **1974**, *2*, 117-35.
224. Larson, R. A.; Hunt, L. L.; Blankenship, D. W., Formation of toxic products from a #2 fuel oil by photooxidation. *Environ. Sci. Technol.* **1977**, *11*, 492-6.
225. Larson, R. A.; Bott, T. L.; Hunt, L. L.; Rogenmuser, K., Photooxidation products of a fuel oil and their antimicrobial activity. *Environ. Sci. Technol.* **1979**, *13*, 965-9.
226. Patel, J. R.; Overton, E. B.; Laseter, J. L., Environmental photooxidation of dibenzothiophenes following the Amoco Cadiz oil spill. *Chemosphere* **1979**, *8*, 557-61.
227. Payne, J. R.; Phillips, C. R., Photochemistry of petroleum in water. *Environ Sci Technol* **1985**, *19*, 569-79.
228. Bobinger, S.; Andersson, J. T., Photooxidation Products of Polycyclic Aromatic Compounds Containing Sulfur. *Environ. Sci. Technol.* **2009**, *43*, 8119-8125.
229. Sterling, M. C., Jr.; Bonner, J. S.; Page, C. A.; Fuller, C. B.; Ernest, A. N. S.; Autenrieth, R. L., Partitioning of Crude Oil Polycyclic Aromatic Hydrocarbons in Aquatic Systems. *Environ. Sci. Technol.* **2003**, *37*, 4429-4434.
230. Sterling, M. C.; Bonner, J. S.; Ernest, A. N. S.; Page, C. A.; Autenrieth, R. L., Chemical dispersant effectiveness testing: influence of droplet coalescence. *Mar. Pollut. Bull.* **2004**, *48*, 969-977.
231. Barbosa, G. C. L.; Di, M. E.; Antunes, V.; Mangrich, A. S., Photochemical weathering study of Brazilian petroleum by EPR spectroscopy. *Mar. Chem.* **2003**, *84*, 105-112.
232. McAuliffe, C. D.; Johnson, J. C.; Greene, S. H.; Canevari, G. P.; Searl, T. D., Dispersion and weathering of chemically treated crude oils on the ocean. *Environ. Sci. Technol.* **1980**, *14* (12), 1509-18.
233. Ducreux, J.; Berthou, F.; Bodennec, G., Study of the weathering of a crude petroleum spread on the surface of seawater under natural conditions. *Int. J. Environ. Anal. Chem.* **1986**, *24*, 85-111.
234. Rojo, F., Degradation of alkanes by bacteria. *Environ. Microbiol.* **2009**, *11* (10), 2477-2490.
235. Brooijmans, R. J. W.; Pastink, M. I.; Slezen, R. J., Hydrocarbon-degrading bacteria: the oil-spill clean-up crew. *Microb. Biotechnol.* **2009**, *2* (6), 587-594.
236. Dutta, T. K.; Harayama, S., Fate of Crude Oil by the Combination of Photooxidation and Biodegradation. *Environ. Sci. Technol.* **2000**, *34*, 1500-1505.
237. Li, Z.; Wrenn, B. A.; Mukherjee, B.; Lee, K.; Venosa, A. D., Impacts of Iron, Nutrients, and Mineral Fines on Anaerobic Biodegradation of Canola Oil in Freshwater Sediments. *Soil Sediment Contam.* **2010**, *19*, 244-259.
238. Yang, G.; Zhang, L.; Sun, X.; Jing, W., Photochemical degradation of crude oil in seawater. *Chin. J. Oceanol. Limnol.* **2006**, *24*, 264-269.
239. Grzechulska, J.; Hamerski, M.; Morawski, A. W., Photocatalytic decomposition of oil in water. *Water Res.* **2000**, *34*, 1638-1644.
240. Garrett, R. M.; Pickering, I. J.; Haith, C. E.; Prince, R. C., Photooxidation of Crude Oils. *Environ. Sci. Technol.* **1998**, *32*, 3719-3723.
241. Pernyeszi, T.; Dekany, I., Photooxidation of oleic acid, toluene, asphaltene and crude oil in titanium dioxide aqueous suspensions. *Prog. Min. Oilfield Chem.* **2001**, *3*, 233-244.

242. Berry, R. J.; Mueller, M. R., Photocatalytic decomposition of crude oil slicks using TiO₂ on a floating substrate. *Microchem. J.* **1994**, *50*, 28-32.
243. Nicodem, D. E.; Guedes, C. L. B.; Correa, R. J., Photochemistry of petroleum I. Systematic study of a Brazilian intermediate crude oil. *Mar. Chem.* **1998**, *63*, 93-104.
244. Lloyd, J. B. F., Synchronized excitation of fluorescence emission spectra. *Nature (London), Phys. Sci.* **1971**, *231*, 64-5.
245. Warner, I. M.; Callis, J. B.; Davidson, E. R.; Christian, G. D. In *Oil characterization by multicomponent fluorescence analysis*, IEEE: 1977; pp 129-35.
246. Guedes, C. L. B.; Di, M. E.; De, C. A.; Mazzochin, L. F.; Bragagnolo, G. M.; De, M. F. A.; Piccinato, M. T., EPR and fluorescence spectroscopy in the photodegradation study of Arabian and Colombian crude oils. *Int. J. Photoenergy* **2006**, 48462/1-48462/6.
247. Nicodem, D. E.; Guedes, C. L. B.; Conceicao, M.; Fernandes, Z.; Severino, D.; Correa, R. J.; Coutinho, M. C.; Silva, J., Photochemistry of petroleum. *Prog. React. Kinet. Mech.* **2001**, *26*, 219-238.
248. Patra, D.; Mishra, A. K., Total synchronous fluorescence scan spectra of petroleum products. *Anal. Bioanal. Chem.* **2002**, *373*, 304-309.
249. Nahorniak, M. L.; Booksh, K. S., Excitation-emission matrix fluorescence spectroscopy in conjunction with multiway analysis for PAH detection in complex matrices. *Analyst (Cambridge, U. K.)* **2006**, *131*, 1308-1315.
250. Alostaz, M. d.; Biggar, K.; Donahue, R.; Hall, G., Petroleum contamination characterization and quantification using fluorescence emission-excitation matrices (EEMs) and parallel factor analysis (PAPAFAC). *J. Environ. Eng. Sci.* **2008**, *7*, 183-197.
251. Christensen, J. H.; Hansen, A. B.; Mortensen, J.; Andersen, O., Characterization and Matching of Oil Samples Using Fluorescence Spectroscopy and Parallel Factor Analysis. *Anal. Chem.* **2005**, *77*, 2210-2217.
252. Sinski, J. F.; Exner, J.; New, A., Degradation analysis of polycyclic aromatic hydrocarbons by mycobacterium PRY-1 with excitation emission fluorescence spectroscopy. *J. Undergrad. Chem. Res.* **2009**, *8*, 93-97.
253. Tjessem, K.; Aaberg, A., Photochemical transformation and degradation of petroleum residues in the marine environment. *Chemosphere* **1983**, *12* (11-12), 1373-94.
254. Boukir, A.; Aries, E.; Guiliano, M.; Asia, L.; Doumenq, P.; Mille, G., Subfractionation, characterization and photooxidation of crude oil resins. *Chemosphere* **2001**, *43*, 279-286.
255. ThomINETTE, F.; Verdu, J., Photooxidative behavior of crude oils relative to sea pollution. Part I. Comparative study of various crude oils and model systems. *Mar. Chem.* **1984**, *15* (2), 91-104.
256. Rontani, J. F.; Giral, P. J. P., Significance of photosensitized oxidation of alkanes during the photochemical degradation of petroleum hydrocarbon fractions in seawater. *Int. J. Environ. Anal. Chem.* **1990**, *42* (1-4), 61-8.
257. Ehrhardt, M. G.; Burns, K. A.; Bicego, M. C., Sunlight-induced compositional alterations in the seawater-soluble fraction of a crude oil. *Mar. Chem.* **1992**, *37* (12), 53-64.
258. Bobinger, S.; Andersson, J. T., Photooxidation Products of Polycyclic Aromatic Compounds Containing Sulfur. *Environ. Sci. Technol.* **2009**, *43* (21), 8119-8125.
259. Eldridge, J. C.; Stevens, J. T.; Editors, *Endocrine Toxicology, Third Edition. [In: Target Organ Toxicol. Ser., 2010; 27{1}]*. Informa Healthcare: 2010; p 408 pp.
260. Page, C. A.; Bonner, J. S.; McDonald, T. J.; Autenrieth, R. L., Behavior of a chemically dispersed oil in a wetland environment. *Water Res.* **2002**, *36*, 3821-3833.

261. Okpokwasili, G. C.; Odokuma, L. O., Effect of salinity on biodegradation of oil spill dispersants. *Waste Manage.* **1990**, *10*, 141-6.
262. Odokuma, L. O.; Okpokwasili, G. C., Role of composition in degradability of oil spill dispersants. *Waste Manage. (N. Y.)* **1992**, *12*, 39-43.
263. Yang, G.; Zhang, L.; Sun, X.; Jing, W., Photochemical degradation of crude oil in seawater. *Chin. J. Oceanol. Limnol.* **2006**, *24* (Copyright (C) 2012 American Chemical Society (ACS). All Rights Reserved.), 264-269.
264. Tjessem, K.; Aaberg, A., Photochemical transformation and degradation of petroleum residues in the marine environment. *Chemosphere* **1983**, *12* (Copyright (C) 2011 American Chemical Society (ACS). All Rights Reserved.), 1373-94.
265. Pesarini, P. F.; Silva, d. S. R. G.; Correa, R. J.; Nicodem, D. E.; de, L. N. C., Asphaltene concentration and compositional alterations upon solar irradiation of petroleum. *J. Photochem. Photobiol., A* **2010**, *214*, 48-53.
266. Rontani, J. F.; Giral, P. J. P., Significance of photosensitized oxidation of alkanes during the photochemical degradation of petroleum hydrocarbon fractions in seawater. *Int. J. Environ. Anal. Chem.* **1990**, *42* (Copyright (C) 2012 American Chemical Society (ACS). All Rights Reserved.), 61-8.
267. Rontani, J. F., Mechanistic aspects of saturated hydrocarbon photooxidation induced by hydrogen atom abstraction. *Trends Photochem. Photobiol.* **1997**, *4*, 125-136.
268. Pongratz, H.; Kiermaier, J.; Wiegerebe, W., Photochemical degradation of crude oils on sea surfaces under simulated conditions. *Toxicol. Environ. Chem.* **1997**, *59*, 151-166.
269. Pilpel, N., Sunshine on a Sea of Oil. *New Scientist* **1973**, *59*, 656.
270. Krajnak, K.; Kan, H.; Waugh, S.; Miller, G. R.; Johnson, C.; Roberts, J. R.; Goldsmith, W. T.; Jackson, M.; McKinney, W.; Frazer, D.; Kashon, M. L.; Castranova, V., Acute Effects of COREXIT EC9500A on Cardiovascular Functions in Rats. *J. Toxicol. Environ. Health, Part A* **2011**, *74*, 1397-1404.
271. Sriram, K.; Lin, G. X.; Jefferson, A. M.; Goldsmith, W. T.; Jackson, M.; McKinney, W.; Frazer, D. G.; Robinson, V. A.; Castranova, V., Neurotoxicity Following Acute Inhalation Exposure to the Oil Dispersant COREXIT EC9500A. *J. Toxicol. Environ. Health, Part A* **2011**, *74*, 1405-1418.
272. Roberts, J. R.; Reynolds, J. S.; Thompson, J. A.; Zacccone, E. J.; Shimko, M. J.; Goldsmith, W. T.; Jackson, M.; McKinney, W.; Frazer, D. G.; Kenyon, A.; Kashon, M. L.; Piedimonte, G.; Castranova, V.; Fedan, J. S., Pulmonary Effects after Acute Inhalation of Oil Dispersant (COREXIT EC9500A) in Rats. *J. Toxicol. Environ. Health, Part A* **2011**, *74*, 1381-1396.
273. Maki, H.; Sasaki, T.; Harayama, S., Photo-oxidation of biodegraded crude oil and toxicity of the photo-oxidized products. *Chemosphere* **2001**, *44*, 1145-1151.
274. Lehto, K. M.; Vuorimaa, E.; Lemmetyinen, H., Photolysis of polycyclic aromatic hydrocarbons (PAHs) in dilute aqueous solutions detected by fluorescence. *J. Photochem. Photobiol., A* **2000**, *136*, 53-60.
275. D'Auria, M.; Racioppi, R.; Velluzzi, V., Photodegradation of Crude Oil: Liquid Injection and Headspace Solid-Phase Microextraction for Crude Oil Analysis by Gas Chromatography with Mass Spectrometer Detector. *J. Chromatogr. Sci.* **2008**, *46*, 339-344.
276. Kim, Y.-C.; Jordan, J. A.; Nahorniak, M. L.; Booksh, K. S., Photocatalytic degradation-excitation-emission matrix fluorescence for increasing the selectivity of polycyclic aromatic hydrocarbon analyses. *Anal. Chem.* **2005**, *77*, 7679-7686.

277. Patra, D.; Sireesha, K. L.; Mishra, A. K., Determination of synchronous fluorescence scan parameters for certain petroleum products. *J. Sci. Ind. Res.* **2000**, *59*, 300-305.
278. Patra, D.; Mishra, A. K., Recent developments in multi-component synchronous fluorescence scan analysis. *TrAC, Trends Anal. Chem.* **2002**, *21*, 787-798.
279. Patra, D., Simple luminescence method for estimation of benzo[a]pyrene in a complex mixture of polycyclic aromatic hydrocarbons without a pre-separation procedure. *Luminescence* **2003**, *18*, 97-102.
280. Saeed, T.; Ali, L. N.; Al-Bloushi, A.; Al-Hashash, H.; Al-Bahloul, M.; Al-Khabbaz, A.; Al-Khayat, A., Effect of environmental factors on photodegradation of polycyclic aromatic hydrocarbons (PAHs) in the water-soluble fraction of Kuwait crude oil in seawater. *Mar. Environ. Res.* **2011**, *72*, 143-150.
281. Klein, A. E.; Pilpel, N., Oxidation of n-alkanes photosensitized by 1-naphthol. *J. Chem. Soc., Faraday Trans. 1* **1973**, *69*, 1729-36.
282. Guiliano, M.; El, A.-L. F.; Doumenq, P.; Mille, G.; Rontani, J. F., Photooxidation of n-alkanes in simulated marine environmental conditions. *J. Photochem. Photobiol., A* **1997**, *102*, 127-132.
283. Herbes, S. E.; Whitley, T. A., Characterization and toxicity of water-soluble photooxidants produced during irradiation of coal liquids by sunlight. *Environ. Pollut., Ser. B* **1983**, *6*, 221-40.
284. Little, E. E.; Cleveland, L.; Calfee, R.; Barron, M. G., Assessment of the photoenhanced toxicity of a weathered oil to the tidewater silverside. *Environ. Toxicol. Chem.* **2000**, *19*, 926-932.
285. Finch, B. E.; Wooten, K. J.; Smith, P. N., Embryotoxicity of weathered crude oil from the gulf of Mexico in mallard ducks (*Anas platyrhynchos*). *Environ. Toxicol. Chem.* **2011**, *30*, 1885-1891.
286. Milroy, S. P., Moshogianis, A.M., Brunner, C.A., Howden, S., Yeager, K. In *Polycyclic Aromatic Hydrocarbon (PAH) Contamination within Mississippi Sound Biota: Preliminary Analyses of Bioaccumulation, Depuration, and Likely Routes of Exposure*, Northern Gulf Institute Annual Conference, Mobile, AL, May 17-19, 2011; Mobile, AL, 2011.
287. Administration, N. O. a. A. 2010-2011 Cetacean Unusual Mortality Event in Northern Gulf of Mexico. http://www.nmfs.noaa.gov/pr/health/mmume/cetacean_gulfofmexico2010.htm (accessed September 9, 2011).
288. Administration, N. O. a. A. Sea Turtle Strandings in the Gulf of Mexico. <http://www.nmfs.noaa.gov/pr/species/turtles/gulfofmexico.htm> (accessed September 6, 2011).
289. Uno, S.; Koyama, J.; Kokushi, E.; Monteclaro, H.; Santander, S.; Cheikyula, J. O.; Miki, S.; Anasco, N.; Pahila, I. G.; Taberna, H. S., Jr.; Matsuoka, T., Monitoring of PAHs and alkylated PAHs in aquatic organisms after 1 month from the Solar I oil spill off the coast of Guimaras Island, Philippines. *Environ. Monit. Assess.* **2010**, *165*, 501-515.
290. Ogata, M.; Fujisawa, K., Organic sulfur compounds and polycyclic hydrocarbons transferred to oyster and mussel from petroleum suspension. Identification by gas chromatography and capillary mass chromatography. *Water Res.* **1985**, *19*, 107-18.
291. Botello, A. V.; Goni, J. A.; Castro, S. A., Levels of organic pollution in coastal lagoons of Tabasco State, Mexico; I: petroleum hydrocarbons. *Bull. Environ. Contam. Toxicol.* **1983**, *31*, 271-7.

292. Kumar, K. S.; Sajwan, K. S.; Richardson, J.; Loganathan, B. G., Polycyclic aromatic hydrocarbons in sediment and American oyster from marsh and estuarine ecosystem in Savannah, GA, USA. *Organohalogen Compd.* **2007**, *69*, 348/1-348/5.
293. Luna-Acosta, A.; Kanan, R.; Le, F. S.; Huet, V.; Pineau, P.; Bustamante, P.; Thomas-Guyon, H., Enhanced immunological and detoxification responses in Pacific oysters, *Crassostrea gigas*, exposed to chemically dispersed oil. *Water Res.* **2011**, *45*, 4103-4118.
294. Shelton, T. B.; Hunter, J. V., Aerobic decomposition of oil pollutants in sediments. *J. Water Pollut. Control Fed.* **1974**, *46*, 2172-82.
295. Soniat, T. M.; King, S. M.; Tarr, M. A.; Thorne, M. A., Chemical and Physiological Measures on Oysters (*Crassostrea Virginica*) from Oil-Exposed Sites in Louisiana. *Journal of Shellfish Research* **2011** (in press).
296. Gratz, S.; Mohrhaus, A.; Gamble, B.; Gracie, J.; Jackson, D.; Roetting, J.; Ciolino, L.; McCauley, H.; Schneider, G.; Crockett, D.; Krol, W.; Arsenault, T.; White, J.; Flottmeyer, M.; Johnson, Y.; Heitkemper, D.; Fricke, F., Screen for the Presence of Polycyclic Aromatic Hydrocarbons in Select Seafoods Using LC-Fluorescence. 07/26/2010 ed.; FDA, Ed. 2010; pp 1-29.
297. Michel, J.; Henry, C. B., Jr., Oil uptake and depuration in oysters after use of dispersants in shallow water in El Salvador. *Spill Sci. Technol. Bull.* **1997**, *4*, 57-70.
298. Neff, J. M.; Boehm, P. D.; Haensly, W. E., Petroleum contamination and biochemical alterations in oysters (*Crassostrea gigas*) and plaice (*Pleuronectes platessa*) from bays impacted by the Amoco Cadiz crude oil spill. *Mar. Environ. Res.* **1985**, *17*, 281-3.
299. Kelly, C.; Santillo, D.; Johnston, P.; Fayad, G.; Baker, K. L.; Law, R. J., Polycyclic aromatic hydrocarbons in oysters from coastal waters of the Lebanon 10 months after the Jiyeh oil spill in 2006. *Mar. Pollut. Bull.* **2008**, *56*, 1215-1218.
300. Barszcz, C.; Yevich, P. P.; Brown, L. R.; Yarbrough, J. D.; Minchew, C. D., Chronic effects of three crude oils on oysters suspended in estuarine ponds. *J. Environ. Pathol. Toxicol.* **1978**, *1*, 879-95.
301. Wilson, E. A.; Powell, E. N.; Craig, M. A.; Wade, T. L.; Brooks, J. M., The Distribution of *Perkinsus marinus* in Gulf Coast Oysters: Its Relationship with Temperature, Reproduction, and Pollutant Body Burden. *Internationale Revue der gesamten Hydrobiologie und Hydrographie* **1990**, *75* (4), 533-550.
302. Soniat, T. M., Epizootiology of *Perkinsus Marinus* disease of Eastern Oysters in the Gulf of Mexico. *Journal of Shellfish Research* **1996**, *15* (1), 35-43.
303. Powell, E. N.; Klinck, J. M.; Hofmann, E. E., Modeling Diseased Oyster Populations. II. Triggering Mechanisms for *Perkinsus Marinus* Epizootics. *Journal of Shellfish Research* **1996**, *15* (1), 141-165.

VITA

Sarah King was born in New Orleans, Louisiana in August of 1982. She grew up in the New Orleans metropolitan area until moving to Sun, Louisiana. In 2000, she attend Southeastern Louisiana University. She received her B.S. in Chemistry (ACS Certified) and a minor in Biology in the Spring of 2005. In the Fall of 2006 she started her graduate career in chemistry at the University of Memphis. The Fall of 2007 she transferred to the University of New Orleans. Later that semester she joined Professor Matthew Tarr's research group.